

Development of Advanced Controller to Achieve Complete Peak Shifting in Light-Weight
Residential Buildings Located in Cold Climate

Jianing Luo

A Thesis in
The Department
of
Building, Civil and Environmental Engineering

Presented in Partial Fulfillment of the Requirements
for the Degree of Master of Applied Science (Building Engineering) at
Concordia University
Montreal, Québec, Canada

August 2019

© Jianing Luo, 2019

CONCORDIA UNIVERSITY
School of Graduate Studies

This is to certify that the thesis prepared

By: **Jianing LUO**

Entitled: **Development of Advanced Controller to Achieve Complete Peak Shifting in Light-Weight Residential Buildings Located in Cold Climate**

and submitted in partial fulfillment of the requirements for the degree of

Master of Applied Science (Building Engineering)

complies with the regulations of the University and meets the accepted standards with respect to originality and quality.

Signed by the final examining committee:

Dr. R. G. Zmeureanu Chair / Examiner

Dr. A. Dolatabadi Examiner

Dr. L. Wang Examiner

Dr. F. Haghghat Supervisor

Approved by Dr. F. Haghghat
Chair of Department or Graduate Program Director
Dr. A. Asif
Dean of Faculty

Date August 06, 2019

ABSTRACT

In the cold northern climate of Canada, building energy consumption for space heating during the winter have caused huge stress on electrical grids, especially during the peak hours. Shifting or shaving the peak demand can avoid additional capital investment required to meet extra peak demand for the electrical suppliers. Consequently, in the recent years, several utility companies adopted time-based rates to encourage the customers to shift their consumption from high demand hours to those with lower demand. In this regard, the two most commonly used time-based rates are time-of-use tariffs and critical peak pricing. Achieving peak shifting can reduce the heating cost under time-based rates for consumers. Overall, peak shaving is benefit not only for the electrical suppliers but also for the consumers.

Most Canadian residential houses are equipped with a concrete slab in their basement primarily for structural integrity. Such high thermal mass concrete slab can be exploited for heat storage to shift the peak power consumption. To take benefit of the concrete slabs in the basement, in previous research works, the self-learning control system and the heat extraction system were proposed to achieve peak shifting in the basement and in the other floors of the buildings, respectively. Despite several advantages, the major limitation of these studies is that the developed self-learning control system focused only on peak shifting in the basement, while the heat extraction system concept was investigated separately from the self-learning control system.

Accordingly, this study focused on developing an advanced controller, which can efficiently operate both electrically heated floor and heat extraction system with the objective of achieving the peak shifting, heating cost savings and guaranteeing the thermal comfort in the whole building. As a preliminary work of this study, the peak shifting ability and heating cost savings potential of the self-learning control system operated electrically heated floor under two electrical tariffs (i.e. time-of-use tariffs and critical peak pricing) was analyzed using a validated TRNSYS-MATLAB model. Later, the advanced controller was developed for extending the peak shifting from the floor with high thermal mass to that without high thermal mass by the electrically heated floors integrated with the heat extraction system. In this regard, the developed TRNSYS-MATLAB model was integrated with the heat extraction system. Consequently, the peak shifting

ability, heating cost savings of the advanced controller was compared with the other commonly used peak shifting control strategies (i.e. constant set point control and rule-based control) and the respective results are presented. At last, a parametric study using Taguchi method was performed to explore the effective parameters that significantly influence the performance of electrically heated floor, heat extraction system in terms of peak shifting ability, thermal comfort and capital cost. For this purpose, three levels were considered for five factors (A) concrete slab thickness, (B) insulation thickness, (C) fan flow rate, (D) indoor air temperature upper limit and (E) floor surface temperature upper limit. Based on the results of the parametric study, overall recommendation to design the optimal electrically heated floors and heat extraction system was provided.

Regarding the results, the peak shifting, thermal comfort and heating cost saving are presented for two tariffs (time-of-use tariffs and critical peak pricing) considering the floor with concrete. The simulation results showed that the peak shifting can be achieved at 99.7% in critical peak pricing and 97.6% in time-of-use tariffs, respectively. On the other hand, to extend the peak shifting in the whole building, self-learning control integrated with a fan (heat extraction system) can improve the peak shifting in basement (up to 97%) and second floor (up to 88%). The cost saving can also increase around 35%, which can be proven financially attractive to both supplier and owner. At last, through parametric study, the optimal condition for efficient design and operation of electrically heated floor system and heat extraction system was found to be concrete slab thickness of 152.4 mm, an insulation thickness of 101.6 mm, a fan flow rate of 400 CFM, air indoor upper limit of 24.5 °C and floor surface temperature upper limit of 28 °C.

ACKNOWLEDGMENTS

First of all, I would like to express my deepest gratitude to my supervisor, Dr. Fariborz Haghighat. I benefited greatly from his excellent guidance throughout my graduate studies. His extensive expertise and charismatic personality enabled me to learn a lot during the research period. Because of his strong support and great patience, I could finish my master degree project successfully.

I would also like to extend my sincere gratitude and appreciation to my friends, Dr. Mahmood Mastani Joybari and Dr. Karthik Panchabikesan, for their valuable suggestions on my research and tremendous efforts to improve the quality of this thesis. Without their help, I could not finish this thesis.

I extend my deepest thanks to Dr. Zhun (Jerry) Yu, Professor, Hunan University, China. His personal and professional advice made me to have interest in research. Also, his recommendations gave me the opportunity to start the master's program in Concordia.

I would like to thank all those with whom I worked during this project: Alain Moreau and Stéphane Boyer from Laboratoire des technologies de l'énergie d'Hydro-Québec, Miguel Robichaud from Ouellet Canada, and my colleagues (Ying, Hélène and Dave). Their expertise and patience helped me to get familiar and confident about this project.

Then, I would like also to thank all my colleagues (Behrang, Emilie, Jun, Chao, Maryam, Soroush, Saba, Niousha and Myriam) for their help and kindness with my English and research. It was a fantastic experience to work with them.

Last but not least, I am deeply thankful to my family members (Chunwen, Wenli, Jimin, Xiuhua, Chunyu and Dalong) for their continuous encouragement and understanding. Without their love and support, this master's degree would not have been possible.

CONTRIBUTION OF AUTHORS

Chapter	3, 4
Title	Performance analysis of a predictive model free self-learning controller for heat storage under different tariffs
Authors	Jianing (Tom) Luo, Mahmood Mastani Joybari, Karthik Panchabikesan, Ying Sun, Fariborz Haghighat, Alain Moreau, Miguel Robichaud
Status	Under review in Sustainable Cities and Society
Description	TRNSYS-MATLAB model was validated according to the measurement data. Base on two different time-based rates, the peak shifting potential, cost saving and thermal comfort have been analyzed.

TABLE OF CONTENTS

ABSTRACT	III
ACKNOWLEDGMENTS	V
CONTRIBUTION OF AUTHORS.....	VI
TABLE OF CONTENTS.....	VII
LIST OF FIGURES	X
LIST OF TABLES	XII
LIST OF SYMBOLS AND ABBREVIATIONS.....	XIII
1. INTRODUCTION	15
1.1. Background.....	15
1.2. Objectives.....	17
1.3. Thesis Outline.....	18
2. CHAPTER 2 – LITERATURE REVIEW	19
2.1. Non-Predictive Control.....	19
2.1.1. Classical control.....	19
2.1.2. Rule-based control	21
2.2. Predictive Control	27
2.2.1. Model based predictive control.....	27
2.2.2. Model free control.....	33
2.3. Summary and Limitations of Previous Studies	36
3. CHAPTER 3 – BUILDING AND SIMULATION MODEL DESCRIPTION	37
3.1. Building and Fan Information	37

3.1.1.	Building description.....	37
3.1.2.	Heat extraction system installing the building.....	39
3.2.	Research Methodology.....	40
3.3.	Task A: Investigation on the Peak Shifting Potential of SLC in the Basement under Different Time Schedule.....	41
3.3.1.	Task A.1: Model development (TRNSYS-MATLAB model)	41
3.3.2.	Task A.2: Comparison of the controllers with two different schedules	43
3.4.	Task B: Extend Peak Shifting Investigation for the ENTIRE House with Different Control Strategies	47
3.4.1.	Task B.1: Controller development.....	47
3.4.2.	Task B.2: Development of TRNSYS-MATLAB model intergrated with HES.....	52
3.4.3.	Task B.3: Comparision of the peak shifting potential of different control strategies	53
3.5.	Task C: A parametric study.....	56
3.5.1.	Task C.1: Minitab model	56
3.5.2.	Task C.2: Simulation design by Taguchi method.....	58
4.	CHAPTER 4: RESULTS.....	60
4.1.	Task A: Investigation on the Peak Shifting Potential of SLC in the Basement under Different Tariffs	60
4.1.1.	Task A.1: Model validation (TRNSYS-MATLAB model)	60
4.1.2.	Task A.2: Study of the peak shifting potential, thermal comfort and cost saving for the basement.....	63
4.2.	Task B: Extend Peak Shifting Investigation for the Whole House with Different Control Strategies	75
4.2.1.	Task B.1 Parametric study of the floor surface upper limit temperature.....	75
4.2.2.	Task B.3 Comparison results among these cases.....	76

4.3. Task C: Results for Parametric Study by Taguchi method	82
4.3.1. Task C.1: Analysis for the output results.....	82
4.3.2. Task C.2: ANOVA methods for analysis output results.....	86
5. CONCLUSION.....	91
5.1. Summary and Conclusion	91
5.2. Future Work and Recommendations	93
6. REFERENCES	94

LIST OF FIGURES

Figure 2.1: Principle of the ON/OFF controller ("Control," 2014)	20
Figure 2.2: Different RBC strategies	22
Figure 3.1: The photograph of the investigation house considering in the study	37
Figure 3.2: Floor plan of the house (a) basement, (b) ground floor and (c) second floor	38
Figure 3.3: The photographs of the HES installed in the house	39
Figure 3.4: Overview of research works carried out in this study	40
Figure 3.5: Schematic representation of the TRNSYS-MATLAB model.....	42
Figure 3.6: Time schedule based on (a) the CPP tariff in Quebec and (b) the TOU tariff in Ontario	44
Figure 3.7: Low-level controller operation principle in two scenarios for easing overshoot: setting upper limit (a) and fan method (b).....	48
Figure 3.8: Working principle of the proposed advanced controller	51
Figure 3.9: Schematic of the TRNSYS-MATLAB model integrated with the HES	52
Figure 3.10: Schematic representation of the parametric studies with combinations of the software box in TRNSYS and MATLAB	56
Figure 4.1: Exemplary comparison of energy consumption profile between measurement data and simulation results	61
Figure 4.2: Comparison of (a) energy consumption and (b) average power consumption among the cases for Quebec during critical days	65
Figure 4.3: Comparison of the average indoor air temperature among the cases for Quebec during critical days (a) real variation and (b) box plot.....	66
Figure 4.4: Comparison of the heating cost among the cases for Quebec during critical days	68
Figure 4.5: Comparison of the total heating cost among the cases for Quebec during the entire winter	68
Figure 4.6: Comparison of (a) energy consumption and (b) average power consumption between the cases for Ontario during the entire winter.....	70
Figure 4.7: Indoor air temperature in different rooms using Case O-SLC for Ontario during the entire winter	71

Figure 4.8: Comparison of the total heating cost between the cases for Ontario during the entire winter	72
Figure 4.9: Energy consumption and peak energy shaving potential of the SLC system under different temperature categories	73
Figure 4.10: Heating cost saving potential of Case O-SLC compared to Case O-NoSLC.....	74
Figure 4.11: Peak power consumption for each temperature category depending on the occurrence	75
Figure 4.12: Frequency of the PTC for different floor surface upper limit temperatures	76
Figure 4.13: Comparison of average demand per period per day for the different cases	77
Figure 4.14: Peak shifting potential (%) of different cases in the second floor and basement.....	78
Figure 4.15: Energy shifting potential (%) of different cases during 2nd off-peak period (10:00-16:00)	79
Figure 4.16: Average indoor air temperature for different cases in (a) the basement and (b) the second floor.....	80
Figure 4.17: Comparison of thermal comfort potential among the cases	81
Figure 4.18: Comparison of the total heating cost savings for different these cases.....	82
Figure 4.19: S/N ratio main effect plots of different factors and levels	85
Figure 4.20: Comparison of regression models with simulation results.....	89

LIST OF TABLES

Table 2.1: Summary of investigations on SPC with energy storage for peak load shifting and cost saving	26
Table 2.2: Summary of previous studies for load shifting using MBPC in latent heat storage....	30
Table 2.3: Summary of previous studies for load shifting using MBPC in the building envelop storage	32
Table 2.4: Performance of the MFC for achieving the load shifting with different kinds of energy storage	35
Table 3.1. The distribution of heating systems in the building.....	38
Table 3.2: Fan flow rate levels and its power consumption	39
Table 3.3: Acceptance criteria (in %) for energy model validation.....	43
Table 3.4: Description of the investigated cases.....	46
Table 3.5: Summary of various cases and their control strategies.....	54
Table 3.6: Setpoint temperature schedule based on CPP	55
Table 3.7: The considered factors in parametric study and their levels.....	58
Table 3.8: The L27 orthogonal array indicating the factors and their levels according to Table 3.7	58
Table 4.1: Energy validation results	62
Table 4.2: Total energy consumption and deviations for the two stages	62
Table 4.3: Temperature validation results	62
Table 4.4: Electricity pricing in Quebec ("Residential rates," 2018)	67
Table 4.5: TOU electricity pricing in Ontario (HydroOne 2017).....	71
Table 4.6: The responses and their corresponding signal-to-noise ratio for each simulation in Table 3.6.....	83
Table 4.7: S/N for factorial effects and contribution ratio.....	86
Table 4.8: ANOVA results based on the data in Table 4.6.....	87
Table 4.9: Optimal condition for each response as well as overall (equal weight)	89
Table 4.10: Verification of optimal conditions for each output parameter.....	90

LIST OF SYMBOLS AND ABBREVIATIONS

Symbols

C	Heat capacity of the air (kJ/kgK)
C_c	Concrete slab cost (\$)
$C_{c,l}$	Concrete slab cost per unit volume (\$.m ⁻³)
C_f	Fan cost (\$)
D	Duration (hr)
E_{fan}	Energy consumption by fan (kWh)
I	Time step
K	Room number
N	Final time step
R	Response
T	Time (hr)
$T_{i,out}$	Outlet air temperature (°C)
$T_{i,in}$	Inlet air temperature (°C)
V_i	Fan speed (m ³ /s)
W	Volumetric weight ratio
y	Output parameter
ρ	Air density (kg/m ³)

Abbreviations

ANOVA	Analysis of variance
ASHRAE	American society of heating, refrigeration and air-conditioning engineers
BIM	Building Information Modeling
BITES	Building-integrated thermal energy storage
CHS	Convective heating system
COP	Coefficient of performance

CPP	Critical peak pricing
CSC	Constant setpoint control
CVRMSE	Coefficient of variance of the root mean square error
EHF	Electrically heated floor
FEMP	Federal energy management program
FHS	Floor heating system
FRP	Flat rate pricing
HCS	Hybrid control strategies
HES	Heat extraction system
HVAC	Heating, ventilation, and air conditioning
MBPC	Model based predictive control
MFC	Model free control
MPC	Model predictive control
MS	Mean square
NMBE	Normalized mean bias error
ORC	Organic Rankine cycle
PCM	Phase change material
PID	Proportional integrative derivative
PSP	Peak shave potential
PTC	Poor thermal comfort
RBC	Rule-based control
RTP	Real-time pricing
SHS	Sensible heat storage
SLC	Self-learning control
SS	Sum of squares
TBR	Time-based rate
TCP	Thermal comfort potential
TOU	Time-of-use
TRNSYS	TRaNsient SYstems Simulation program

INTRODUCTION

1.1.BACKGROUND

Building energy consumed by heating, ventilation and air-conditioning (HVAC) is over 40% of the total energy (A. Sharma, Saxena, Sethi, & Shree, 2011). In Canada, residential buildings consume about 17% of the total energy, a major part of which is dedicated to space heating (up to 63%) ("Energy Efficiency Trends in Canada 1990 to 2013," 2016). In several provinces (e.g. Quebec and Ontario), electricity is the main source to maintain the thermal comfort in buildings. Consequently, with respect to exterior weather conditions and occupant behavior, electrical grids face critical issues to meet the space heating demands during the peak hours (Québec, Lanoue, & Mousseau, 2014). As a result, peak periods create stress on the electrical grids, where utility companies have to use mostly fossil fuel-based systems to meet the peak demand, causing a lot of CO₂ emissions. Hence, investigations on peak shifting control strategies are worthwhile not only to decrease the CO₂ emissions but also to achieve cost saving for both electrical suppliers as well as the customers.

Several approaches have been studied to achieve peak shifting. One of the methods is to set different electricity tariffs for different hours of the day (i.e. peak, mid-peak and off-peak periods). Four common electricity tariffs include time-of-use (TOU) rates (Greenage, 2019), critical peak pricing (CPP) (Herter, 2007), peak time rebate (PTR) (Alexander, 2010) and dynamic pricing (DP) (Triki & Violi, 2009). The electrical tariff in TOU as the most common rule has different rates though-out the day. In other words, different electricity rates are set at different time of each day according to the stress exerted on the electrical grid. Commonly, TOU rates are set based on the season (e.g. Hydro One (HydroOne 2017)). CPP sets critical peak rates on specific critical days. In the critical peak time, the electrical rates are substantially higher than normal rates (e.g. Hydro Quebec ("Residential rates," 2018)). In the PTR, no extra electrical rates are set during the peak periods. On the other hand, the customers who consume less energy during peak hours are rewarded. DP also known as real-time pricing is dynamic according to supply and demand, and other external factors in the market. This typical electrical rate can be altered each hour

according to the stress on the electrical grid. In this way, electrical suppliers encourage the consumers to decrease their energy consumption especially during the peak periods.

In line with the above mentioned tariffs, peak load shifting can be achieved by charging the thermal mass of building during off-peak periods. In other words, heat can be stored in building thermal mass during cheap off-peak hours so as to be use later during peak hours, meeting thermal comfort requirements. Most Canadian residential buildings are equipped with a thick concrete slab in their basement. The amount of heat storage in such slabs depends on the thickness of the concrete slab and its insulation. However, thicker concrete and insulation means more initial investment. A major issue is that the concrete and insulation thicknesses cannot be altered for existing buildings. Consequently, heat storage in concrete slabs requires some modifications to achieve peak load shifting.

Energy must be stored during off-peak and mid-peak periods, which can be consumed during the peak periods to meet the demand. In this regard, control strategies can be used to achieve load shifting. Self-learning control (SLC) as one kind of the peak shifting control has been studied for typical residential buildings with thick concrete per room (Hélène Thieblemont, 2017). So far, building thermal mass, phase change material (PCM) and water tank have been frequently used for thermal energy storage (TES) (Bastani & Haghghat, 2015; Bastani, Haghghat, & Kozinski, 2014; Nkwetta & Haghghat, 2014; Nkwetta et al., 2014). Among them, building thermal mass is regarded as the simple method for energy storage.

Consequently, among these different types of TES, EHF by storing energy in concrete slab is applied in the residential sector during winter. EHF can adapt different charge methods (i.e. air duct, water pipe or electricity (Olsthoorn, Haghghat, Moreau, Joybari, & Robichaud, 2019)) in application. Hence, during the off-peak and mid-peak periods, EHF charges the slab and the stored heat can be consumed to maintain the thermal comfort during the peak period. By employing proper control strategies for the EHF, the peak load could be reduced. Several studies for the control strategies with EHF focused on peak shifting and cost saving (Hu, Xiao, Jørgensen, & Li, 2019; Le Dréau & Heiselberg, 2016).

As mentioned earlier, most residential buildings have thick concrete slabs only in their basements for structural integrity which are equipped with electrical cables for heating. As a result, merely using the building thermal mass to store energy is not enough for the whole building to

meet the peak demand. Therefore, a fan can be used to transfer the stored energy from the room with thick concrete to those without lower thermal mass. Such fan systems, also known as heat extraction systems (HES), have been studied using manual control (Ying Sun, 2018).

Despite of several advantages, the major limitations of the previous research works (Ying Sun, 2018; H el ene Thieblemont, 2017) are: i) the developed SLC system focused only on the efficient operation of electrically heated floors (EHFs) installed in the basement and hence, the peak shifting is possible only in the basement of the building; ii) though HES concept is proposed to shift the peak in the floors without high thermal mass (by transferring the warm air from the basement to other floors), the operation of EHF and HES does not involved any control system, which means both EHF and HES were operated manually. Therefore, for the combined operation of both EHF and HES, an advanced controller is recommended to enhance the peak shifting ability of the EHF not only in the basement but also to the entire house. To increase the peak load shaving, this thesis focused on developing an advanced controller to achieve peak shifting, thermal comfort and heating cost saving in the entire house rather than the particular floor with thick concrete slab. Parametric study as the recommendation were also conducted to analyze the parameters for the combination of these components. Therefore, HES (i.e. fan flowrate), TES (i.e. thickness of concrete and insulation) and thermal comfort (i.e. setting upper limit values) have been investigated based on the peak shifting potential, thermal comfort and economic analysis. Moreover, comparison results of different peak shifting control strategies are presented to guide both the consumers and electrical suppliers.

1.2.OBJECTIVES

The main objectives of the research are:

- Investigation of peak shifting, heating cost saving potential of SLC under two different types of time-based rates of electricity pricing.
- Development of an advanced controller, which can control the heat storage in the EHF together with the heat extraction to other floor while maintaining thermal comfort and increasing the peak shifting potential.

- Conduct of parametric study using Taguchi method to explore the effective factors (fan flow rate, thickness of the concrete slab and insulation, upper limit for air, floor surface temperature) influencing the peak shifting potential of EHF system integrated with HES.

1.3. THESIS OUTLINE

Chapter 2 presents a literature review on control strategies applied to different types of the TES. Chapter 3 reports the research methodology, model development and control algorithms as well as parametric study by Taguchi method. Chapter 4 discusses the results obtained for different control strategies as well as the parametric study. Finally, conclusions of this research and recommendations for future studies are presented in Chapter 5.

CHAPTER 2 – LITERATURE REVIEW

In this chapter, literature review is carried out on various types of control strategies used for the purpose of achieving peak shifting with different energy storage options in buildings. Building-integrated thermal energy storage (BITES) is used for cool and/or heat storage in order to cover or shave the peak load. Depending on its mechanism, BITES can be divided into active and passive categories. The passive BITES is operated using uncontrollable natural forces (such as natural convection) while active BITES includes controllable mechanical systems. The control strategies used for active BITES can be divided into two categories: non-predictive control (or local control) and predictive control (or supervisory control) (Yu, Huang, Haghghat, Li, & Zhang, 2015). Among non-predictive control strategies, classical control (i.e. ON/OFF and PID) and rule-based control are frequently used. On the other hand, model based predictive control (MBPC) and model free control (MFC) are classified as predictive control.

Energy storage in buildings is proved to be an effective way to achieve the load shifting, maintain the thermal comfort and reduce temperature swings (Heier, Bales, & Martin, 2015). Three main types of the energy storage in buildings are: sensible heat storage (using concrete, water tank, etc.), latent heat storage (using PCMs) and thermochemical storage (using batteries).

2.1. NON-PREDICTIVE CONTROL

Non-predictive control includes a series of control strategies with no prediction for the future states. Among these control strategies, classical control is most frequently used, whose objectives are to guarantee the thermal comfort and decrease the swings of the temperature. In addition, based on the difference of the electrical tariffs in different hours of each day, the power consumption can be adapted using manual control. According to different rules or objectives, RBC can be used.

2.1.1. CLASSICAL CONTROL

Classical control uses Laplace transform to adapt the dynamic building energy consumption to maintain the indoor temperature. In general, the most commonly used classical

control systems are ON/OFF and proportional–integral–derivative (PID) control. Based on the feedback (i.e. the difference between the measured indoor air temperature and the setpoint temperature), ON/OFF or PID control provides the relative rate for cooling and/or heating systems. Consequently, ON/OFF or PID control (Bai & Zhang, 2007) can maintain the thermal comfort in a proper indoor air temperature range once applied in HVAC systems.

2.1.1.1. ON/OFF control

ON/OFF control is like operating a switch, which is widely used for temperature control. Figure 2.1 shows the principle of the temperature controller under ON/OFF control in a heater ("Control," 2014). Once the feedback temperature is below (or above) the setpoint values, the heater is turned ON (or OFF). This kind of control normally includes a delay, hysteresis and/or a cycle time to reduce the cycling or "hunting" when the feedback variable is close to the setpoint.

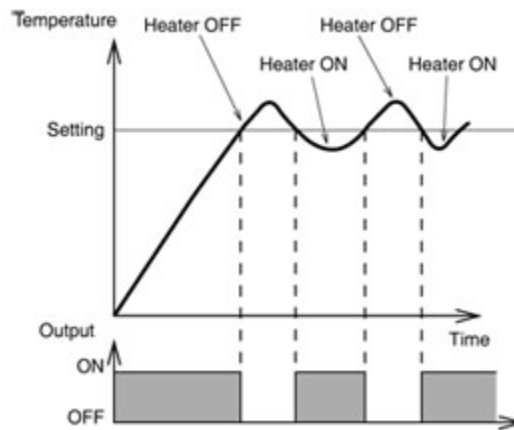


Figure 2.1: Principle of the ON/OFF controller ("Control," 2014)

ON/OFF control can provide simple control actions. Liu et al. (L. Liu, Fu, & Jiang, 2012) used wireless ON/OFF control to decrease the household waste heat in China. The energy consumption for controlled users was 30% lower than the users without controller in the same place. Kattan et al. (Kattan, Ghali, & Al-Hindi, 2012) investigated an under-floor heating system with ON/OFF control. By setting the upper limit of floor surface temperature as 30 °C during the off-peak period, the under-floor heating system could save 26% of the peak demand and a 30% reduction in energy consumption comparing with the conventional system. However, poor thermal comfort was reported (i.e. PMV below -0.5 sometimes).

2.1.1.2. PID control

PID control constitutes calculating the error values between the measured feedback and the desired values based on proportional, integral and derivative terms. The main advantage of PID control over ON/OFF control is achieving less discrepancy between the measured data and the desired value. Consequently, PID control is usually regarded as the sub-control systems in investigation to achieve peak load shifting as well as to guarantee the thermal comfort. Yang et al. (Q. Yang, Li, & Kang, 2008) studied a PID control integrated with fuzzy control to operate the heating system. This typical hybrid controller provided joint control from the boiler to the power station in the heating system. Saving energy and decreasing heating cost was achieved by giving the reasonable joint control signal. Lavrova et al. (Lavrova et al., 2012) studied operation of battery charge/discharge by PID control for load shifting. Upon testing different strategies with manual handling for starting charging time, 15% peak shifting was achieved by the substation-sited photovoltaic (PV) system and large-scale utility storage. In such cases, adding the battery system is the main reason for achieving the peak shifting and the control is only applied to maintain system operation.

Despite its simplicity and advantages, the major drawback of PID controller is it cannot find satisfy answers by itself. Note that, PID control cannot achieve peak shifting on its own as it lacks effective control strategies for building energy management.

2.1.2. RULE-BASED CONTROL

In general, two types of RBC control strategies are commonly used: night setback control (NSC) and setpoint control (SPC). Figure 2.2 depicts an example for the temperature setting level of NSC and SPC for space heating application during different periods of a given day. Note that, Level 2 and Level 1 means higher and lower temperature setting during space heating, respectively. As the figure shows, SPC enables the charging based on the electrical tariff (off-peak/peak periods), while NSC enables charging only during night. In other words, the higher electrical tariffs will lead to the lower/higher setpoint in heating/cooling system for SPC. On the other hand, NSC charges the building at night when the stress on the electrical grids is low. Unless thermal comfort is jeopardized, the control system would not charge during the day. In order to store more energy

at night, thermal comfort cannot be considered simultaneously. Hence, NSC is widely used in the commercial or office buildings since they are not normally occupied at night. Therefore, considering the thermal comfort during the night for residential buildings, SPC is the suitable option.

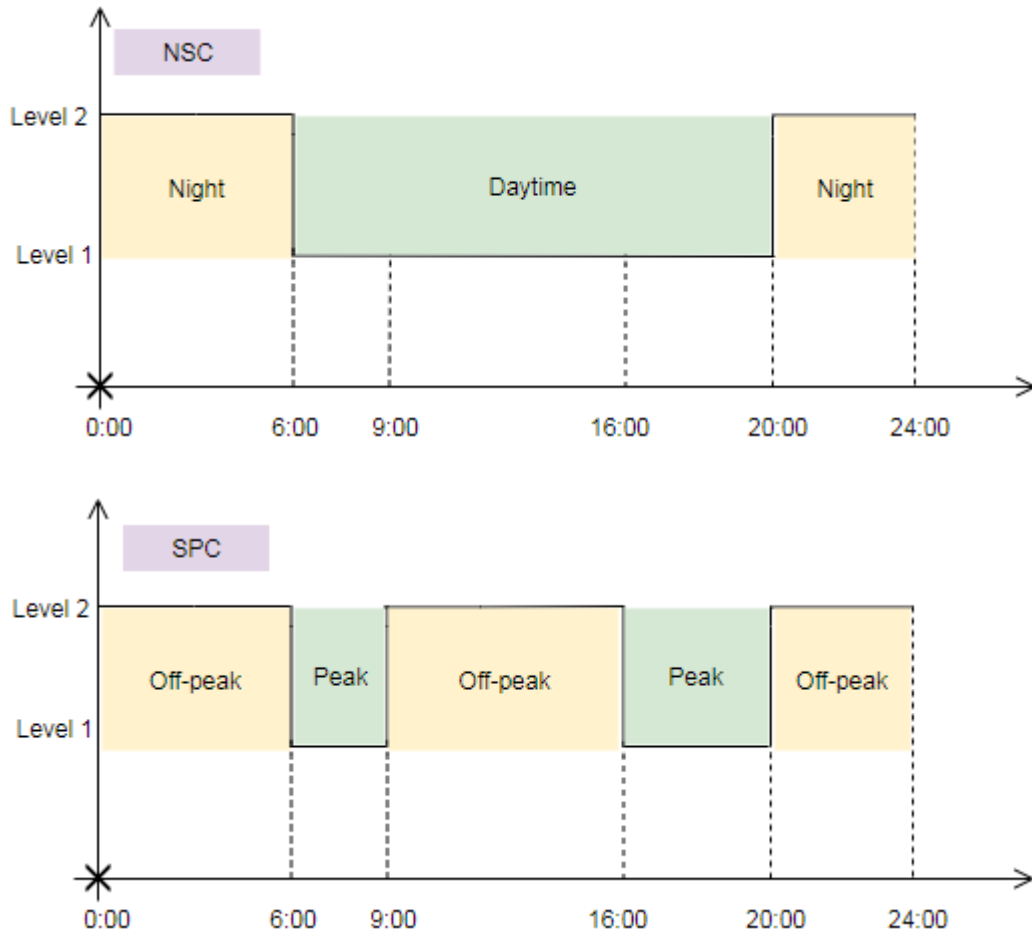


Figure 2.2: Different RBC strategies

Alonso and Mathisen (Alonso & Mathisen, 2017) studied the NSC for a cooling system to achieve load shifting. The system was simulated by IDA ICE model for an office building located in Norway. Their results conveyed that NSC as a simple and useful control strategy could achieve load shifting up to 12%. Lin et al. (Lin et al., 2005) investigated an under-floor electric heating system with PCM using NSC in a single zone office building. NSC was used to charge the system during the night (i.e. 23:00 to 8:00). Considering that there are no occupants at this period, the

average indoor air temperature was and floor surface temperature was maintained at 31 °C and 45 °C, respectively. During the discharging time, the minimum average indoor air temperature was maintained at 19 °C. As a result, a peak shifting potential of 54% was achieved. Cheng et al. (Cheng, Xie, Zhang, Xu, & Xia, 2015) also studied an under-floor heating system with PCM under NSC in experiment and simulation. In the experiments, charging was continued for 10 hours during the night while the under-floor heating system was discharged during the other 14 hours of the day. With exterior temperature within 0-6 °C, the average room temperatures were low (within 15-16 °C) resulting in poor thermal comfort. Thus, the inference from the literature is that, though NSC could achieve the peak shifting potential, the poor thermal comfort should be considered.

Mazo et al. (Mazo, Delgado, Marin, & Zalba, 2012) investigated a floor heating system (FHS) integrated with PCM for peak shifting using NSC. By operating the heat pump at night to meet the building load, energy could be shifted (by 78%) during the peak period. Besides, heating cost savings of around 18% were achieved. Moreover, Li et al. (J. Li, Xue, He, Ding, & Han, 2009) developed an under-floor heating system using concrete and micro-encapsulated paraffin of various thicknesses. To achieve the peak load shifting, NSC was applied for charging between 22:00 to 6:00, while during discharging time thermal comfort was guaranteed. The results indicated that 80% of energy consumption could be shaved during the peak period. Overall, NSC can achieve peak load shifting; however, the poor thermal comfort during the night is the barrier for its application in residential buildings. Meanwhile, excess energy storage during the night also causes energy waste in terms of heat loss.

On the other hand, SPC strategy can be used to adapt to the time-based rates for the energy price and achieve peak shifting. SPC system can trigger a signal action based on temperature, time-based rates or occupancy load based on the setpoint to control the power level for achieving load shifting (Péan, Salom, & Costa-Castello, 2018). For different types of energy storage, charging or discharging strategies have an impact on the load shifting potential. However, once the schedule for the SPC strategy is fixed, it can be used in most of the buildings located in the same climatic condition with the same energy TOU price. Several studies have been conducted, some of which integrated or compared the SPC with NSC in terms of peak load shifting and cost saving.

As for integrated control strategies, Keeney and Braun (K. R. Keeney & Braun, 1997) developed and tested a cooling control strategy in a large office building. By precooling the fluid

in the chiller with different setpoint temperatures, peak load shifting could be achieved. At the same time, NSC was also applied to decrease the energy consumed for the chiller during unoccupied periods. It is reported that by adopting the proposed control strategy, the cooling cost savings of \$25,000 per month is possible. Braun et al. (Braun, 2003) provided the optimal SPC considering electricity price and thermal comfort in a small commercial building. Comparing with NSC, SPC could reduce the peak energy in cooling load within 18-31% for the interior, east, south and west zones in experiment with several test zones. Moreover, the optimal control strategy for SPC (considering more factors including zone direction and occupied load) could achieve peak shifting up to 40% compared to NSC.

Andresen and Brandemuehl (Andresen & Brandemuehl, 1992) developed an SPC precooling strategy based on TOU electricity rates for a single residential building. Internal air and thermal mass (i.e. building furnishings) were considered in energy storage using SPC, leading to 50% peak load shifting in simulations. Moreover, for energy storage in SPC, a three-floor office building located in Phoenix was studied by Henze et al. (Henze, Le, & Florita, 2005). They studied the influence of the thickness of building structure, occupancy period temperature setpoint range, and weather as characterized by diurnal temperature and relative humidity swings in achieving peak shifting with the same control strategy. Moreover, internal gains were another influencing factor. Considering these factors, the running process for the chilled water setpoint was optimized and load shifting was enhanced within 21-28% compared to NSC.

As for energy storage using RBC strategy, Klein et al (Klein, Herkel, Henning, & Felsmann, 2017) studied four different types of energy storage systems (i.e. batteries, fuel switch, water tanks and building thermal mass) to achieve peak shifting and cost saving improvements using TOU prices. An RC model based on a 6-story office building was developed to perform simulations of the heating and cooling systems. The inference from the simulation results is that energy storage via batteries showed best energy saving potential (up to 10%), while the building thermal mass possessed an energy saving potential of 4%. Batteries stored energy directly without affecting heating or cooling system. However, if the RBC with batteries can balance load shifting in electricity grid and customers' requirements including thermal comfort, more complex control strategies should be applied. The reason is that the charging and discharging time for battery as

well as the stress swing on the electrical grid should be considered. Consequently, building thermal mass as the simplest option is more suitable for RBC.

Table 2.1 shows a summary of the investigations on SPC with energy storage regarding peak load shifting and cost saving. Overall, comparison of the result shows that SPC has a superior performance in load shifting and cost saving.

Table 2.1: Summary of investigations on SPC with energy storage for peak load shifting and cost saving

Ref.	Building type	System type	Location	Study type	Storage type	Achievement (criteria)
(Xu, Haves, Piette, & Braun, 2004)	Office building	Cooling	USA	Simulation	Building thermal mass	Peak power decreasing 2.3 W/ft ²
(Xu, 2006)	Commercial building	Cooling	USA	Simulation	Building thermal mass	Load shifting 25%
(Hu, Xiao, & Wang, 2017)	Residential building	Cooling	Hong Kong	Simulation	Building thermal mass	Load shifting
(Zhu, Wang, Ma, & Sun, 2011)	Commercial building	Cooling	Hong Kong	Simulation	PCM wall	Electricity cost saving 11%
(Péan, Salom, & Ortiz, 2017)	Residential flat	Heating	Spain	Simulation	Water tank	Electricity cost saving 22-26%
(Le Dréau & Heiselberg, 2016)	Two Single-family houses	Heating	Denmark	Both	Floor	Heating cost saving 3-10%
(Reynders, Diriken, & Saelens, 2015)	Residential house	Heating	Belgium	Simulation	Building thermal mass	Load shifting 75%

In summary, based on the literature review, energy storage control by RBC could achieve the peak shifting in the range of 25-75%. Meanwhile, since it is a simple control strategy lacking load prediction, achieving peak shifting is affected by the room direction, occupancy, energy storage type and building characteristics. Therefore, to achieve higher peak shifting, predictive control of energy storage should be applied.

2.2.PREDICTIVE CONTROL

In predictive control, based on the prediction for the future system states in the building, the control actions can be determined by considering increasing efficiency of the storage system and/or economic factors. Predictive control provides the control signal to calculate the preheating/precooling time and the power level required by the system. Regarding the prediction approaches, weather forecast (e.g. exterior temperature, solar radiation, etc.) and building parameters are the main inputs for the predictive based control system. The building demand can be determined using the weather forecast data and building energy consumption pattern.

In the predictive control for peak shifting, MBPC and MFC are most commonly used to achieve peak shifting. MBPC requires development of a specific building model. Hence, accurate calculation is the main advantage for MBPC. On the other hand, MFC calculates the building demand using one unique universal model or even without model. Therefore, the exact building demand cannot be calculated at the beginning of the MFC operation. Based on the feedback or accumulation of historical data, the model can be trained to get more accurate prediction gradually. Hence, the main advantage for MFC is that this control can be widely used in application since a specific model is not mandatorily required.

Henze et al. (Henze, Dodier, & Krarti, 1997) investigated the performance of prediction controller in a large 20-floor office building with ice storage technology. By optimizing the charging and discharging time for the energy storage in control strategies, cost saving values of 3-60% were achieved, proving that control strategies integrated with the energy storage are important for achieving load shifting and cost saving.

2.2.1. MODEL BASED PREDICTIVE CONTROL

MBPC uses a specific model for each building to predict the future states (i.e. dynamic building demand and cost saving). When dealing with energy storage, other states (i.e. peak

shifting and pre-charging power) should also be included in the model. Accurate future states can be provided from the specific building model, determining the proper control actions according to the objectives. Consequently, MBPC can achieve several various objectives such as guaranteeing thermal comfort, load shifting (Robillart, Schalbart, Chaplais, & Peuportier, 2018) and cost function minimization (I. Sharma et al., 2016). Keeney and Braun (K. Keeney & Braun, 1996), using a validated model (Morris, Braun, & Treado, 1994), studied the peak load shifting potential using MBPC. Compared to NSC it was found that 95-97% cost saving can be achieved in cooling system using MBPC. Moreover, based on an RC model for a residential building, Masy et al. (Masy, Georges, Verhelst, Lemort, & André, 2015) compared the predictive control with SPC in terms of load shifting and electricity cost saving for a FHS. The results showed that MBPC could achieve peak load shifting up to 80%, while decreasing the electricity cost by 2-19% compared to the setpoint control.

In addition, Clauß et al. (Clauß, Finck, Vogler-Finck, & Beagon, 2017) studied the specific energy flexibility key performance indicators (KPI) between the building performance and electrical grid by comparing the MBPC with RBC. According to the KPI, multiple “objective functions” can be considered by MBPC in system optimization by taking into account the energy flexibility. On the other hand, if only a single objective is pursued, RBC was reported as an effective control strategy. In this section, the studies which investigated MBPC in conjunction with energy storage are presented.

2.2.1.1. Thermochemical energy storage with MBPC

Thermochemical energy storage can be used for load shifting and to decrease the stress on the electrical grids by charging batteries during the off-peak period and using the stored electricity during the peak period (Lund, Lindgren, Mikkola, & Salpakari, 2015). Kuboth et al. (Kuboth, Heberle, König-Haagen, & Brüggemann, 2019) developed a thermal RC model for the building envelope of a single family residential building in Germany and used Simulink MATLAB (by means of the component a library CARNOT (Wemhöner, Hafner, & Schwarzer, 2000)) to describe the energy storage system. Photovoltaic panels as well as a battery energy storage were utilized while two hot water storages were applied in the space heating and domestic hot water systems. As for predictive control, both load shifting and cost function were considered in control strategies.

The energy consumption performance was improved, and the energy cost was decreased by about 12%.

The performance and lifetime of thermochemical storages can be significantly impacted by ambient temperature and the methods used for charging and discharging (Salpakari, Rasku, Lindgren, & Lund, 2017). Investigation of thermochemical storage is still being investigated under ideal conditions. Moreover, thermochemical storages face barriers in terms of economic factors and also environmental issues for dealing with their disposal. As the initial and operational cost of batteries is still high, they are not popular options for achieving peak shifting.

2.2.1.2. Latent heat storage with MBPC

As its name implies, the latent heat capacity of some suitable materials is exploited in this type of storage. To shift the peak load, latent heat storage can be used with phase change materials (PCMs) (Kalnæs & Jelle, 2015), where the most commonly PCM is ice (Yau & Rismanchi, 2012). Overall, PCMs can be used in both cooling and heating systems for energy storage. PCMs are proved as an effective type of energy storage for achieving peak shifting with energy management in different building sizes (J. Ma, Qin, Salsbury, & Xu, 2012). PCMs can be integrated within the building envelopes, which means no space scarification would be required within the buildings. Also, it can increase the energy storage capacity during the off-peak period. The higher heating capacity is necessary to increase peak shifting potential under proper control strategy. However, aside from higher initial investment, it may cause longer pre-cooling time to meet demand during summer (Xu et al., 2004). A method to solve this is to use PCM tanks. However, extended piping system would be needed to transfer the energy to the storage tank. In addition, comparing the initial investment, the price of the PCMs is much higher than ice applications. Table 2.2Figure 2.1 shows a summary of previous studies for load shifting using MBPC for latent storage.

Table 2.2: Summary of previous studies for load shifting using MBPC in latent heat storage

Ref.	Building type	System type	Location	Study type	Model type	Storage type	Achievement (criteria)
(Bastani, Haghghat, & Manzano, 2015)	Bungalow	Heating	Canada	Simulation	TRNSYS model	PCM wallboard	Decrease the peak heating time
(Touretzky & Baldea, 2016)	Single zone building	Heating	USA	Simulation	Mathematical model	PCM wall	Load shifting 84%-66%
(Barzin, Chen, Young, & Farid, 2015)	Hut	Heating	New Zealand	Experimental	LabVIEW software	PCM floor	Heating cost saving 62.6%
(Wang & Niu, 2009)	Office room	Cooling	Hong Kong	Experimental	Mathematical model	PCM slurry tank	Load shifting 48.5%
(Zhu, Hu, & Xu, 2013; Zhu, Liu, Hu, Liu, & Jiang, 2015)	One room	Both	China	Simulation	RC model	PCM wall	Load shifting: 3.1–3.8% (cooling); 8.6–11.3% (heating)
(Yau & Lee, 2010)	Tropical building	Cooling	Malaya	Simulation	TRNSYS model	Ice tank	Energy cost saving 24%
(Hajiah & Krarti, 2012)	Commercial buildings	Cooling	Kuwait	Experimental	Mathematical model	Ice tank	Energy cost savings 10.8%
(Henze, Felsmann, & Knabe, 2004)	Three-story office building	Cooling	USA	Simulation	EnergyPlus model TRNSYS model	Ice tank	Electricity cost saving 46%
(Morgan & Moncef Krarti PhD, 2010)	School building	Cooling	USA	Simulation	EnergyPlus model	Ice tank	Electricity costs saving 47%
(Luo, Hong, Li, Jia, & Weng, 2017)	Commercial building	Cooling	China	Simulation	MATLAB model	Ice tank	Energy costs saving 5.7–11.3%

2.2.1.3. Sensible heat storage with MBPC

In this type of storage, the material undergoes sensible temperature increase. Existing building envelope and water tanks are few examples for sensible heat storage. Pedersen et al. (Pedersen, Hedegaard, & Petersen, 2017) investigated MBPC to achieve load shifting and cost saving. For an apartment located in Denmark, a model was developed in EnergyPlus. By preheating and storing the energy in building structure, up to 6% cost saving could be achieved by this MBPC. Ma et al. (Y. Ma, Kelman, Daly, & Borrelli, 2012) investigated an MBPC system integrated with a water tank for heating and cooling applications. For simulation, an RC model was developed for a university building in USA. The MBPC could effectively shift the load by precooling/preheating of the water tank. Hot water tank can be used for space heating (Haines, Kyriakopoulou, & Lawton, 2019), which is an accepted option for existing buildings (Gupta & Irving, 2013). Finck et al. (Finck, Li, & Zeiler, 2016) developed an MBPC for a heating system equipped with a water tank. An RC model was used for the simulation to test the load shifting. The daily electricity peak load of a small-scale office building was found to be reduced by 72%. Patteeuw et al. (Patteeuw, Henze, & Helsen, 2016) also studied MBPC to achieve load shifting by storing energy in a water tank. An individual building with heat pumps was used to develop the RC model. Heat pumps were used for preheating and 60-90% cost saving could be achieved.

Building envelop has also been used for sensible storage (Balaras, 1996). Table 2.3 shows a summary of previous studies for load shifting using MBPC in the building envelop. According to the table, building thermal mass is the main energy storage for achieving peak shifting. Compared with public buildings (e.g. office or commercial buildings), residential buildings can get better performance in terms of peak shifting. The reason is that smaller areas have lesser demand during the peak period since the building thermal mass cannot store more energy. Note that floor was the main storage for heating using MBPC; however, its lower heat capacity (compared to latent storage) is the main limit. Nevertheless compared to the latent storage, sensible storage is simpler and easier to implement in application. Besides, model development is also easier for sensible storages, which leads to promote its application.

Table 2.3: Summary of previous studies for load shifting using MBPC in the building envelop storage

Ref.	Building type	System type	Location	Study type	Model type	Storage type	Achievement (criteria)
(Perez, Baldea, & Edgar, 2016)	Individual house	Cooling	USA	Simulation	Linear autoregressive with exogenous model	Building thermal mass	Load shifting: 25.5% (18.2 kW)
(Turner, Walker, & Roux, 2015)	Residential building	Cooling	USA	Simulation	REGCAP model	Building thermal mass	Load shifting 75%
(Salsbury, Mhaskar, & Qin, 2013)	Single story commercial building	Cooling	USA	Simulation	EnergyPlus model	Building thermal mass	Cost saving 25.52%
(X. Li & Malkawi, 2016)	Small office building	Cooling	USA	Simulation	EnergyPlus model	Building thermal mass	Energy costs saving 20-60%
(Pavlak, Henze, & Cushing, 2015)	Office building	Cooling	USA	Experimental	RC model	Building thermal mass	Load shifting 1.2-18.1%
(Avci, Erkok, Rahmani, & Asfour, 2013)	Typical house	Cooling	USA	Experimental	Mathematical model	Building thermal mass	Load shifting:44.2% Cost saving: 43.3%
(Fadejev, Simson, Kurnitski, & Bomberg, 2017)	Single-family house	Cooling	Poland	Simulation	IDA ICE model	Floor and wall	Load shifting 16%
(Schmelas, Feldmann, & Bollin, 2015)	Office building	Both	Germany	Both	RC model	Slab	Load shifting: 2-9% (cooling); 1-5% (heating);
(Klein, Kalz, & Herkel, 2015)	Office building	Heating	Germany	Simulation	Modelica building library model	Floor	Shifting peak power: 28kW to 2kW
(Favre & Peuportier, 2014)	Single-family house	Heating	France	Simulation	Mathematical model	Floor	Weekly cost saving 12%
(Halvgaard, Poulsen, Madsen, & Jørgensen, 2012)	House	Heating	Denmark	Simulation	Mathematical model	Floor	Electricity cost saving 25-30%
(Hu et al., 2019)	Residential building	Heating	Denmark	Simulation	TRNSYS model	Floor	Daily electricity costs saving: 1.82-18.65%
(Masy et al., 2015)	Residential building	Heating	Belgium	Simulation	RC model	Floor	Electricity cost saving 8-13%
(Georges, Masy, Verhelst, Andre, & Lemort, 2014)	Residential building	Heating	Belgium	Simulation	RC model	Floor	Electricity cost saving 2-14%

Overall, these studies illustrate that MBPC can be utilized for accurate prediction, load shifting and decreasing energy cost. However, since MBPC requires a unique model for any specific building/application, it is inherently limited to that case. As such, MFC has been presented in the following part to overcome this shortcoming.

2.2.2. MODEL FREE CONTROL

MFC does not need a specific building model (Spall & Cristion, 1998) for prediction. Instead, a universal building model or historical data can be used for load prediction (Hélène Thieblemont, Haghghat, Ooka, & Moreau, 2017). Therefore, MFC can predict the load to control indoor environment for instance based on weather forecast, time schedule of the electricity prices, energy storage potential, etc. Since a specific building model is not required, accurate load prediction cannot be achieved at the beginning of the MFC implementation. Historical data prediction (HDP) can be used based on the accumulated data of building energy consumption over time for instance according to the exterior conditions. This typical load prediction for the MFC is regarded as a simple prediction method. Besides, two main learning methods (reinforce learning control and self-learning control) can be applied for load prediction in MFC to update the database or training coefficients of the system. The MFC can adapt the parameters of the universal model or update the database according to the feedback from measurements such as indoor air temperature or building energy consumption (Spall & Cristion, 1993). Comparing among these three methods (i.e. HDP, reinforce learning and self-learning), HDP lacks the updating and learning process. The simpler calculation process results in lower prediction accuracy than the other two learning methods. By this approach, (unlike MBPC) MFC can be utilized for various buildings/applications. As such, MFC can be implemented more simply and cheaply than MBPC (Hélène Thieblemont, 2017).

In terms of improving the predictive accuracy for MFC, because of using the universal building model or historical load values in prediction, reinforce learning control (RLC) would face difficulties. Moreover, there is still a research gap for investigating accurate prediction of RLC during the training period. On the other hand, SLC can achieve high prediction accuracy. For instance, Omar et al. (Omar, Bushby, & Williams, 2017) developed an SLC system for a single-family residence, comparing the prediction results from the SLC system with the actual data in 362 days. An RMSE value of lower than 4% was achieved, indicating a well-trained SLC.

RLC is regarded as an effective cost saving method in the building energy consumption. Yang et al. (L. Yang, Nagy, Goffin, & Schlueter, 2015) compared the RLC with RBC in the annual output power for the PV/T panels. RLC strategy got gradually better performance in terms of generating total higher net power output than RBC at 5.73%, 9.78%, and 11.47% for the first three years. Chen et al. (Chen, Norford, Samuelson, & Malkawi, 2018) developed an RLC as a black-box building model to save energy. The energy saving from 13-23% could be implemented in different buildings located in two areas (Miami and Los Angeles). As for achieving the task (i.e. peak shifting), RLC mostly can be used for demand response (DR) (Vázquez-Canteli & Nagy, 2019), which means not only considering the building energy consumption from the HVAC system but also considering other influencing factors of the electrical grid (such as domestic hot water, solar PV, electrical vehicle, etc.). In addition, RLC can achieve the load shifting with energy storage, which led to around 8-25% cost saving. The details of the studies are presented in Table 2.4.

SLC is another learning process for energy and cost savings in buildings. As for load shifting, Zhang et al. (Zhang, Pipattanasomporn, & Rahman, 2017) developed an SLC system for small and medium size commercial buildings to reduce the peak demand of the electricity grid. An office building was tested to develop and optimize peak load reduction by training data, validation and improvement algorithms for SLC. Table 2.4 shows the summary performance of the MFC for achieving the load shifting with various kinds of energy storage.

According to Table 2.4, MFC could achieve peak shifting with different types of energy storage. HDP and RLC were the main training methods for commercial buildings under MFC, while SLC was mainly used for residential buildings. Regarding the SLC, compared to the HDP, the database update can provide more accurate prediction, which improves the energy pre-charging. A proper and sufficient energy storage can lead to higher peak shifting potential. On the other hand, SLC as a simpler typical MFC than other learning methods, is widely accepted in application (Hélène Thieblemont, 2017).

Table 2.4: Performance of the MFC for achieving the load shifting with different kinds of energy storage

Ref.	Building type	System type	Location	Study type	Prediction	Storage type	Achievement (criteria)
(Yongjun Sun, Wang, & Huang, 2010)	Commercial building	Cooling	Hong Kong	Experimental	HDP	Chilled water storage	Monthly cost saving 8.51%
(Henze, Kalz, Felsmann, & Knabe, 2004)	Office building	Cooling	USA	Simulation	HDP	Chilled water storage	Cost saving 11-24%
(Braun, Montgomery, & Chaturvedi, 2001)	Commercial building	Cooling	USA	Simulation	HDP	Building thermal mass	Cost saving 40%
(Yin, Xu, Piette, & Kiliccote, 2010)	Commercial building	Cooling	USA	Simulation	HDP	Building thermal mass	Load shifting 15-30%
(Henze & Schoenmann, 2003)	Commercial building	Cooling	USA	Simulation	RLC	Ice tank	Annual cost saving 25%
(S. Liu & Henze, 2007)	Commercial building	Cooling	USA	Simulation	RLC	Chilled water storage	Cost saving 12.3%
(S. Liu & Henze, 2006a, 2006b)	Commercial building	Heating	USA	Simulation	RLC	Building thermal mass	Cost saving 8.3%
(Huang & Liu, 2011, 2013)	Residential house	Electricity	USA	Simulation	SLC	Battery	Weekly cost saving 30.5%
(Massie, 2002)	Laboratory	Heating	USA	Simulation	SLC	Water tank	Load shifting 60%
(H Thieblemont, Moreau, Lacroix, & Haghghat, 2017)	Residential building	Heating	Canada	Simulation	SLC	Floor	Load shifting 98%
(Hélène Thieblemont, Haghghat, Moreau, & Lacroix, 2018)	Residential building	Heating	Canada	Simulation	SLC	Floor	Weekly cost saving 10% Load shifting 55-97%

2.3.SUMMARY AND LIMITATIONS OF PREVIOUS STUDIES

According to the literature, the achieved peak shifting potential depends upon the implemented control strategy and the type of energy storage. A few studies reported satisfactory results for achieving peak shifting and cost saving while guaranteeing thermal comfort. Several types of non-predictive control (i.e. RBC system) can meet the requirements. As for the simple control strategy, it is mostly investigated for building thermal mass, which has low peak shifting potential because of the small heating/cooling capacity. Instead, the predictive control has been investigated to calculate the proper pre-charging values to achieve peak shifting. MBPC with complex model can obtain accurate predictions. However, the main limitation of the MBPC is that a specific model is required for each building to be able to provide accurate predictions. Considering the residential buildings, the number is more than 1.6 million in (Canada., 2017) therefore, MBPC requires too much time for model development. Consequently, MBPC is not a reasonable selection for this type of buildings. On the other hand, MFC uses a universal model or historical data for effective load management in buildings. Compared to the classical control, MFC can predict the peak load, which can give effective predictions for charging and discharging duration of energy storage systems. Consequently, promising performance can be achieved in terms of peak load shifting and cost saving.

In addition, using the energy storage in each room to shift its load can be achieved by SLC (Hélène Thieblemont et al., 2018; H Thieblemont et al., 2017). However, it is only focus on the EHF in the floor with thick concrete floor. Sun et al. (Ying Sun et al., 2018) investigated a heat extraction system (HES) with manual control. The HES can transfer warm air from the floor with energy storage (thicker concrete floor) to the floor without energy storage. However, there is still a research gap in terms of extending the energy storage of the floors using more advanced control strategies. Therefore, considering above mentioned limitations of previous studies, the present study focuses on a universal smart controller for the floors with energy storage and those without energy storage. The integration of the EHF's with HES in MFC has been conducted in this work.

CHAPTER 3 – BUILDING AND SIMULATION MODEL DESCRIPTION

3.1. BUILDING AND FAN INFORMATION

3.1.1. BUILDING DESCRIPTION

A residential single detached house (shown in) located in Boischatel, Quebec, Canada was considered for this study. It has one semi-underground floor (basement) and two floors (ground floor and the second floor) above the ground. There are three types of space heating systems in the house (1) buried EHF system (in which the electrical heating wires are buried inside a 152 mm concrete slab), (2) surface EHF system (with electrical heating wires directly installed below the floor cover and over a 0.6 cm layer of concrete), and (3) convective heating system (electrical baseboard heaters). Note that only buried EHF's can be applied for peak load shifting. All the heating devices are controlled by thermostats as shown by red blocks in

Figure 3.2. The mentioned heating systems are distributed in the house as shown in Table 3.1. Note that under normal operation conditions, a constant set-point indoor air temperature (i.e. 21.5 °C (Hélène Thieblemont et al., 2018)) is used in the house to meet the thermal comfort requirements, representing a typical residential building application.



Figure 3.1: The photograph of the investigation house considering in the study

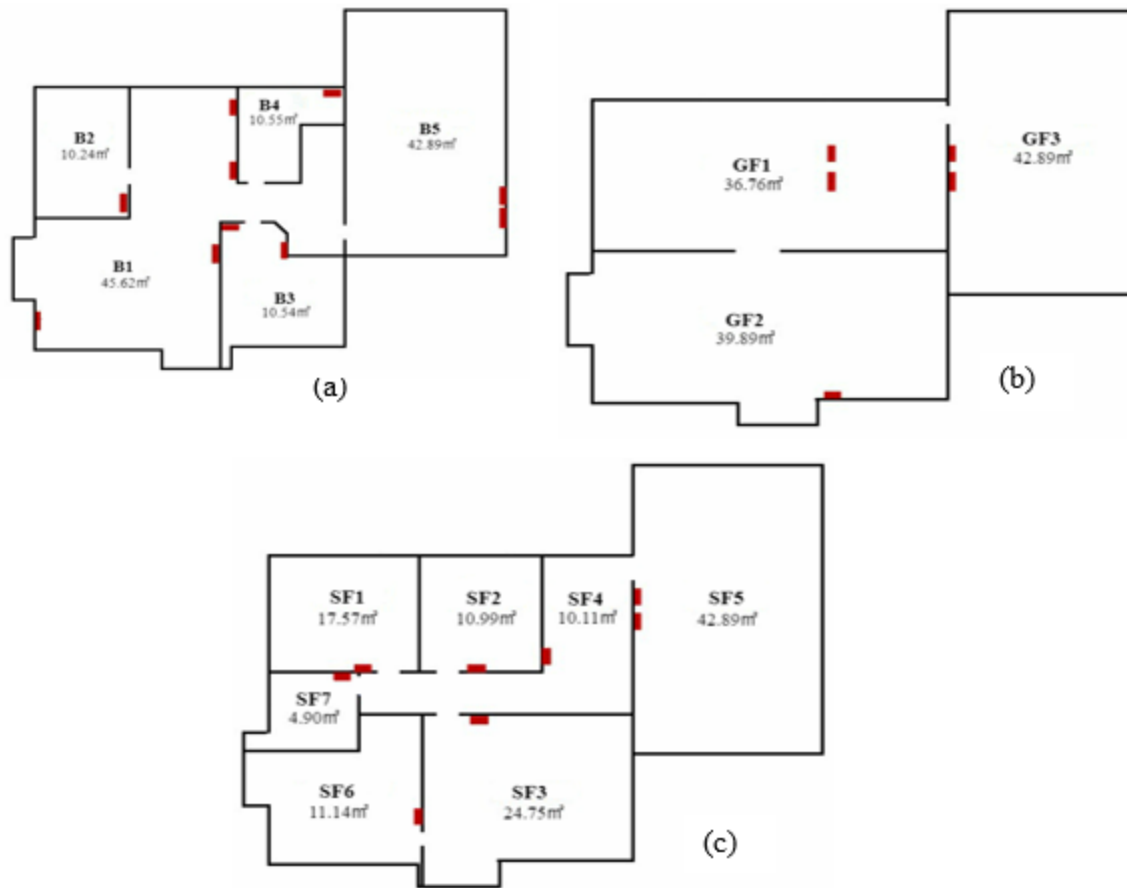


Figure 3.2: Floor plan of the house (a) basement, (b) ground floor and (c) second floor

Table 3.1. The distribution of heating systems in the building

Basement			Ground floor			Second floor		
Room	Functionality	Equipment	Room	Functionality	Equipment	Room	Functionality	Equipment
B1	Living room	CHS, BEHF	GF1	Kitchen	SEHF	SF1	Bedroom	CHS
B2	Bedroom	BEHF	GF2	Living room	CHS	SF2	Bedroom	CHS
B3	Bedroom	BEHF	GF3	Garage	BEHF	SF3	Bedroom	CHS
B4	Bathroom	BEHF				SF4	Hallway	CHS
B5	Laundry room	BEHF				SF5	Office room	CHS
						SF6	Bathroom	CHS
						SF7	Bathroom	CHS

CHS: Conventional heating system BEHF: Buried electrically heated floor SEHF: Surface electrically heated floor

3.1.2. HEAT EXTRACTION SYSTEM INSTALLING THE BUILDING

As mentioned earlier, the floors above the ground have lower thermal mass. To be able to exploit the heat stored in the concrete slab of the basement, the HES has been introduced (Ying Sun et al., 2018). The system transfers the warm air from the basement to the other floors by operating a fan during peak hours. The HES installed in the house is shown in Figure 3.3. The fan can transfer the warm air to the second floor using a duct. Table 3.2 shows the fan performance based on the measurement data. This fan information has been used to develop a model to test the control system.

Table 3.2: Fan flow rate levels and its power consumption

Level	Flow rate (CFM)	Power (W)
1	247	158
2	550	297
3	804	410



(a)



(b)

Figure 3.3: The photographs of the HES installed in the house

3.2. RESEARCH METHODOLOGY

Figure 3.4 shows the overview of the research tasks carried out in the study. Three tasks with the research procedures are presented.

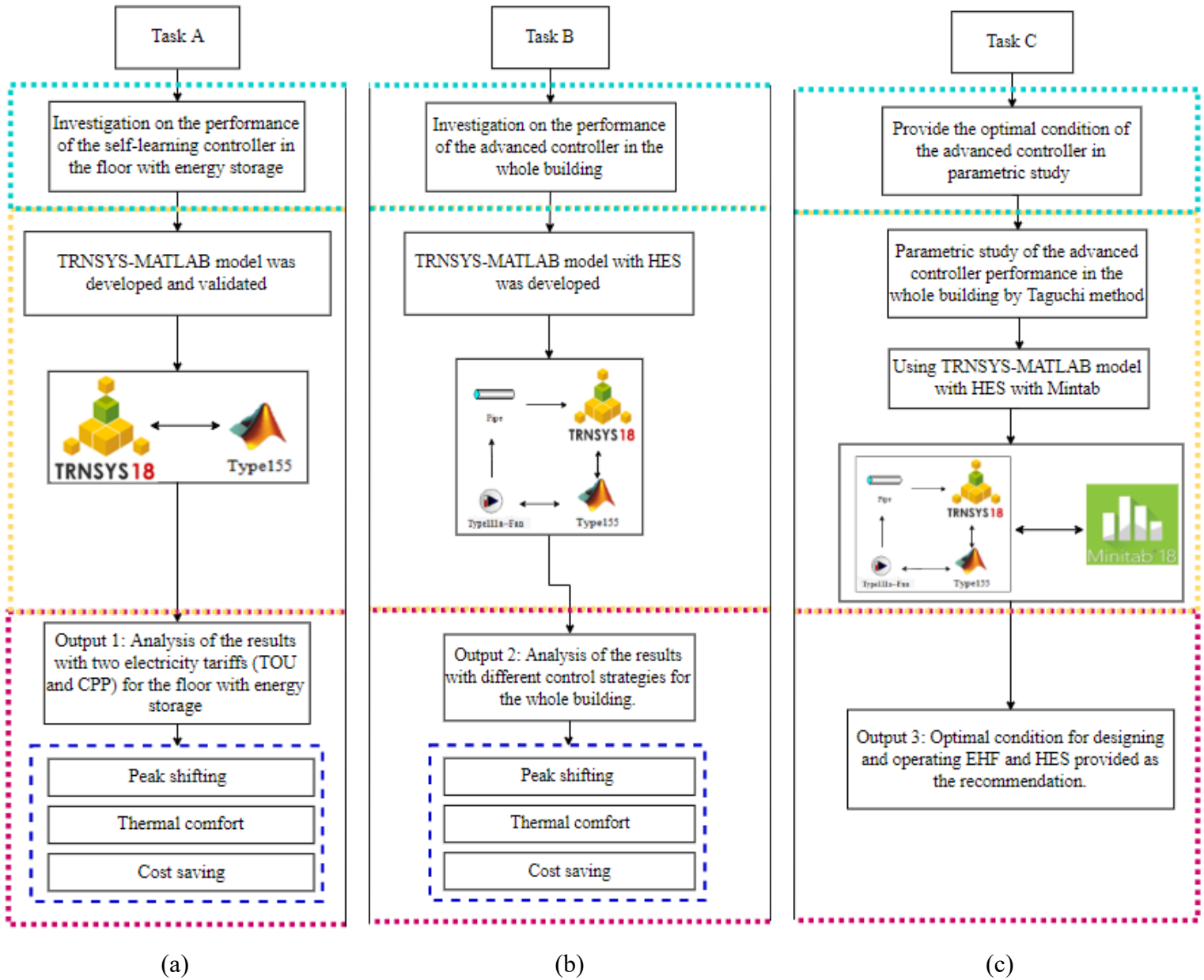


Figure 3.4: Overview of research works carried out in this study

3.3. TASK A: INVESTIGATION ON THE PEAK SHIFTING POTENTIAL OF SLC IN THE BASEMENT UNDER DIFFERENT TIME SCHEDULE

3.3.1. TASK A.1: MODEL DEVELOPMENT (TRNSYS-MATLAB MODEL)

In this section, a brief description on the model development was presented. Different components of the model have been presented. As a result, a TRNSYS-MATLAB model was developed as presented in the following section.

3.3.1.1. TRNSYS-MATLAB model

To simulate the SLC system, the previous TRNSYS model was connected to MATLAB using Type 155 (as shown in Figure 3.5 with red box). Previous TRNSYS model (Ying Sun et al., 2018) using the controller (Type 108) as setpoint control strategy, which only can maintain the thermal comfort. Consequently, SLC only can be implemented by controller in MATLAB. In other words, Type 155 (MATLAB) replaced the TRNSYS model's controller (Type 108) to control the building energy consumption and indoor temperature. Therefore, in the TRNSYS-MATLAB model, control strategies are generated in MATLAB while the indoor conditions are simulated in TRNSYS. Type 155 acted as a bridge to convey the building information (i.e. indoor air and floor surface temperatures as well as the building energy consumption).

The weather data (e.g. exterior dry bulb temperature, solar radiation, humidity and wind velocity) was obtained from the closest weather station (i.e. Jean Lesage International Airport, Quebec City, Canada). Based on the weather data, the exterior soil temperature were calculated. Three main factors such as exterior air temperature, rainfall and snowfall were considered for soil temperature calculation at different ground depths (Qian, Gregorich, Gameda, Hopkins, & Wang, 2011). The exterior soil was divided into two parts below the ground (Ying Sun et al., 2018) (1) from 0 m to 1 m and (2) from 1 m to 2 m. In this model, the former was calculated as functions of exterior air temperature and the latter was assumed based on the contact parts with the exterior walls and insulated floors. Multi-zone building was developed using Type 56 based on the characteristics of the experimental house. Basic information of the building was imported (from an external file) to Type 56 including its zones, room volumes, envelopes and materials as well as

their properties. Within a building, the air flows due to the pressure difference among the zones. This inter-zonal air flow should be considered in the model. To do so, Type 97 (CONTAM model) was used to account the dynamic inter-zonal heat air airflow as well as the infiltration. Note that, the building infiltration was calculated using the experimentally measured leakage area values (Olsthoorn, 2018), which is used in this type (Type 97) to calculate the dynamic infiltration. Consequently, the dynamic internal temperatures were provided by the multi-zone building (Type 56), while Type 97 returned the dynamic pressure difference and the resulting air flows as well as the infiltration of each zone.

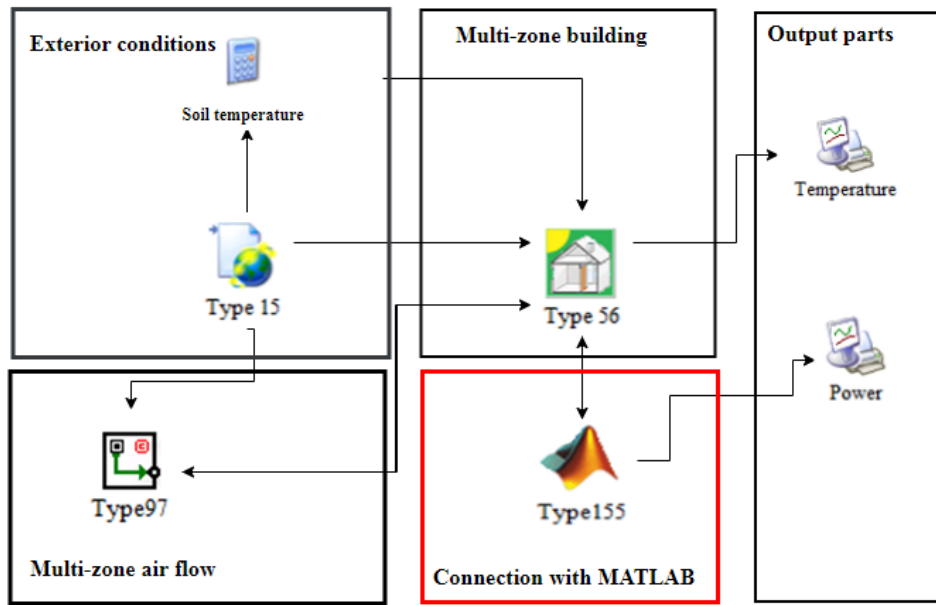


Figure 3.5: Schematic representation of the TRNSYS-MATLAB model

3.3.1.2. Model validation

For the validation of the developed TRNSYS-MATLAB model, two mathematical criteria were considered: Normalized Mean Bias Error (NMBE) and Coefficient of Variance of the Root Mean Square Error (CVRMSE). The NMBE and CVRMSE are calculated using Equations 1 and 2, respectively.

$$NMBE(\%) = \frac{\sum_{t=1}^N (m_t - s_t)}{\bar{m}(N-p)} \times 100 \quad (1)$$

$$CVRMSE(\%) = \frac{\sqrt{\sum_{t=1}^N \frac{(m_t - s_t)^2}{N-p}}}{\bar{m}} \times 100 \quad (2)$$

where m_t and s_t denote the measured and simulated values at time t . N is the number of measured data points, \bar{m} is the average value of the measurement and p is the number of adjustable model parameters. Table 3.3 shows the requirements of ASHRAE (ASHRAE, 2014) and FEMP (Webster et al., 2015) standards for these statistical criteria. The standards assign a limit for the NMBE and CVRMSE values for hourly and monthly levels.

Table 3.3: Acceptance criteria (in %) for energy model validation

Index	Standard	
	ASHRAE (ASHRAE, 2014)	FEMP (Webster et al., 2015)
NMBE _{hourly}	±10	±10
NMBE _{monthly}	±5	±5
CVRMSE _{hourly}	±30	±30
CVRMSE _{monthly}	±15	±15

3.3.2. TASK A.2: COMPARISON OF THE CONTROLLERS WITH TWO DIFFERENT SCHEDULES

3.3.2.1. Two different schedules

Peak shifting, thermal comfort and cost saving potential of SLC were investigated for two tariff settings of CPP and TOU (i.e. for the provinces of Quebec and Ontario, respectively). The time schedule for the tariffs in Quebec and Ontario are shown in Figure 3.6(a) and (b), respectively. During the off-peak (or non-critical) hours (shown by black portions in Figure 3.6), the SLC system can operate the EHF at any capacity (i.e. from 0% to 100%). The white portions illustrate the peak (or critical) hours where preferably no consumption should occur. Note that the TOU tariff in Ontario includes mid-peak hours (the gray portion) in Figure 3.6b, which means that the SLC system can operate the heaters during the mid-peak hours, but at a lower capacity.

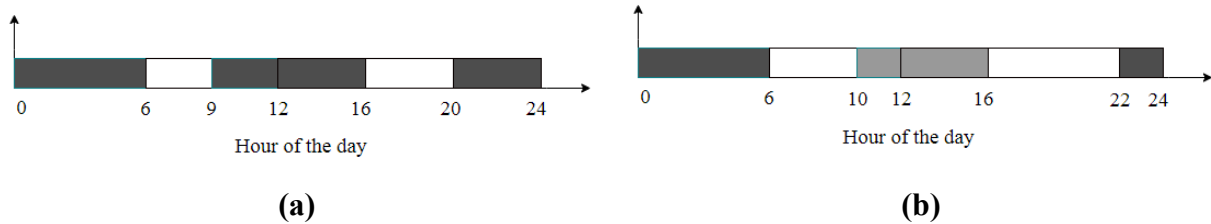


Figure 3.6: Time schedule based on (a) the CPP tariff in Quebec and (b) the TOU tariff in Ontario

Note that, residential customers in Quebec can select from two options (1) FRP tariff (also known as Rate D ("Residential rates," 2018)) which is a flat rate throughout the year irrespective of critical hours and (2) CPP tariff which is a two-level rate where during non-critical hours the electricity cost would be lower than FRP tariff; however, during critical hours (maximum 100 hours annually) it would cost more. In other words, the customers who opt into CPP tariff might be financially penalized should their consumption occur during critical hours. The CPP tariff is only effective during the winter (from Dec. 1 to Mar 31) and for the rest of the year it is the same as the FRP.

3.3.2.2. Comparison of the controllers

To achieve peak shifting, the self-learning algorithm was implemented to predict the half-daily heating load (based on building energy consumption data) (Hélène Thieblemont et al., 2018). The SLC system considered the two most influencing outdoor parameters namely exterior temperature and solar radiation. Therefore, during the SLC system operation, weather forecast was obtained from Environment Canada ("Québec, QC - Hourly Forecast," 2018). This information is used to predict the required heating load for the next day. During the normal operation (i.e. the reference case), a constant set point was considered for the indoor air temperature, representing a typical residential building application. Consequently, for the reference case, the thermostats maintained the indoor air temperature at 21.5°C. In this study, the self-learning algorithm proposed by Thieblemont et al. (Hélène Thieblemont et al., 2018) was adopted with some modifications. The modifications are related to the characteristics of the CPP tariff. Such a temperature categorization is suitable for Ontario, where the TOU tariff applicable for the entire winter. However, for Quebec, where CPP is adopted only during the days with critical hours (i.e. days

with extreme cold temperatures ($> -15^{\circ}\text{C}$), a similar profiling of temperature category is not suitable for CPP time-based tariff (i.e. for Quebec) since the SLC system can operate only during the critical days. In the SLC system developed by Thieblemont et al. (Hélène Thieblemont et al., 2018), for accurate prediction and to account for the temperature variation within a day, each day is divided into two half days. Subsequently, for predicting the heating demand, the temperature categories were categorized in the intervals of 10°C (i.e., $[-40^{\circ}\text{C} -30^{\circ}\text{C}]$, $[-30^{\circ}\text{C} -20^{\circ}\text{C}]$, $[-20^{\circ}\text{C} -10^{\circ}\text{C}]$ and $[20^{\circ}\text{C} 30^{\circ}\text{C}]$), where the category is determined by considering the minimum temperature recorded for each half day. For instance, if the half day hourly exterior temperature is from -9°C to -21°C , the lowest temperature is -16°C , which belongs to category $[-20^{\circ}\text{C} -10^{\circ}\text{C}]$.

However, a similar profiling of temperature category is not suitable for CPP time-based tariff (i.e. for Quebec) since the SLC system can operate only during the critical days. In the rest of the year, when an FRP tariff is imposed there would be no need to activate the SLC system. Overall, it is expected that the critical hours occur during lower exterior temperature (creating a huge stress on the grid). According to Figure 3.6a, in Quebec, there are two peak periods 6:00 – 9:00 and 16:00 – 20:00; therefore, approximately 14 days can be considered as critical days. Hence, in Quebec, if the temperature category for predicting the heating load was categorized with 10°C interval (as proposed by Thieblemont et al. (Hélène Thieblemont et al., 2018)), only three temperature categories would be available during the entire winter (i.e. $[-40^{\circ}\text{C} -30^{\circ}\text{C}]$, $[-30^{\circ}\text{C} -20^{\circ}\text{C}]$ and $[-20^{\circ}\text{C} -10^{\circ}\text{C}]$).

For instance, if the forecast coldest hourly exterior temperatures are -29°C and -22°C (i.e. 7°C difference) for the two half days, using the 10°C intervals would result in the same temperature category (i.e. $[-20^{\circ}\text{C} -30^{\circ}\text{C}]$). Consequently, the historical energy consumption value of the two half days would be stored in the same category to be used for heating load prediction. Considering the number of days the SLC system is operated in Quebec (i.e. 14 days) and to accurately predict the heating load, in this study, the outdoor temperature is categorized into 5°C intervals (i.e. $[-40^{\circ}\text{C} -35^{\circ}\text{C}]$, $[-35^{\circ}\text{C} -30^{\circ}\text{C}]$, $[-30^{\circ}\text{C} -25^{\circ}\text{C}]$ and $[-15^{\circ}\text{C} -10^{\circ}\text{C}]$). If 5°C intervals are used in the previous example the two half days would belong to two different temperature categories (i.e. $[-$

25°C -30°C] and [-20°C -25°C], respectively). This temperature categorization is examined in this study to investigate if it improves load prediction accuracy.

The investigated cases are presented in Table 3.4. For each case, the first alphabetic indicator represents the first letter of the corresponding province while the second indicator shows the characteristic of the case. For instance, **Case Q-SLC-5°C** is for the case with SLC system according to the Quebec’s TBR schedule with the prediction of 5°C interval temperature category. **Case Q-Ref** considers a constant set-point temperature of 21.5°C throughout the day. It represents a customer who selects to stick with the existing FRP tariff. **Case Q-NoSLC** shows a customer who selected the CPP tariff but continues to operate the heaters the same as **Case Q-Ref**. In other words, **Case Q-NoSLC** aims to illustrate whether a household would be financially penalized if it fails to meet the requirements of peak shifting in the CPP tariff. **Case Q-SLC-5°C and Case Q-SLC-10°C** represent a household which implemented the SLC system to shift its load and benefit from lower heating cost. For these cases the SLC system was activated only during the critical days and for the rest (i.e. non-critical days) a constant set-point temperature of 21.5°C was used.

In Ontario, the majority of residential customers use the mandatory TOU pricing ("Electricity pricing and costs," 2018). Therefore, only two cases were investigated for this province. For **Case O-SLC**, the SLC system was used all the days (only during winter), whereas **Case O-NoSLC** shows how much it would cost for the customers using a constant set-point temperature.

Table 3.4: Description of the investigated cases

Province	Case	Controller characteristic	Electricity price
Quebec	Case Q-Ref	Constant set-point (21.5°C)	FRP tariff of Quebec
	Case Q-NoSLC	Constant set-point (21.5°C)	CPP tariff of Quebec
	Case Q-SLC-5°C	SLC system (Quebec schedule)	CPP tariff of Quebec
	Case Q-SLC-10°C	SLC system (Quebec schedule)	CPP tariff of Quebec
Ontario	Case O-NoSLC	Constant set-point (21.5°C)	TOU tariff of Ontario
	Case O-SLC	SLC system (Ontario schedule)	TOU tariff of Ontario

3.4.TASK B: EXTEND PEAK SHIFTING INVESTIGATION FOR THE ENTIRE HOUSE WITH DIFFERENT CONTROL STRATEGIES

3.4.1. TASK B.1: CONTROLLER DEVELOPMENT

In order to exploit the stored heat (within the concrete slab) and use it in other floors, the HES was used. To do so, a fan was installed to transfer the warm air from the rooms with thicker concrete (i.e. from the basement) to the other rooms without energy storage. In this way, the peak load for the rooms without energy storage can also be reduced.

In this task, the fan was located in the basement laundry room (B5 in Figure 3.2), transferring the hot air to the second floor. With the three outlets, the hot air was uniformly distributed in the office room (SF5 in Figure 3.2) and two bathrooms (SF6 and SF7 in Figure 3.2). Note that the number and the location of the outlets were selected based on the results from Sun et al (Ying Sun et al., 2018).

3.4.1.1. Extending the peak shifting

Note that, existing SLC strategies only focused on the floor with energy storage (i.e. the basement with thicker concrete) (Hélène Thieblemont, 2017). Moreover, the HES proposed by Sun et al. (Ying Sun et al., 2018) was operated only during the peak hours using manual control. Hence, there is still a research gap in terms of automation for the heat storage system when combining peak shifting control strategies (SLC) and the HES.

This study develops an advanced controller to integrate the HES with the SLC system, with the aim of increasing the potential of peak shifting (not only in the basement, to the whole house) and at the same time guaranteeing thermal comfort. The operation of HES during the off-peak hours can be controlled by the SLC in the low-level controller. By operation the fan, the overshoot caused by the heat delay can be eased, which is an effective approach to guarantee the thermal comfort. Overall, the developed advanced controller not only can achieve peak shifting for the floors with and without high thermal mass but also can provide a control strategy for the operation

of HES during the off-peak periods to ease the temperature overshoot and also guarantee complete charging.

Low-level controller

Low-level controller plays a vital role on ensuring thermal comfort in control system. Based on the measured values (i.e. indoor air temperatures or floor surface temperatures) from the thermostats, low-level controller can give the control actions to switch the heating system and HES controller, which can achieve the timely supervision in application.

Figure 3.7 depict the principle of the low-level controller and the fan working schedule during different periods with two different approaches to ease overshoot. During the peak periods, the fan would operate with the maximum flow rate to transfer the energy from the basement to the second floor as highlighted in green box in both Figure 3.7a and Figure 3.7b, respectively.

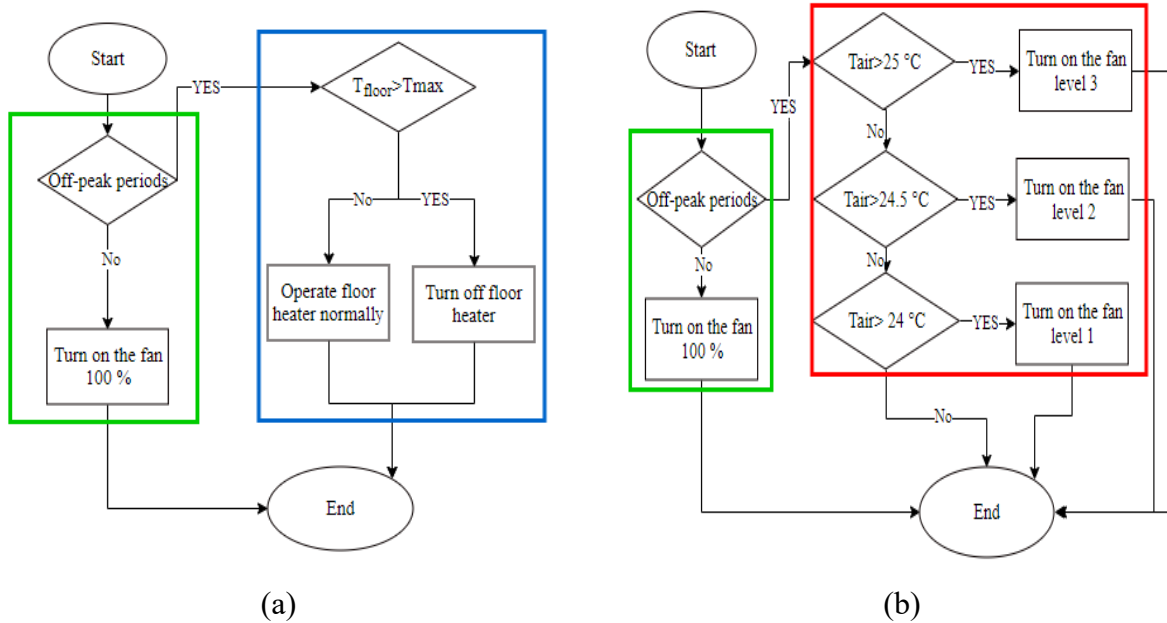


Figure 3.7: Low-level controller operation principle in two scenarios for easing overshoot: setting upper limit (a) and fan method (b)

Temperature overshoot in the basement while charging the EHF

As the SLC system operates the EHF while learning from historical values, there is a chance for poor thermal comfort. In the basement, sometimes the temperature overshoot might occur as there is a time delay from when the heaters are turned OFF until the time the indoor temperature responds. To guarantee thermal comfort and ease the overshoot during the charging period, an upper limit can be set in the low-level controller in Figure 3.7a for blue box as scenario one. During the off-peak period, Figure 3.7a shows how the upper limit of the floor surface temperature is set in the low-level controller. The floor surface temperature is monitored and if it exceeds the maximum floor surface temperature T_{max} , the EHF will turn OFF immediately as illustrated in Figure 3.7a (with the blue boundary). Upper limit as a common method in controller based on the setpoint rules (i.e. floor surface temperature) can control (using ON/OFF) the EHF during the charging period. In such cases, if the indoor air temperature exceeds the upper limit, a control action signal would be sent to switch the EHF OFF immediately. However, a disadvantage of setting an upper limit to ease overshoot during the charging period is that complete charging cannot be guaranteed. In other words, energy storage might be insufficient to cover the entire peak load due to the interruption of charging by the upper limit. In such conditions, insufficient energy storage not only decreases the peak shifting potential but also can cause poor thermal comfort during the peak periods. Consequently, a novel approach should be investigated satisfying both the thermal comfort as well as complete charging.

Regarding the second scenario in Figure 3.7b, using fan to ease the overshoot is developed. Note that in Figure 3.7b the term “level” denotes fan flow rate. To ease overshoot during the off-peak periods, the fan is operated to transfer the excess warm air to the second floor with different levels according to the indoor air temperature as shown in Figure 3.7b (with the red boundary). For instance, if the indoor air temperature reached 24.3 °C at 5:30 am (i.e. during the first off-peak period), the fan would operate at its flow rate level 1. As a result, the EHF would continue heating while the fan running at the lowest flow rate. In this way, the thermal comfort can be guaranteed while the incomplete charging can be avoided. At the same time, the partial energy (resulting in overshoot) has been transferred to preheat the second floor, which can avoid energy wasting as

well. According to recording the fan operation time and flow rates in off-peak periods, the record as the feedback can be calculated by the SLC in advanced controller.

3.4.1.2. Proposed control strategy

Regarding the SLC strategy, the EHF in the basement can be operated by the approach presented by Thieblemont et al. (Hélène Thieblemont et al., 2018). A brief representation of the strategy is shown in Figure 3.8 without the pink boundary. First, according to the weather forecast downloaded from Environment Canada ("Québec, QC - Hourly Forecast," 2018), exterior temperature and solar radiation can be identified. This is the input to the historical database which has been classified by temperature-solar categories. Then, the EHF's are operated normally by output values from the database.

The existing SLC system (Hélène Thieblemont et al., 2018) can adjust the daily energy consumption at the end of the day. Nevertheless, discomfort is an existing issue during the operation, especially at its beginning, regarded as the training time. At the end of each day, the daily maximum and minimum indoor air temperature as well as energy consumption during different hours are used in the SLC. For each period, if the maximum indoor air temperature is higher than 25 °C (or minimum indoor air temperature lower than 22 °C), the corresponding energy consumption of the period will decrease (or increase). Although the training can eventually tend the daily energy consumption to a proper range, the temperature overshoot remains a concern.

To guarantee the thermal comfort by easing the overshoot and at the same time guarantee complete charging, fan operation can be applied during off-peak periods instead of setting any upper limit. In such conditions, the low-level controller as the supervisory control provides different action signals (fan as well as EHF operation) based on the building feedback (i.e. indoor air temperature) during different daily periods. This novel approach has been presented by the pink boundary in Figure 3.8.

The low-level controller can record the fan operation time and fan flow rate level. According to the recorded results, the amount of energy transferred from the basement to the second floor during the off-peak periods can be calculated which will be used by the learning

process. In the learning process, these values are used as the reference to judge the energy value (denoted by E_{fan_Mod} in Figure 3.8) to increase or decrease. Finally, E_{fan_Mod} values are stored in the historical database to adjust the energy consumption prediction values (E_{Mod}) accordingly.

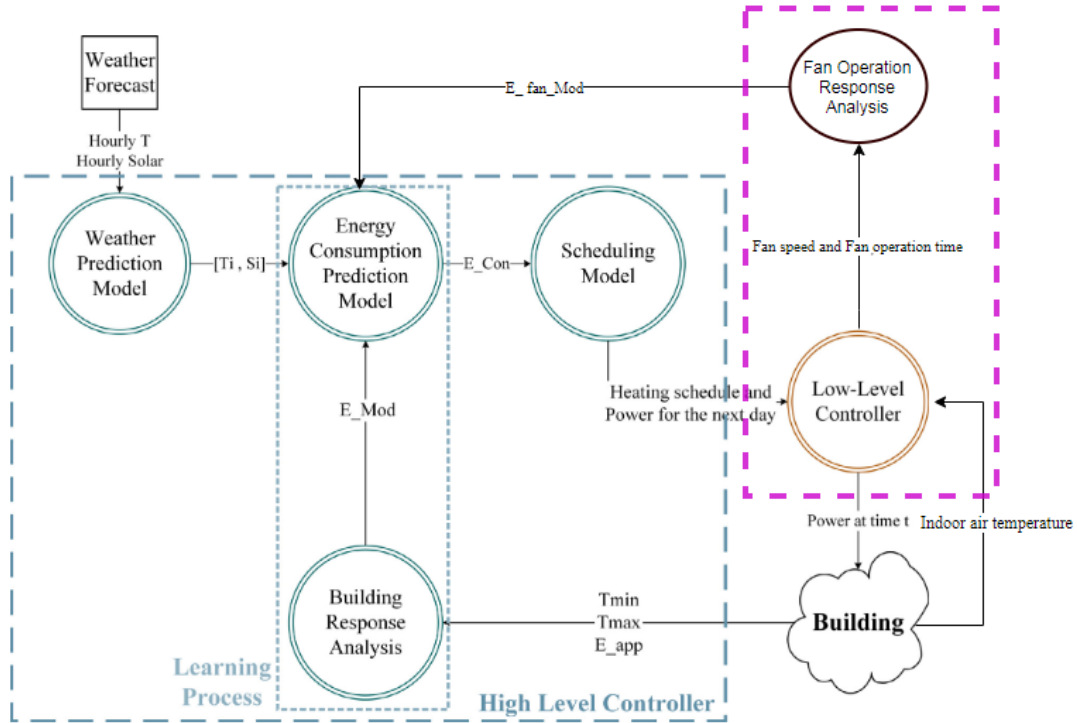


Figure 3.8: Working principle of the proposed advanced controller

In this task, the matrix E_{fan} can be calculated by Equation (3) based on the fan flow rate and operation time. The objectives of transferring the air in the off-peak period are (1) to guarantee thermal comfort, (2) to improve the incomplete charging during the off-peak period and (3) to preheat the second floor avoiding energy waste.

$$E_{fan} = \rho C \sum_{i=1}^n [V_i (T_{i,out} - T_{i,in})] \quad (3)$$

where E_{fan} (kW) is the real applied energy consumption of the previous day, $T_{i,out}$ (°C) is the outlet air temperature and $T_{i,in}$ is the inlet air temperature in the laundry room (B5) where the fan

is installed. C (kJ/(kg°C)) is the specific heat capacity of the air and ρ is the air density. Moreover, V_i (m³/s) is the volumetric flowrate in the simulation and n is the total step.

According to Equation (3), the amount of the transferring energy in off-peak period can be calculated at the end of each day. If keep this part of energy in the basement, the indoor air temperature in the basement would be high than the proper range caused overshoot. This part of the energy is reduced from the total energy consumption implemented by EHF next time by learning process. In this way, the database is updated for training of the SLC system. Once the SLC finds the same exterior weather forecast, the updated value from the database can provide the energy consumption prediction to control the indoor air temperature and floor surface temperature as well as the energy storage in the concrete.

3.4.2. TASK B.2: DEVELOPMENT OF TRNSYS-MATLAB MODEL INTEGRATED WITH HES

The TRNSYS-MATLAB model (explained in Section 3.3.1) was modified to include the HES. As shown in Figure 3.9 all main components were the same except for addition of a fan (Type 111a). The fan transferred the warm air from the basement laundry room (B5) to the second floor (three outlets).

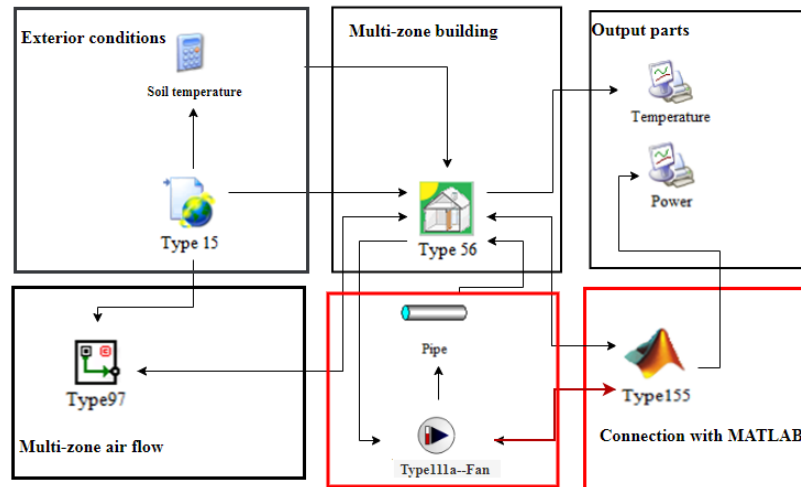


Figure 3.9: Schematic of the TRNSYS-MATLAB model integrated with the HES

The electricity tariff plans adopted in Quebec is shown in Figure 3.6a. The electricity pricing is a two-level rate where during non-critical hours (shown by black portions in Figure 3.6a) the electricity cost would be normal; however, during critical hours (maximum 100 hours annually) it would cost more. Overall, it is expected that the critical hours occur when the outdoor temperature is extremely cold (creating a huge stress on the grid). Therefore, in this task, the coldest winter days were selected to cover the 100 critical hours. According to Figure 3.6a, the critical period last for 14 days. Consequently, during the off-peak hours (shown by black portions in Figure 3.6a), the SLC system can operate the heaters at any capacity. The white portions illustrate the peak (or critical) hours where preferably no consumption should occur.

3.4.3. TASK B.3: COMPARISON OF THE PEAK SHIFTING POTENTIAL OF DIFFERENT CONTROL STRATEGIES

In this task, several control strategies were investigated for the basement and the second floor. Taking into account the feasibility of the experiment in practice, maintain thermal comfort of the ground floor is utilized by CSPC (21.5 °C) in all the cases. Briefly, Reference case was operated under constant setpoint control (the same as the experimental house). Several control strategy combinations were investigated in the basement and second floor by six combinations (see Table 3.5) of three different control strategies (i.e. constant setpoint temperature, self-learning control and rule-based control), some resulting in hybrid control strategies. In this section, the cases are described individually.

Table 3.5: Summary of various cases and their control strategies

Case		Control strategies	Setpoint
Reference case	Basement Second floor	Constant setpoint control	21.5 °C
Case 1	Basement Second floor	Rule-based control	Peak: 21.5 °C; Off-peak: 23.5 °C Peak: 21.5 °C; Off-peak: 23.5 °C
Case 2	Basement Second floor	Self-learning control with upper limit Constant setpoint control	21-25 °C 21.5 °C
Case 3	Basement Second floor	Self-learning control with upper limit Rule-based control	21-25 °C Peak: 21.5 °C; Off-peak: 23.5 °C
Case 4	Basement Second floor Fan control	Self-learning control with upper limit Constant setpoint control ON/OFF control	21-25 °C 21.5 °C N/A
Case 5	Basement Second floor Fan control	Self-learning control with upper limit Constant setpoint control Self-learning control	21-25 °C 21.5 °C N/A
Case 6	Basement Second floor Fan control	Self-learning control without upper limit Constant setpoint control Self-learning control	21-25 °C 21.5 °C N/A

3.4.3.1. Reference case

Using the constant setpoint control (CSPC) is one of the most common control strategies in the residual applications. This simple control strategy can maintain the thermal comfort; however, it cannot meet the requirements of the peak shifting. In this case, electrical baseboard heaters and EHF system (in the basements) was used to meet the space heating demand of the considered house throughout the day.

3.4.3.2. Rule-based control

Rule-based control (RBC) is regarded as a typical simplified control strategy considering both thermal comfort and peak shifting. Without load prediction and specific building model, the setpoint for indoor air temperature is adjusted based on the electricity price schedule. Therefore, RBC strategy is one of the most simple, but effective methods to achieve peak shifting while maintaining thermal comfort. Case 1 (see Table 3.5) uses RBC in both the basement and second floor.

The setpoint temperatures in different periods have a significant impact on the peak shifting potential and thermal comfort. Considering the building thermal mass and the variation of external temperatures, an indoor air temperature span of ± 2 °C is recommended to prevent discomfort (Le Dréau & Heiselberg, 2016). Consequently, peak and off-peak setpoint of RBC can be defined at 21.5 °C and 23.5 °C, respectively. According to the schedule of the CPP in Figure 3.6a, Table 3.6 shows the changes of the setpoint temperature based on different electricity prices. Note that, this is my assumption.

Table 3.6: Setpoint temperature schedule based on CPP

Time period	Setpoint temperature (°C)
0:00-6:00	23.5
6:00-9:00	21.5
9:00-16:00	23.5
16:00-20:00	21.5
20:00-24:00	23.5

3.4.3.3. *Self-learning control*

SLC, as one typical MFC, can be used to control the heating systems within concrete slab for energy storage. Case 2 mentioned in Table 3.5 is similar to the investigation carried out by (Hélène Thieblemont, 2017) on an SLC system which only considered the heat storage in the basement while the other floors continued to operate using the setpoint control. Case 3 used RBC for energy management in second floor while SLC would be used in the basement. Cases 4-6 also used the SLC system in the basement while a fan system was used to cover the peak demand in the second floor. In Case 4, a simple ON/OFF control was implemented for the fan and the fan is operated only during the peak hours to transfer the warm air from the basement to the second floor. To guarantee the thermal comfort, an upper limit for easing overshoot during the charging time has been set in the SLC system. In Case 5, the fan control was integrated in the SLC system itself while keeping the upper limit. In Case 6, the SLC system itself is used to operate both the heaters and the fan. During the learning process, no upper limit was set letting the controller operate the fan according to the requirements. Note that in Cases 4-6, a setpoint of 21 °C was set during peak period in the second floor to guarantee the thermal comfort.

3.5.TASK C: A PARAMETRIC STUDY

3.5.1. TASK C.1: MINITAB MODEL

Figure 4.10 shows the schematic of the procedure followed in this study with regards to the software used. First, the parameters and their levels were fed to Minitab ("Minitab 18 Statistical Software (2010)," 2014.2.14) which then produced an orthogonal array for simulations. Then, simulations were conducted using the TRNSYS-MATLAB model whose results were returned to Minitab. Note that, the simulation results were analyzed in Minitab using the Taguchi method. Taguchi method provides not only standard sets of orthogonal arrays, but also a method to analyze the results according to signal-to-noise (S/N) ratio (Peace). The identification of significant factors and their ranking was performed. Finally, the proper combination of parameters was identified.

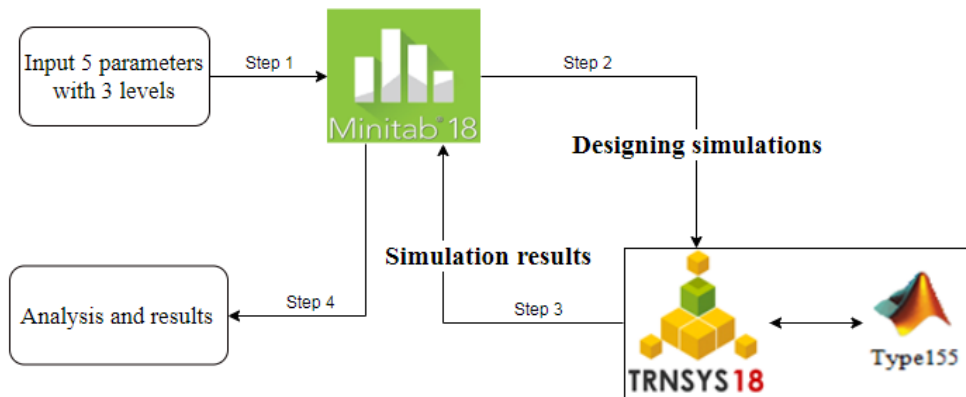


Figure 3.10: Schematic representation of the parametric studies with combinations of the software box in TRNSYS and MATLAB

The ultimate purpose to use the heat storage system is to achieve peak shifting and benefit from the lower electricity cost. However, thermal comfort might be compromised, and capital cost might be affected accordingly. Therefore, in this study, three responses were selected (1) average peak power consumption, (2) thermal comfort potential and (3) capital cost. Thermal comfort potential (TCP) is defined as:

$$TCP = \frac{\sum_k (D - t_k) w_k}{D} \times 100 \quad (4)$$

where ‘ t ’ is the duration of poor thermal comfort (indoor air temperature higher than 25 °C or lower than 21 °C (ASHRAE, 2013; Schiavon, Hoyt, & Piccioli, 2014)), ‘ k ’ is the number of the room, ‘ w ’ is the volumetric weight ratio of the rooms and ‘ D ’ is the total duration of critical days (i.e. 336 hours).

According to the results of earlier simulations (Ying Sun et al., 2018) and experimental campaigns (Olsthoorn et al., 2019), five main factors influencing the performance of the system are identified and considered in this study as shown in Table 3.7. Commercially, concrete slab and insulation material are available in 51 mm increments (Olsthoorn, 2018) and their levels have been selected accordingly. Among these factors, the floor and air temperature upper limits can be handled at no cost (with being defined in the controller). On the other hand, concrete slab and insulation thicknesses as well as fan flow rate affect the capital cost. To consider this, cost functions were used where for the concrete and insulation, they are functions of their volumes. For the concrete slab (Varaee & Ahmadi-Nedushan, 2011):

$$C_c = A_f T_c C_{c,1} \quad (5)$$

where ‘ C_c ’ is the concrete slab cost where ‘ T_c ’ and ‘ A_f ’ are the concrete slab thickness and floor area while ‘ $C_{c,1}$ ’ is the cost of concrete slab per unit volume (\$/m³). A similar functionality was used for the insulation.

The fan cost function is obtained from (Mosaffa, Farshi, Ferreira, & Rosen, 2016):

$$C_f = 155(\dot{V} + 1.43) \quad (6)$$

where ‘ \dot{V} ’ is the fan volumetric flow rate in m³/s.

Table 3.7: The considered factors in parametric study and their levels

Code	Factor	Unit	Level 1	Level 2	Level 3	Ref.
A	Concrete slab thickness	mm	101.6	152.4	203.2	(Olsthoorn, 2018; Olsthoorn et al., 2019)
B	Insulation thickness	mm	50.8	101.6	152.4	(Olsthoorn, 2018; Olsthoorn et al., 2019)
C	Fan flow rate	CFM	400	600	800	(Ying Sun, 2018; Ying Sun et al., 2018)
D	Upper limit for air temperature	°C	23.5	24	24.5	(ASHRAE, 2013; De Dear & Brager, 2002; Schiavon et al., 2014)
E	Upper limit for floor surface temperature	°C	26	27	28	(Olesen & Brager, 2004)

3.5.2. TASK C.2: SIMULATION DESIGN BY TAGUCHI METHOD

Based on the described parameters and their levels, an L27 orthogonal array (shown in Table 3.8) was generated by the Minitab software tool and accordingly. Therefore, a total of 27 simulations were conducted in TRNSYS – MATLAB model with HES.

Table 3.8: The L27 orthogonal array indicating the factors and their levels according to Table 3.7

#	A	B	C	D	E	#	A	B	C	D	E	#	A	B	C	D	E
1	1	1	1	1	1	10	2	1	2	3	1	19	3	1	3	2	1
2	1	1	1	1	2	11	2	1	2	3	2	20	3	1	3	2	2
3	1	1	1	1	3	12	2	1	2	3	3	21	3	1	3	2	3
4	1	2	2	2	1	13	2	2	3	1	1	22	3	2	1	3	1
5	1	2	2	2	2	14	2	2	3	1	2	23	3	2	1	3	2
6	1	2	2	2	3	15	2	2	3	1	3	24	3	2	1	3	3
7	1	3	3	3	1	16	2	3	1	2	1	25	3	3	2	1	1
8	1	3	3	3	2	17	2	3	1	2	2	26	3	3	2	1	2
9	1	3	3	3	3	18	2	3	1	2	3	27	3	3	2	1	3

Consequently, the S/N ratio is defined based on Equation (7) with two conditions. S/N ratio as the evaluation criteria is used in Taguchi method. When the objective should be maximized the top one will be used according to Equation (7). Otherwise, the below one is used according to Equation (7). Note that thermal comfort potential should be maximized, whereas the other outputs should be minimized.

$$S/N = -10 \log \left(\frac{1}{y^2} \right)$$

Objective: maximization

$$S/N = -10 \log (y^2)$$

Objective: Minimization

(7)

where 'y' is the response.

CHAPTER 4: RESULTS

4.1. TASK A: INVESTIGATION ON THE PEAK SHIFTING POTENTIAL OF SLC IN THE BASEMENT UNDER DIFFERENT TARIFFS

In this task, an SLC system based on the Ontario's TOU schedule was developed and implemented in the experimental house (mentioned in Section 3.1). The SLC system was activated during two stages in winter 2018 (the first stage: Jan. 1- Jan 14 and the second stage: Feb. 1- Feb. 15). In this section, validation results are presented for these two stages using the TRNSYS-MATLAB model.

4.1.1. TASK A.1: MODEL VALIDATION (TRNSYS-MATLAB MODEL)

4.1.1.1. Energy consumption validation

The two experimental stages (which is lesser than a month) were not long enough to focus on monthly criteria. Moreover, in this investigation, hourly NMBE and CVRMSE cannot be compared between the simulation and measurement results. Because, the heaters implemented in the experimental house cannot be assigned (by the SLC) to exact percentages of total heater capacity. For instance, if the SLC system assigns a heating level of 50% capacity for 10 minutes, the heater turns ON in full power (i.e. 100% capacity) for instance during the first five minutes; therefore, it would have a 0% capacity during the next five minutes. The real time energy consumption follows a seismic instant power profile, whereas in simulations, the exact heating level can be smoothly achieved. As an example, Figure 4.1 compares the energy consumption between measurement data and simulation results for 4 hours. Note that despite fluctuations in instantaneous measurement results (dash orange line), the average measured energy consumption (dash gray line) is very close to the simulation (solid blue line).

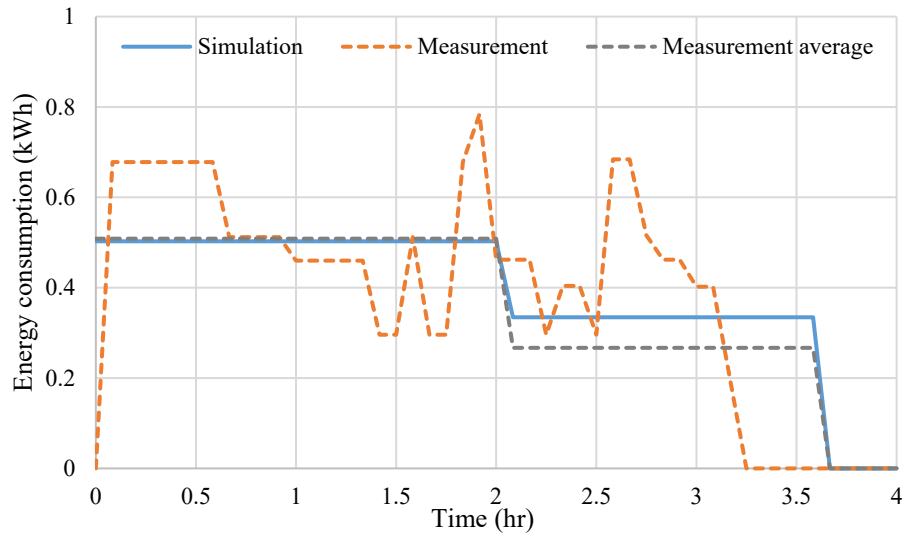


Figure 4.1: Exemplary comparison of energy consumption profile between measurement data and simulation results

This fundamental mechanism difference between simulation and experiments inhibits reasonable comparison of data in terms of hourly energy consumption. Besides, the SLC system goes through day-by-day learning; thus, it functions on a daily basis. Therefore, it is reasonable to regard the overall daily energy consumption as a cycle to validate the TRNSYS-MATLAB model.

A closer look at Table 3.3 can be helpful to better evaluate these criteria at the daily level. The requirement values are lower for monthly level as compared to hourly ones. The reason is that sudden changes of values can be smoothed over the course of a month. Overall, for validation, it is expected that the daily values at least fall between hourly and monthly requirements. Table 4.1 shows the NMBE and CVRMSE values for both stages at the daily level. The NMBE values of these two stages are desirably lower than the monthly criteria of the standards, indicating the validity of the model based on this criterion. Moreover, the CVRMSE values suitably lie between monthly and hourly requirements. Therefore, the model can be considered as validated in terms of both NMBE and CVRMSE criteria.

Table 4.1: Energy validation results

Time stage	NMBE_{daily} (%)	CVRMSE_{daily} (%)
First stage (Jan. 1 – Jan. 14)	1.02	20.80
Second stage (Feb. 1 – Feb. 15)	3.34	12.95

Table 4.2 compares the total energy consumption between measurement and simulation. Overall, there is an acceptable agreement between the measurement data and simulation results in both stages. According to the deviation values in Table 4.2, the prediction accuracy of the TRNSYS-MATLAB model can be validated in terms of accumulated energy consumption.

Table 4.2: Total energy consumption and deviations for the two stages

Items	First stage	Second stage
Measurement (kWh)	1,276	1,292
Simulation (kWh)	1,261	1,305
Deviation (%)	1.02	1.01

4.1.1.2. Temperature validation

To the best of the authors' knowledge, there is no standard criterion for temperature validation. Nevertheless, Table 4.3 tabulates the values of the two criteria for both stages. For the first stage, the values of NMBE and CVRMSE for B4 (i.e. the bathroom) are 6.6% and 14.6%, respectively. The reason is that in the bathroom, the occupancy behaviors (such as showers) cannot be considered in the TRNSYS-MATLAB model. Aside from this room, the average values of NMBE and CVRMSE for both stages are lower than 10%; therefore, the model can be considered to be validated in terms of temperature.

Table 4.3: Temperature validation results

Room	First stage		Second stage	
	NMBE_{daily} (%)	CVRMSE_{daily} (%)	NMBE_{daily} (%)	CVRMSE_{daily} (%)
B1 (living room)	4.35	7.26	3.17	3.68
B2 (bed room)	4.87	8.45	0.44	2.76
B3 (bed room)	4.54	7.58	1.46	2.87
B4 (bathroom)	6.60	14.61	-5.29	4.59
B5 (laundry room)	4.39	7.06	-4.87	4.00
Average	4.27	6.92	-0.53	2.44

4.1.2. TASK A.2: STUDY OF THE PEAK SHIFTING POTENTIAL, THERMAL COMFORT AND COST SAVING FOR THE BASEMENT

4.1.2.1. Electricity price: CPP

To simulate the energy consumption of the reference case (without the SLC system), the TRNSYS model was used with a constant set-point temperature of 21.5°C. For the SLC system, the validated TRNSYS-MATLAB model was used. The energy consumption and the heating costs are compared to show how much saving in the critical days as well as the whole winter (i.e. Dec. 1, 2017 to Mar. 31, 2018) could be achieved.

Energy consumption and peak shifting potential in Quebec

Figure 4.2a compares the energy consumption in different periods among the cases during the critical days. Note that **Case Q-Ref** and **Case Q-NoSLC** have the same energy consumption profile as they both use a constant set-point temperature. Consequently, their difference is in terms of pricing which would be discussed later in this section (cost analysis part). According to the figure, **Case Q-SLC** consumed about 6% more energy compared with **Case Q-Ref**. The reason why these cases consumed more energy than the reference case would be presented in this section (indoor temperature part). Note that despite higher energy consumption, case Q-SLC-10°C and Case Q-SLC-5°C achieved a peak shifting potential of 98.1% and 99.8%, respectively.

From the energy supplier point of view, the peak shave potential (PSP) in terms of power can be defined as (Olsthoorn et al., 2019):

$$PSP = \frac{\sum_{n=1}^N (P_{Ref,n} - P_{SLC,n})}{N} \quad (8)$$

where $P_{ref,n}$ and $P_{SLC,n}$ are the basement power consumption of the reference case and the case with SLC system (see Figure 4.2b) at time n , respectively and N is the total number of time steps in the peak period. Therefore, PSP is the average peak load shave, which for both Case Q-SLC-5°C and Case Q-SLC-10°C, the PSP during first and second peak periods were approximately 5 kW and 4kW, respectively.

Further inference from Figure 4.2a and b is that the energy consumed by EHF when operated under **Case Q-SLC-5°C** is lesser during the first off-peak period (20:00 – 06:00) and relatively higher in the second off-peak period (9:00 – 16:00) compared to **Case Q-SLC-10°C**. This is because, the latter estimated the load by considering the wider temperature range (10°C interval), while in the former, 5°C intervals were considered for the temperature category. For clear explanation, the following example is presented. Consider two days with half-daily forecast minimum exterior temperature as -27°C/-18°C for the first day and -23°C/-18°C for the second. In these two days, -27°C and -23°C belong to the same temperature category (i.e. [-30° -20°]) in **Case Q-SLC-10°C**. In this case, to maintain the thermal comfort, more/excess energy is stored during the first off peak period compared to the second off peak period. However, in **Case Q-SLC-5°C**, -27°C and -23°C belong to different temperature categories. Hence more specific load values (i.e. relatively lesser energy will be stored for -23°C than -27°C) are predicted for these two temperatures. Since, the energy storage in the first off peak period depends strongly on the temperature category (elaborated further in Section 4.1.2.2) and no excess amount of energy is stored in the **Case Q-SLC-5°C**, the additionally required energy to maintain the thermal comfort during the second peak period is stored during the second off-peak period for **Case Q-SLC-5°C** resulting in higher energy consumption compared to **Case Q-SLC-10°C**.

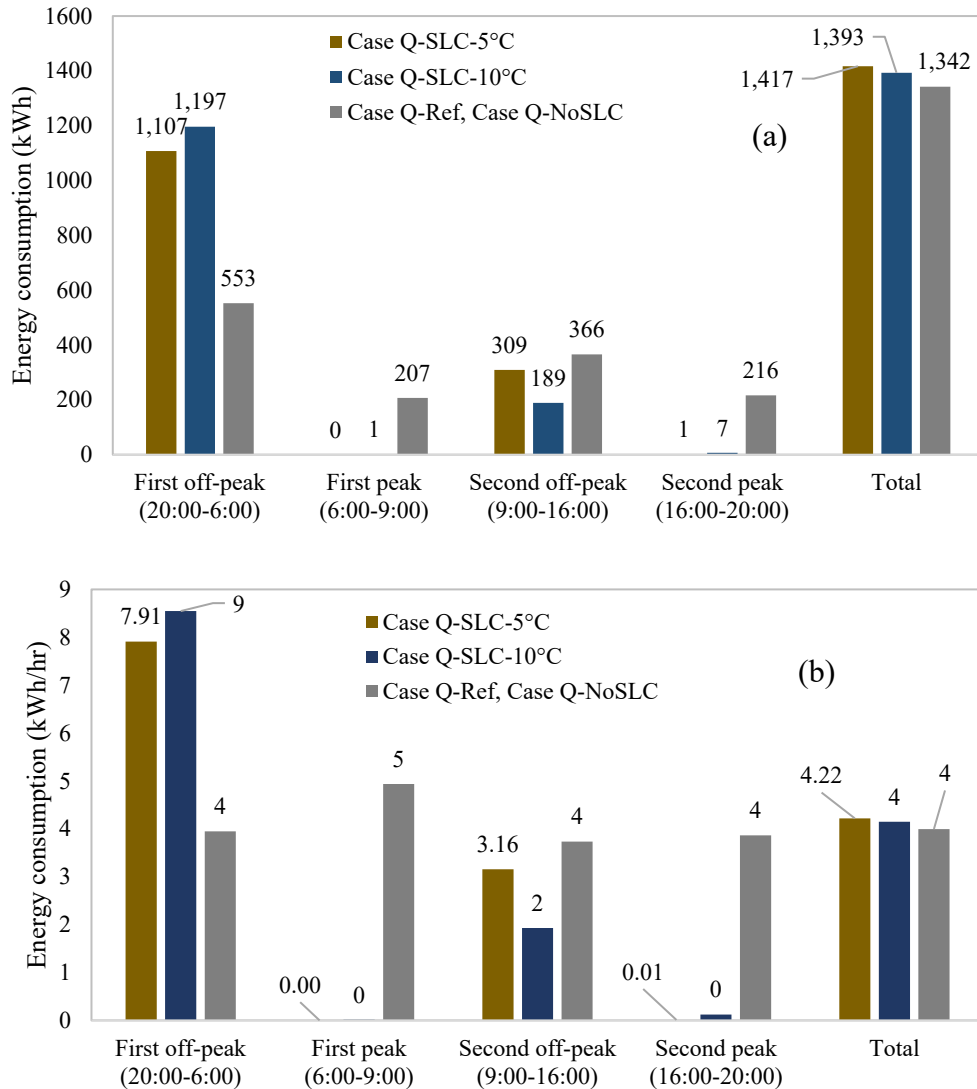


Figure 4.2: Comparison of (a) energy consumption and (b) average power consumption among the cases for Quebec during critical days

Indoor temperature

Figure 4.3 compares the average basement indoor temperature during the critical days among the considered cases. Note that a constant set-point temperature (i.e. 21.5°C) was used in non-critical days. Again, **Case Q-Ref** and **Case Q-NoSLC** have the same profile due to similar energy consumption characteristics. It can be seen from the figure that the indoor air temperature swing of **Case Q-SLC-10°C** and **Case Q-SLC-5°C** were within the range of 21.5 – 23°C and 22.5

- 23.5°C, respectively, which means the SLC system could maintain thermal comfort all the time. The average indoor air temperature of **Case Q-Ref** was almost the same as its set-point temperature (i.e. 21.5°C), which indicates meeting thermal comfort. According to the figure, the temperature of **Case Q-SLC-10°C** and **Case Q-SLC-5°C** are generally higher than **Case Q-Ref**, which is the main reason why the total energy consumption of the SLC system was higher than the reference case.

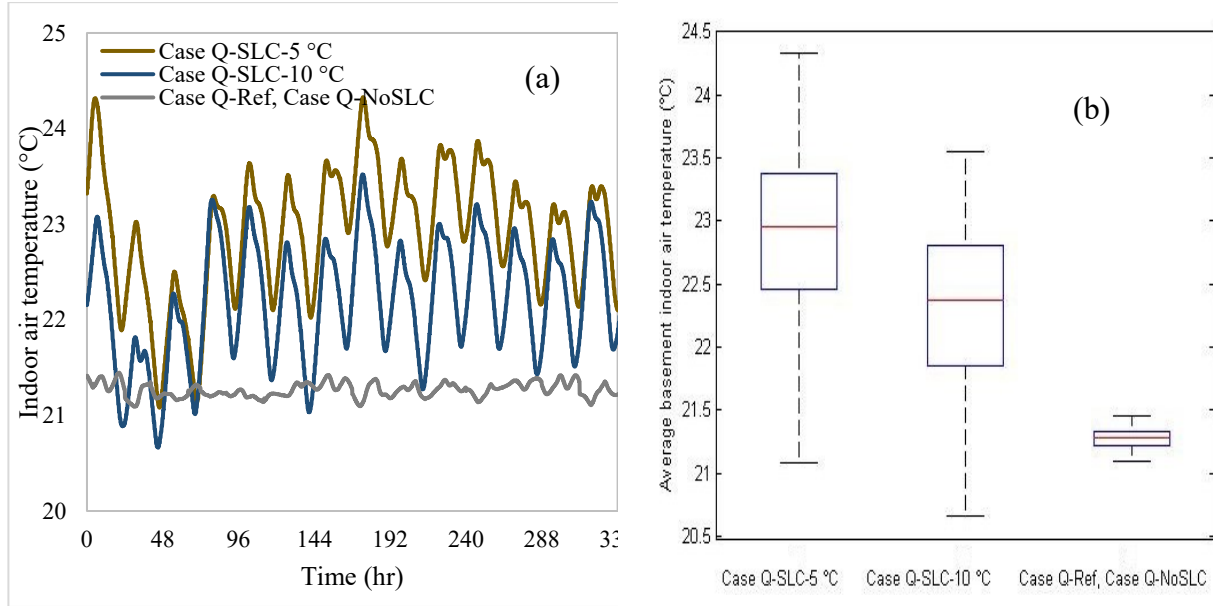


Figure 4.3: Comparison of the average indoor air temperature among the cases for Quebec during critical days (a) real variation and (b) box plot

To guarantee the thermal comfort, the frequency of poor thermal comfort (PTC) occasions by the SLC system was evaluated using:

$$PTC(\%) = \frac{\sum_k t_k w_k}{D} \times 100 \quad (9)$$

where t is the duration of poor thermal comfort (indoor air temperature lower than 21°C or higher than 25°C (Schiavon et al., 2014)), k is the number of the room, w is the volumetric weight ratio of the rooms and D is the total duration of critical days (i.e. 336 hours).

Based on Equation (9), the frequency of PTC is 0%, 0% and 4.9% for **Case Q-Ref**, **Case Q-SLC-5°C** and **Case Q-SLC-10°C**, respectively. This indicates the SLC system can maintain the thermal comfort where **Case Q-SLC-5°C** had a better performance.

Cost analysis

Table 4.4 shows the details of electricity pricing in Quebec. Note that according to Table 3.4, the heating cost of **Case Q-Ref** is evaluated based on the FRP tariff (i.e. Rate D), while for the other cases the CPP tariff (i.e. Rate DPC) was used. Figure 4.4 compares the heating cost among the cases during the critical days. According to the figure, the total heating cost for **Case Q-SLC-5°C** and **Case Q-SLC-10°C** are lower than **Case Q-Ref**, which means a saving of 23.4% and 18.9%, respectively. However, compared to **Case Q-NoSLC**, the SLC system can save heating cost by 64.3% and 62.1%, respectively. Moreover, **Case Q-SLC-5°C** could additionally save 5.99% more than **Case Q-SLC-10°C**.

Table 4.4: Electricity pricing in Quebec ("Residential rates," 2018)

Period	Condition	CPP tariff (Rate DPC)		FRP tariff (Rate D)
		Peak	Off-peak	Constant rating
Electricity price (¢/kWh)	< 40 kWh/per day	50	3.98	6.07
Electricity price (¢/kWh)	> 40 kWh/per day	50	7.03	9.38
Subscription fee (¢/day) *	-		40.64	

* Charged per day irrespective of the actual energy consumption

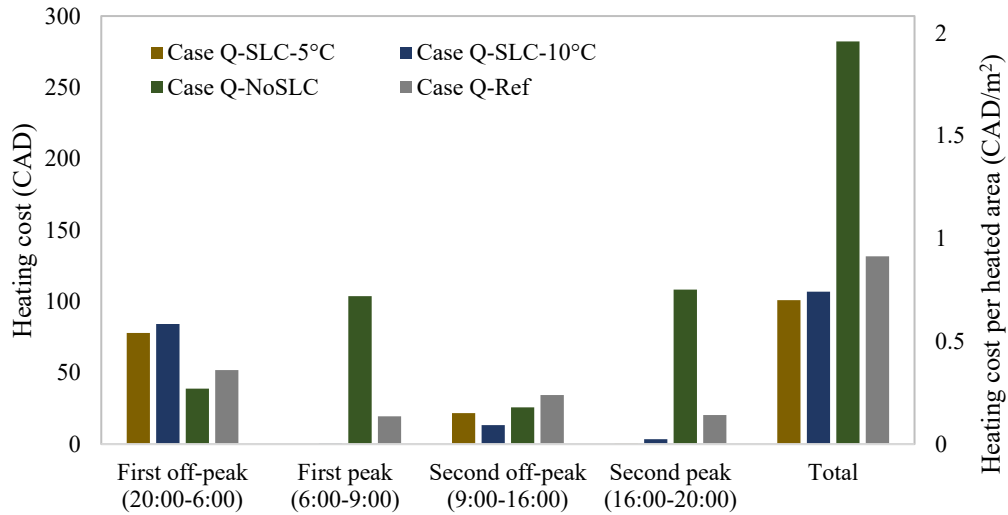


Figure 4.4: Comparison of the heating cost among the cases for Quebec during critical days

For the entire winter (Dec. 1, 2017 to Mar. 31, 2018), Figure 4.5 compares the heating cost among the considered cases. For **Case Q-SLC-5°C** and **Case Q-SLC-10°C**, the total heating cost is lower than **Case Q-Ref**, achieving savings of 23.6% and 22.8%, respectively. Moreover, compared to **Case Q-NoSLC**, they can also save 21.4% and 20.8%, respectively in the heating cost. Overall, **Case Q-SLC-5°C** is the best option to decrease the heating costs in CPP.

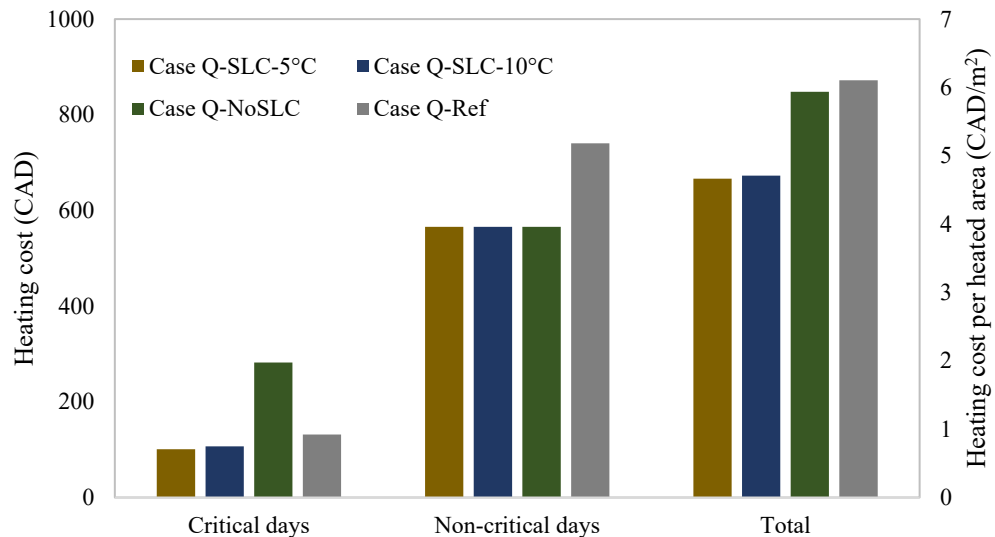


Figure 4.5: Comparison of the total heating cost among the cases for Quebec during the entire winter

For the CPP tariff of Quebec, two prediction methods with different temperature categories have been compared in terms of peak shifting potential, thermal comfort and heating cost saving with a reference case and also without SLC. It was found that during the critical days, although the SLC strategy (i.e. **Case Q-SLC-5°C**) required about 5.5% more heating than the other cases, the heating cost could still be reduced. The comparison results show that the peak shifting potential, thermal comfort and heating cost saving potential is better for **Case Q-SLC-5°C** as the temperature category. For this case, heating cost saving of 64.3% (i.e. \$12.9 per day) and 23.4% (i.e. \$2.20 per day) was achieved compared to **Case Q-NoSLC** and **Case Q-Ref**, respectively.

4.1.2.2. Electricity price: TOU

The peak shifting potential and economic advantages of the SLC system are investigated for the TOU tariff setting in Ontario. The simulation period was from Jan. 1 to Apr. 30, 2018.

Energy consumption and peak shifting potential in Ontario

Figure 4.6a depicts the comparison of the energy consumption between the cases for Ontario. The inference from the figure is that **Case O-SLC** consumed about 12% more energy compared with **Case O-NoSLC** (for the same reasons as mentioned for Quebec cases). Nevertheless, **Case O-SLC** achieved a peak shifting of 97.6%. Figure 4.6b depicts that the peak shifting potential of Case O-SLC during the first and second peak periods compared to Case O-NoSLC are 3.0 kW and 2.9 kW, respectively.

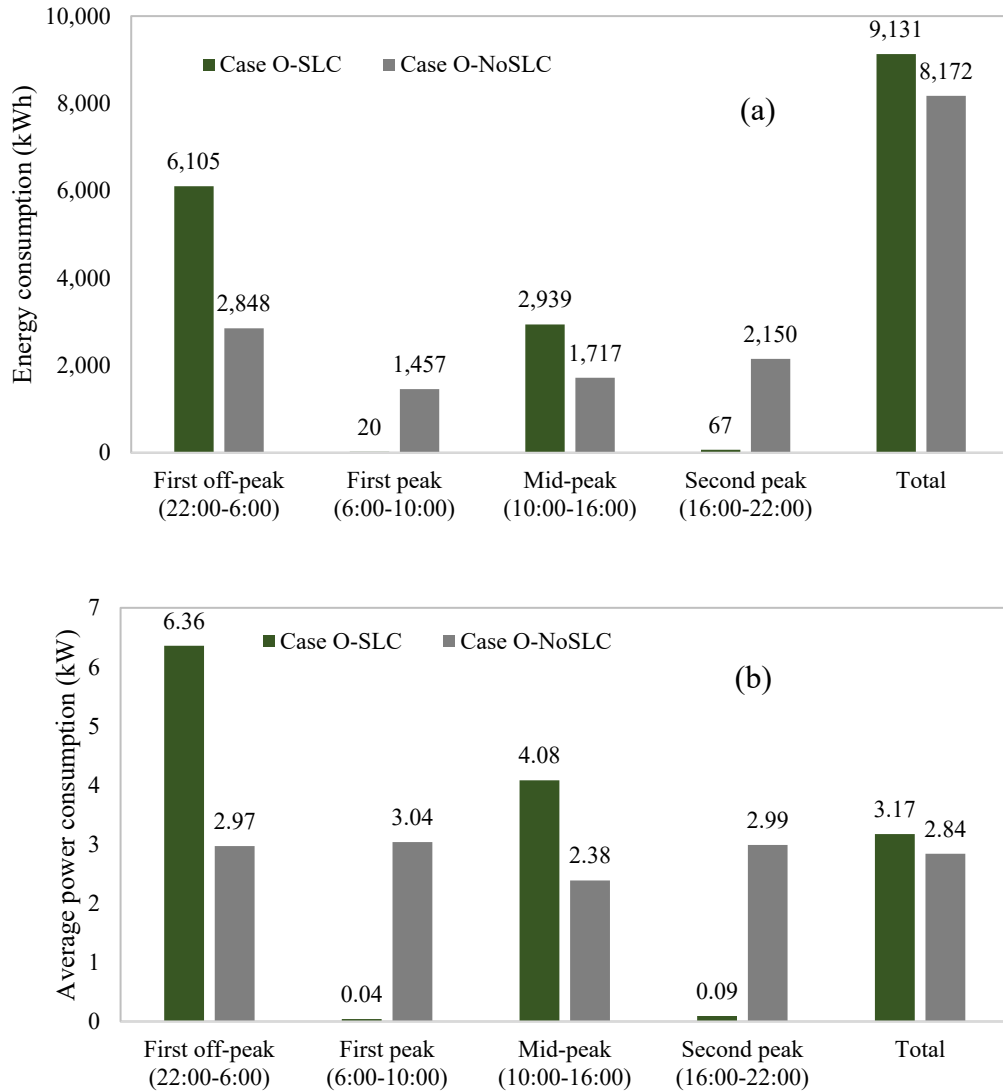


Figure 4.6: Comparison of (a) energy consumption and (b) average power consumption between the cases for Ontario during the entire winter

Indoor air temperature

Figure 4.7 depicts the indoor air temperature in different rooms for **Case O-SLC** during the simulated 120 days. The indoor room air temperatures are close, fluctuating within a proper temperature range (21 – 25°C) for most of the time (Schiavon et al., 2014). Based on Equation (9),

the frequency of PTC is 4.3% for the total simulation time (i.e. 2880 hours), which means the SLC could main the thermal comfort.

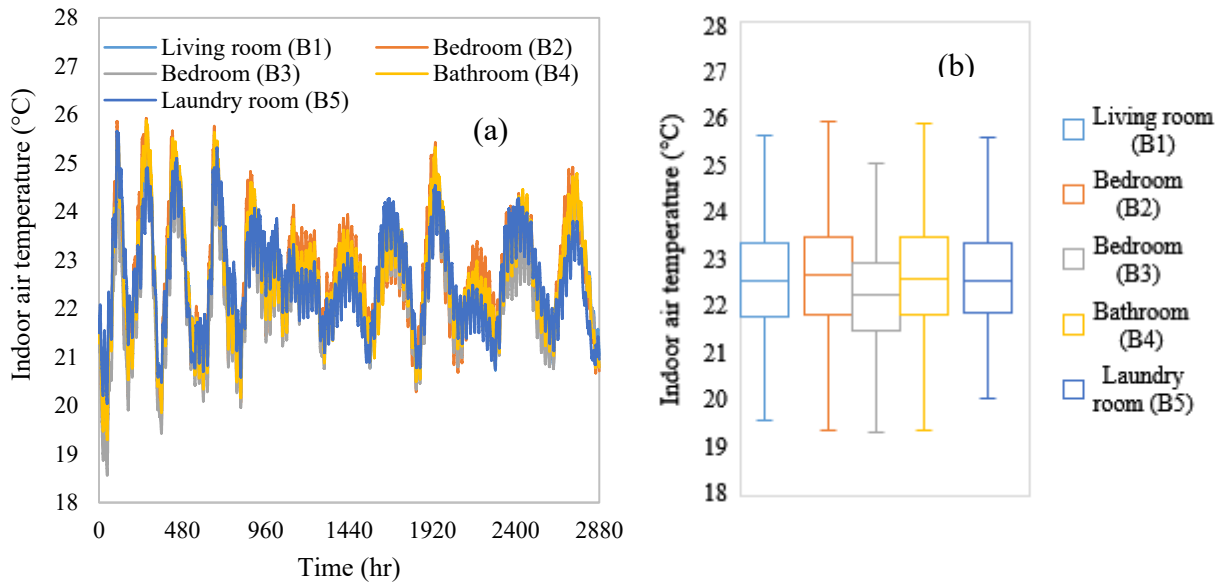


Figure 4.7: Indoor air temperature in different rooms using Case O-SLC for Ontario during the entire winter

Cost saving

Details of the TOU electricity pricing in Ontario are shown in Table 4.5. Figure 4.8 shows the comparison of the total heating cost between **Case O-SLC** and **Case O-NoSLC** from Jan. 1 to Apr. 30, 2018. Compared to **Case O-NoSLC**, **Case O-SLC** can save about 16.9%. Overall, the cost saving of the SLC system under Ontario TOU pricing is lower than Quebec (i.e. **Case Q-SLC-10°C**). The reason is that the TOU electricity pricing includes a mid-peak period (the gray portion in Figure 3.6b) having higher electricity price than the off-peak period in Quebec (the black portion in Figure 3.6a).

Table 4.5: TOU electricity pricing in Ontario (HydroOne 2017)

Price	Peak period	Mid-peak period	Off-peak period
During weekdays (¢/kWh)	18	13.2	8.7
During weekends (¢/kWh)	8.7	8.7	8.7

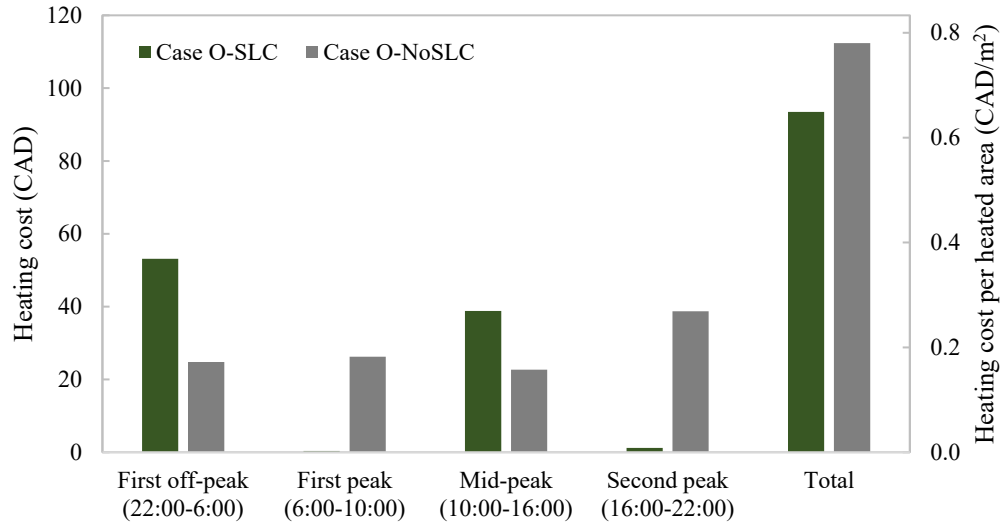


Figure 4.8: Comparison of the total heating cost between the cases for Ontario during the entire winter

SLC performance analysis

Unlike CPP, the SLC system with TOU setting is always in operation during the entire winter. Consequently, it covers a wide range of outdoor temperatures. For the period from Jan. 1 to Apr. 30, 2018, the outdoor temperature varied in the range of $[-30, 10^{\circ}\text{C}]$. Note that the SLC system operates based on half-daily outdoor temperature categories in 10°C intervals. Consequently, a total of 16 combinations are possible for the half-daily temperature categories; however, some combinations never occurred. Figure 4.9 shows the energy consumption results and peak load shaving for the 120 days (i.e. Jan. 1 to Apr. 30, 2018) according to the half-daily outdoor temperature categories. For each first half-daily (noted by morning) temperature category, the x-axis shows the second half-daily (noted by evening) temperature category, the y-axis shows the peak load shaving and the bubble size (values indicated at the center of each bubble) demonstrates the energy consumption (in kWh). The figure shows that as the exterior temperature increases, the bubble size (i.e. the energy consumption) decreases, which is expected. Another inference from the figure is that for the extreme cold outdoor temperature, the peak shifting potential is lesser compared to the higher exterior temperatures. The main reason is that as exterior temperature increases, the heat loss from the storage decreases and subsequently, the storage can cover more load (store more thermal energy) during the peak hours.

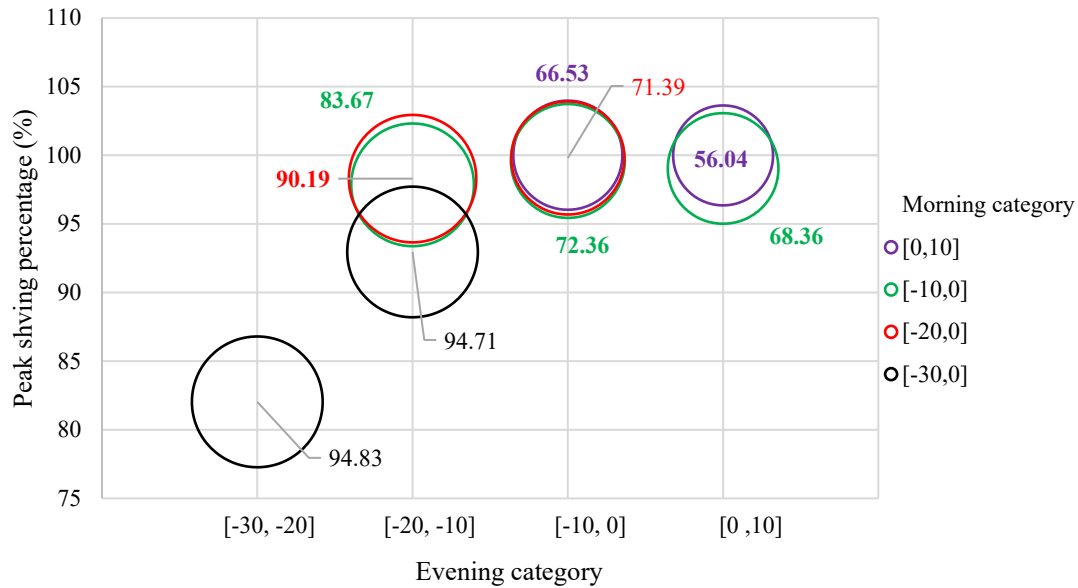


Figure 4.9: Energy consumption and peak energy shaving potential of the SLC system under different temperature categories

Figure 4.10 shows the heating cost saving potential of **Case O-SLC** compared with **Case O-NoSLC**. The x-axis of the figure is the same as Figure 4.9 while the y-axis is the heating cost saving potential and the size of each bubble is the average daily heating cost in CAD (values are shown at the center of each bubble) using the SLC system. According to the figure, for each morning category, as the evening temperature categories get warmer, the bubble size (i.e. total heating cost) becomes smaller, while lower heating cost saving is achieved. The reason is that for **Case O-NoSLC** (i.e. the basis for heating cost saving calculation) energy consumption continues during peak periods (see Figure 4.6); however, for higher exterior temperatures, the energy consumption reduces, resulting in a decreasing heating cost saving potential (from about 30% down to 5%). The trend in this figure can be simply understood when considering two factors. First, the number of occurrences for each temperature category, which helps the learning process in the SLC system towards better control. This can be seen in Figure 4.11 where the y-axis is the power consumption during peak (solid bubbles) and mid peak (dashed bubbles) periods and the bubble sizes indicate the number of occurrences. Second, the performance of thermal energy

storage system depends on outdoor air temperature. For very cold outdoor air temperatures though heat energy is stored during the off-peak periods, the stored heat would not be sufficient to meet the entire heating demand during the peak period. On the other hand, as the exterior temperature increases, the peak shifting potential can be achieved at almost 100%, however the heating cost saving potential is lesser during these days. In overall, the best performance in Figure 4.10 is achieved for the lowest temperature categories, indirectly indicating more cost efficiency under CPP tariff of Quebec.

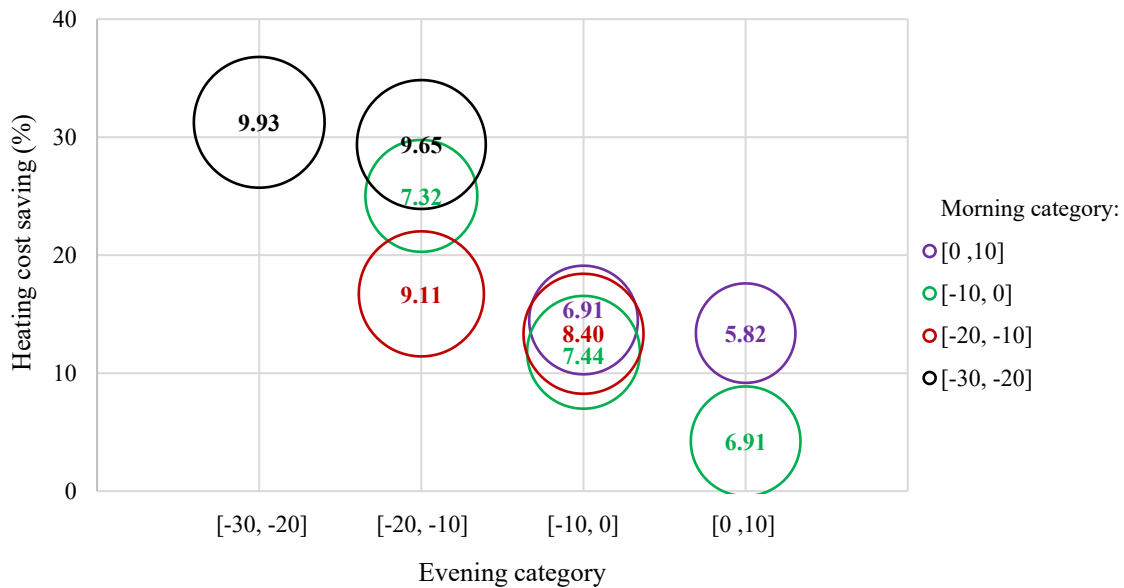


Figure 4.10: Heating cost saving potential of Case O-SLC compared to Case O-NoSLC

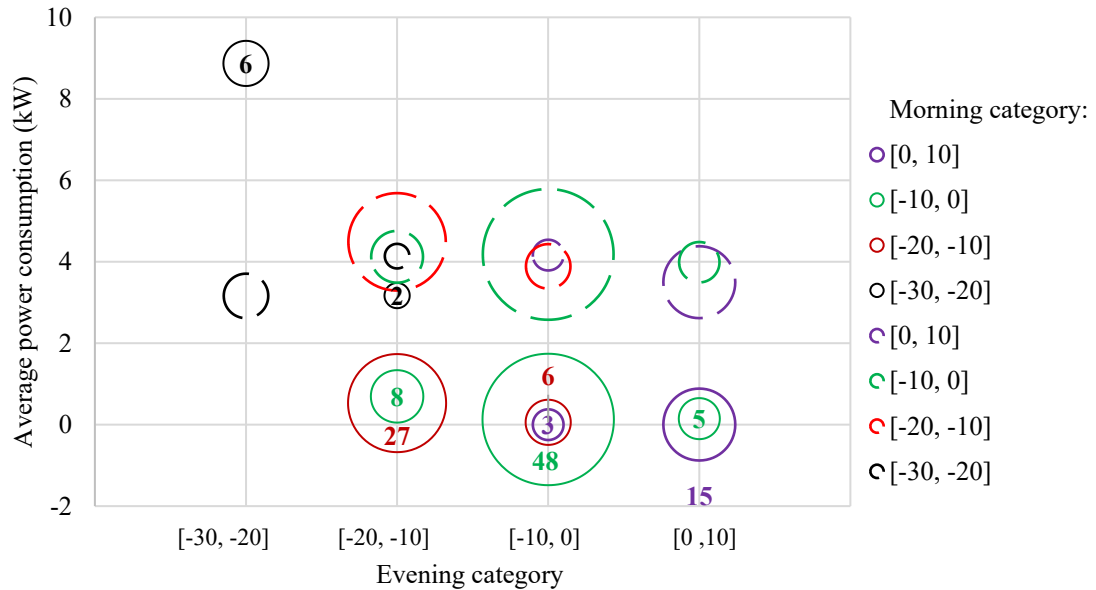


Figure 4.11: Peak power consumption for each temperature category depending on the occurrence

4.2.TASK B: EXTEND PEAK SHIFTING INVESTIGATION FOR THE WHOLE HOUSE WITH DIFFERENT CONTROL STRATEGIES

4.2.1. TASK B.1 PARAMETRIC STUDY OF THE FLOOR SURFACE UPPER LIMIT TEMPERATURE

An upper limit for floor surface temperature can be set to guarantee the thermal comfort by easing the overshoot for the EHF charging time. Regarding the upper limit for floor surface temperature, five various setpoints from 26 to 28 °C were selected (Olesen, 2002; Olesen & Brager, 2004) (as shown in the x axis of Figure 4.12). Due to the delay in thermal response of the concrete, 28 °C was the highest setting value for the upper limit. Figure 4.12 presents the average discomfort hours for indoor air temperature (i.e. in the range of 21-25 °C (Schiavon et al., 2014; Standard, 2013)) for these five upper limits for floor surface temperature. Note that the acceptable thermal comfort temperature range for floor surface temperature could be selected as 19-29 °C (Standard, 2004). The inference from the figure is that the lower upper limit floor surface temperatures acted as a barrier, limiting the amount of energy storage, which in turn caused poor thermal comfort. On the other hand, higher upper limit floor surface temperatures lead to the overshoot in the indoor

air temperature after the charging period, which also caused the poor thermal comfort. Consequently, in this study, 27 °C was selected as the floor surface upper limit temperature due to the frequency of the PTC by Equation (9).

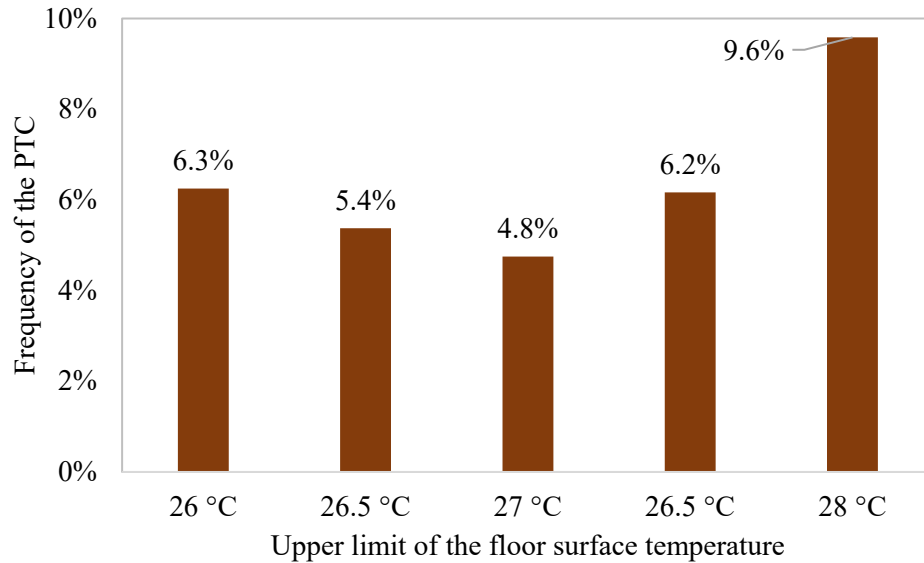


Figure 4.12: Frequency of the PTC for different floor surface upper limit temperatures

4.2.2. TASK B.3 COMPARISON RESULTS AMONG THESE CASES

Since the building's ground floor was not affected in the considered cases, its control strategy was maintained at the CSP, while the peak shifting control strategies were investigated in the basement and second floor. Consequently, the ground floor was set at 21.5 °C throughout the day in all simulations.

4.2.2.1. Peak shifting potential

Figure 4.13 compares the cases in terms of the average power consumption during each period per day. Regarding the peak power, peak shifting control strategies (i.e. Cases 1-6) can decrease the power by about 4.5 kW (which were about 9.7 kW and 8.4 kW during two peak periods, respectively in Reference case) during both peak periods. However, without prediction of next day's energy consumption, Case 1 consumed more energy during the second off-peak period than Reference case. The reason is that the energy storage during the first off-peak period was not

sufficient to meet the demand. Meanwhile, to achieve better peak shifting using SLC, higher amounts of energy were stored during the first off-peak (i.e. above 14 kW). Furthermore, comparing Case 6 with other cases under peak shifting control strategies, less energy has been consumed in both peak periods. Without upper limit setting, more energy can be stored during the first off-peak period, which leads to lower energy consumption during the peak periods.

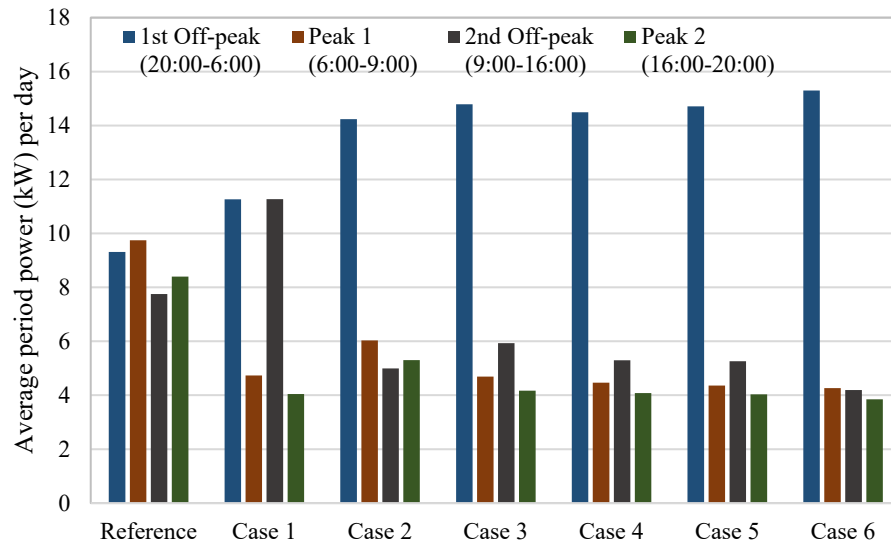


Figure 4.13: Comparison of average demand per period per day for the different cases

Figure 4.14 presents the peak shifting of the basement and second floor among the cases compared with Reference case. Note that in Case 2, the peak shifting was considered only in the basement, which leads to zero percentage for peak shifting in the second floor. In the basement, the RBC (i.e. Case 1) could achieve performance levels in peak shifting as great as the SLC (i.e. Case 2-6), both above 97%. Case 1 and Case 3 had preheating using RBC to store energy in the building thermal mass to extend the peak shifting in the second floor, achieving around 45% peak shifting.

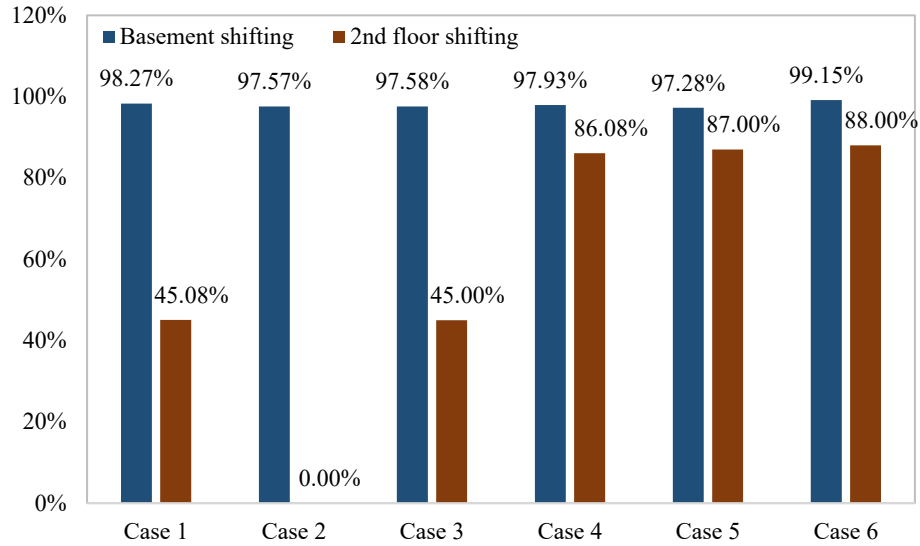


Figure 4.14: Peak shifting potential (%) of different cases in the second floor and basement

In Cases 4-6, better peak shifting results (i.e. more than 86%) were obtained. Meanwhile, for Case 6, the peak shifting potential can increase at 1.87% in the basement and 1.92% in the second floor compared to Cases 4 and 5. Guaranteeing the complete charging is the vital reason. Among the cases with the SLC system with upper limit (Cases 2-5), setting the upper limit influenced the peak shifting. The reason is that when the floor surface temperature gets higher than 27 °C during the charging period, the EHF is turned OFF immediately. Hence, during the peak period the stored energy is not sufficient to maintain the thermal comfort and the EHF would have to operate during the peak period.

In CPP, the electricity price of the second off-peak is the same as the first off-peak period (see Figure 3.6a); however, load shifting from the second off-peak is beneficial. The reason is that the stress on the grid (from the supply side viewpoint) is higher during the second off-peak period, meaning it is prone to become a new peak if peak shifting is not conducted with caution. Figure 4.15 shows the energy shifting potential during the second off-peak period for all the cases compared to Reference case. Case 1 (using RBC) not only cannot decrease the energy consumption during this period, but also consumed 1.5 time higher than Reference case. Case 3 used the RBC in the second floor, which also decreased the second off-peak shifting (7% lower than the SLC

cases). Hence, RBC may cause creating a new peak within the second off-peak period. Indeed, Cases 1 and 3 cannot be considered as reasonable options. Case 2 has the second better performance in terms of load shifting potential during the second off-peak period, but it only focused on the basement. On the other hand, if these two scenarios (i.e. setting upper limit and fan easing overshoot) are used to guarantee the thermal comfort (Case 5), the energy shaved in peak period (Figure 4.14) and 2nd off-peak period (Figure 4.15) cannot get the good performance. Overall, Case 6 is regarded as a proper control strategy in minimizing energy consumption during this period. This could be achieved by fan operation in the proper time during the off-peak period, storing sufficient energy in the basement.

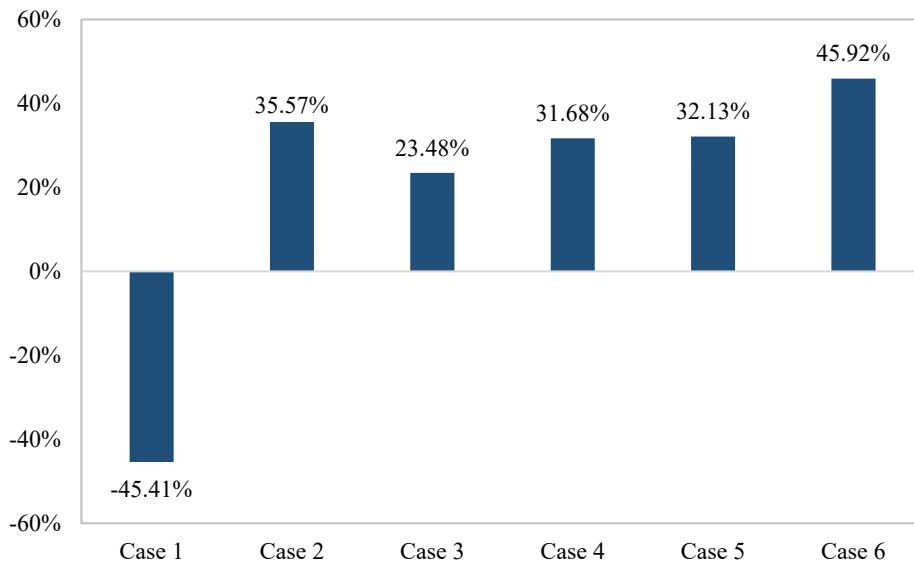


Figure 4.15: Energy shifting potential (%) of different cases during 2nd off-peak period (10:00-16:00)

4.2.2.2. Thermal comfort

Figure 4.16a and Figure 4.16b show the variation of average temperature based on the volumetric weight ratio of the rooms for the basement and second floor, respectively. Regarding RBC, Figure 4.16a shows that Case 1 had lesser temperature swing than the other cases in the basement. Since the RBC required preheating in the second floor, Cases 1 and 3 had wider temperature range than the SLC cases in Figure 4.16b. On the other hand, among SLC cases, Case 6 was the only one to guarantee the thermal comfort without setting upper limit. The reason is that

in Case 6 warm air was transferred to the second floor during the off peak hours for preheating. Hence, indoor air temperature in Case 6 was a little higher than other SLC with fan cases (Cases 4 and 5) in Figure 4.16b. This partial energy did not cause thermal discomfort in the basement, but it was desirably used to preheat the second floor, increasing the peak shifting potential (by 1-2% in Figure 4.14).

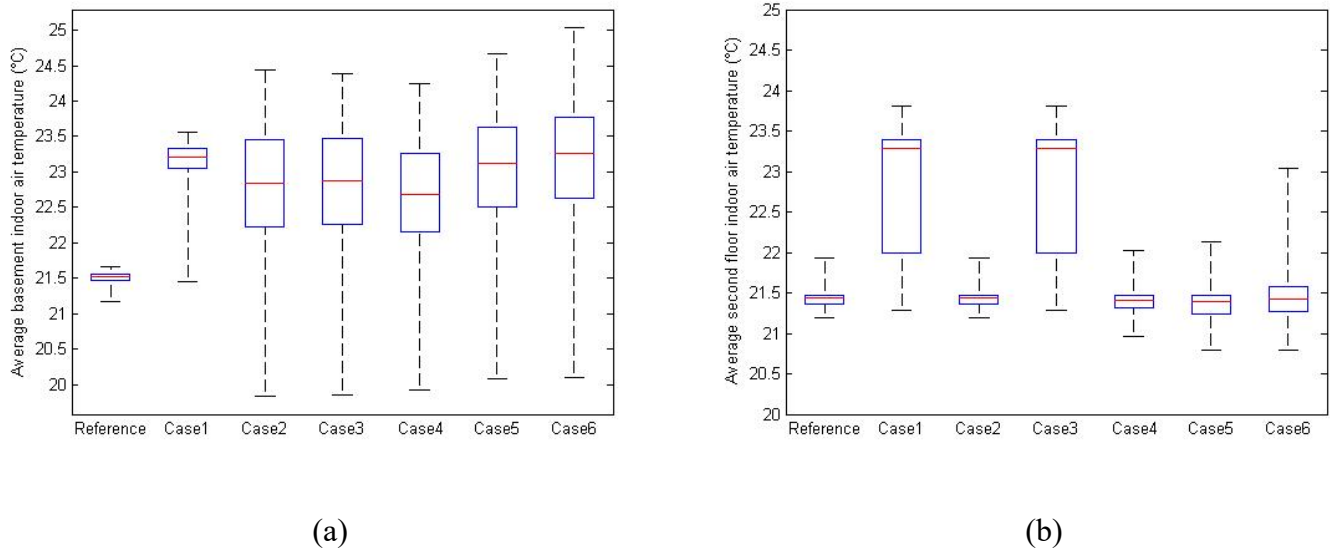


Figure 4.16: Average indoor air temperature for different cases in (a) the basement and (b) the second floor

Figure 4.17 shows the thermal comfort potential among the cases according to Equation (9). Even for the worst case, the thermal comfort percentage is higher than 97.5%, which can indicate that peak shifting control could maintain the thermal comfort. Overall, Case 6 is the best option with lower poor thermal comfort percentages.

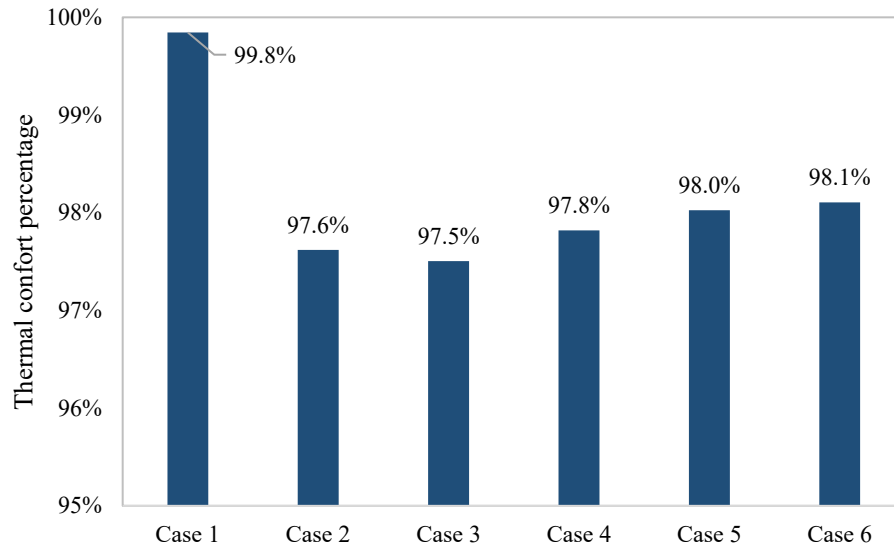


Figure 4.17: Comparison of thermal comfort potential among the cases

4.2.2.3. Cost saving

Table 4.4 shows the details of electricity pricing in Quebec. Figure 4.18 shows the comparison of the total heating cost among the cases. Note that, heating cost saving of all these cases has been calculated by comparing to Reference case. According to the figure, Case 2 which used SLC only for peak shifting in the basement, could save lesser (around 8-14%) than the other cases. Cases 4-6 used a fan, achieving better performance than Case 1 (under RBC) and Case 3 (under HCS). Hence, SLC can get better performance in cost saving (i.e. higher around 2-4%) than other cases. Comparing the cases of SLC with fan controller (i.e. Cases 4-6), Case 6 is regarded as the best options with higher cost saving (i.e. higher around 2%) than Cases 4 and 5. In Case 6, complete charging is the most important factor to have lower heating cost saving than other SLC cases.

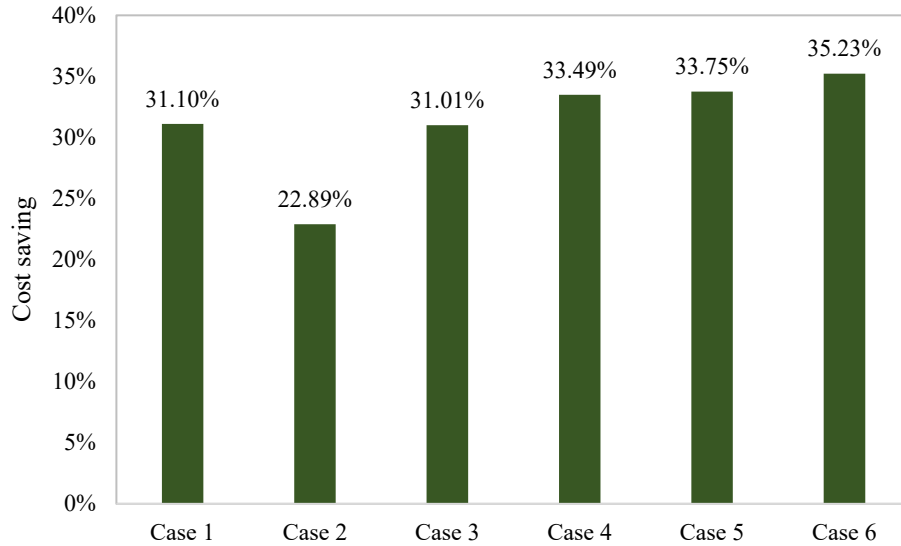


Figure 4.18: Comparison of the total heating cost savings for different these cases

4.3.TASK C: RESULTS FOR PARAMETRIC STUDY BY TAGUCHI METHOD

4.3.1. TASK C.1: ANALYSIS FOR THE OUTPUT RESULTS

4.3.1.1. Simulation results according to the Taguchi design

Regarding Table 4.6 summarizes all the output values as well as their corresponding S/N ratios. For instance, regarding the simulation one (the first row), these five factors are selected in the level one. Considering these three outputs with other simulation results: the peak power (R_1) is higher and the thermal comfort (R_2) is poorer while the capital cost (R_3) is lower. This indicated the lower capital cost (R_3) can decrease investment, which also caused the thinner insulation and concrete. The thinner insulation and concrete cannot achieve the peak shifting well and maintain the thermal comfort. Consequently, these three objectives should be analyzed to propose a trade-off suggestion in the following sections.

In addition, the data in these tables were used to conduct the analysis whose results are presented in the next sections. The output values in Table 4.6 have been used to generate S/N main

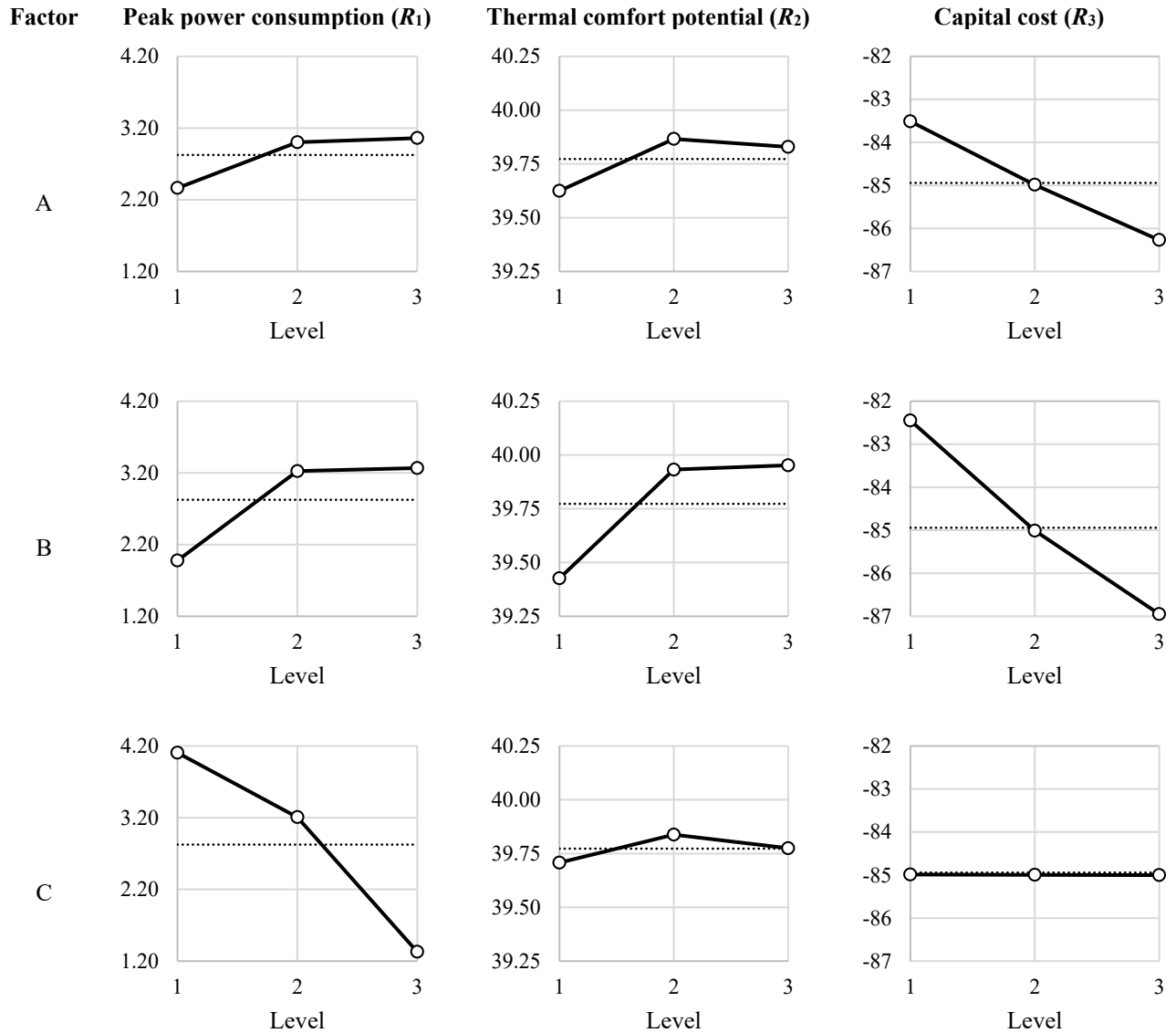
effect plots as shown in Figure 4.19. Figure 4.19 shows S/N ratio main effect plots from the level 1 to level 3 among these five factors.

Table 4.6: The responses and their corresponding signal-to-noise ratio for each simulation in Table 3.6

#	Factors					Peak power consumption (R_1)		Thermal comfort potential (R_2)		Capital cost (R_3)	
	A	B	C	D	E	Response 1 (kW)	S/N 1	Response 2 (%)	S/N 2	Response 3 (\$)	S/N 3
1	1	1	1	1	1	0.79	2.08	89.04	38.99	10,452	-80.38
2	1	1	1	1	2	0.75	2.46	90.57	39.14	10,452	-80.38
3	1	1	1	1	3	0.74	2.60	91.31	39.21	10,452	-80.38
4	1	2	2	2	1	0.71	2.99	97.91	39.82	15,012	-83.53
5	1	2	2	2	2	0.68	3.37	98.51	39.87	15,012	-83.53
6	1	2	2	2	3	0.68	3.41	98.86	39.90	15,012	-83.53
7	1	3	3	3	1	0.85	1.38	98.00	39.82	19,483	-85.79
8	1	3	3	3	2	0.83	1.58	99.36	39.94	19,483	-85.79
9	1	3	3	3	3	0.83	1.67	98.37	39.86	19,483	-85.79
10	2	1	2	3	1	0.79	2.05	94.19	39.48	13,238	-82.44
11	2	1	2	3	2	0.70	3.15	96.85	39.72	13,238	-82.44
12	2	1	2	3	3	0.69	3.17	97.39	39.77	13,238	-82.44
13	2	2	3	1	1	0.84	1.55	99.22	39.93	17,799	-85.01
14	2	2	3	1	2	0.83	1.58	99.43	39.95	17,799	-85.01
15	2	2	3	1	3	0.83	1.58	99.43	39.95	17,799	-85.01
16	2	3	1	2	1	0.58	4.66	99.87	39.99	22,226	-86.94
17	2	3	1	2	2	0.55	5.12	99.92	39.99	22,226	-86.94
18	2	3	1	2	3	0.55	5.25	99.89	39.99	22,226	-86.94
19	3	1	3	2	1	0.93	0.66	92.35	39.31	16,080	-84.13
20	3	1	3	2	2	0.89	0.99	95.22	39.57	16,080	-84.13
21	3	1	3	2	3	0.89	1.04	95.61	39.61	16,080	-84.13
22	3	2	1	3	1	0.58	4.71	99.60	39.97	20,597	-86.28
23	3	2	1	3	2	0.54	5.34	100.00	40.00	20,597	-86.28
24	3	2	1	3	3	0.52	5.69	100.00	40.00	20,597	-86.28
25	3	3	2	1	1	0.66	3.56	99.89	39.99	25,068	-87.98
26	3	3	2	1	2	0.66	3.64	99.89	39.99	25,068	-87.98
27	3	3	2	1	3	0.66	3.64	99.89	39.99	25,068	-87.98

Table 4.6 summarizes all the output values as well as their corresponding S/N ratios. For instance, in the first run (i.e. the first row), the five factors were at their lowest level (i.e. level 1).

Compared to the other runs in Table 4.6, the peak power consumption (R_1) is relatively higher, while the thermal comfort potential (R_2) and the capital cost (R_3) are relatively lower. The reason is that despite costing lower, the least thickness of insulation and concrete slab cannot achieve high peak shifting and maintain the thermal comfort.



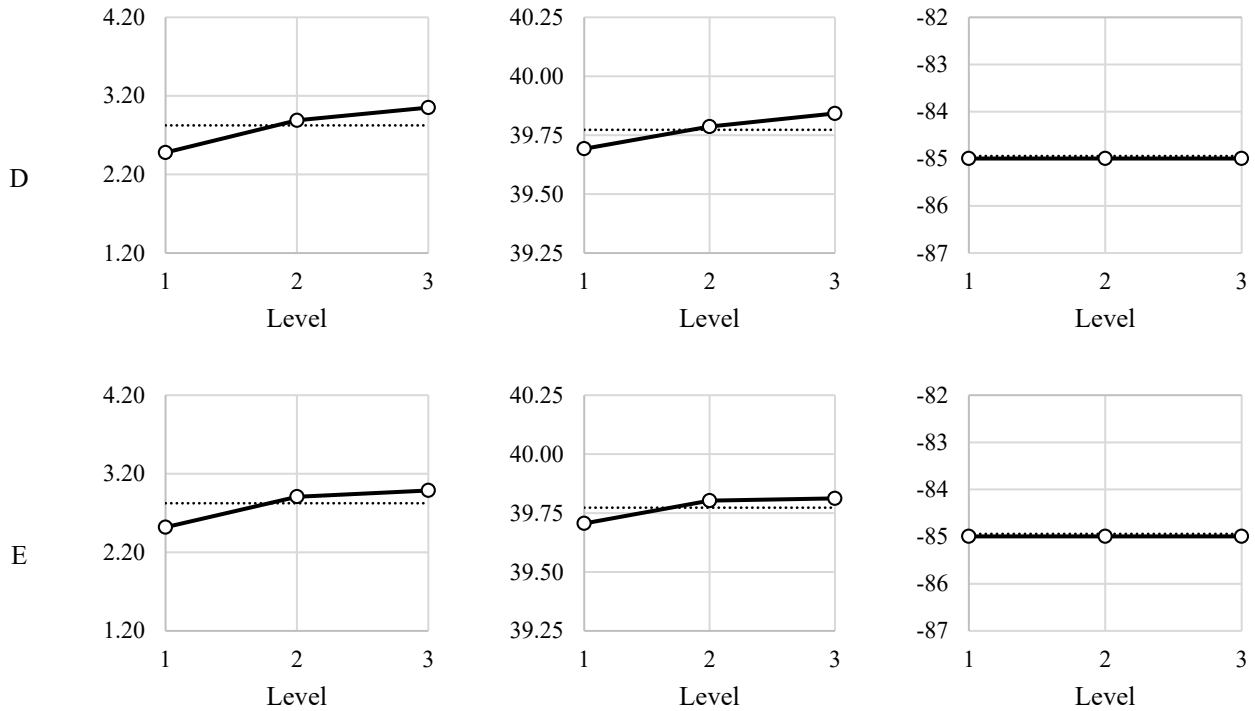


Figure 4.19: S/N ratio main effect plots of different factors and levels

Figure 4.19 can be used to analyze the effect of each factor on each response. For peak power consumption, fan flow rate (C) had the highest effect due to the highest S/N ratio. In addition, concrete slab thickness (A) and insulation thickness (B) show a small effect on average peak power consumption when they go from their second level to the third. This is an important issue which shows the capital cost should be considered. The reason is that the small effect on (i.e. reduction of) average peak power consumption is not sufficient to justify the capital cost for using thicker concrete slab and insulation. In addition, regarding the effect of concrete slab thickness on thermal comfort potential, Figure 4.19 shows that the mid value had the best performance. All these results should be considered simultaneously to be able to obtain the best condition.

4.3.1.2. Ranking of factors

The results obtained from conducting the data analysis based on Taguchi method are shown in Table 4.7. The table shows the S/N ratios for each level based on which the factors are ranked for each output. For instance, for capital cost, the insulation thickness (factor B) was ranked first

followed by concrete thickness. Note that, factors D and E (see Table 3.5 for details) were both ranked 4 as they were found insignificant compared to the other factors. The reason is that they could be achieved with no cost. As the table shows, the insulation thickness (i.e. factor B) was the most significant factor ranking highest in almost all the cases. Aside from this, a universal conclusion cannot be drawn when considering all the outputs as for instance higher peak shifting (desirable) results in higher capital cost (undesirable).

Table 4.7: S/N for factorial effects and contribution ratio

Parameter	Peak power consumption (R_1)					Thermal comfort potential (R_2)					Capital cost (R_3)				
	A	B	C	D	E	A	B	C	D	E	A	B	C	D	E
S/N ratio – Level 1	2.36	1.98	4.11	2.48	2.52	39.62	39.43	39.71	39.69	39.71	-83.51	-82.45	-84.99	-85.00	-85.00
S/N ratio – Level 2	3.00	3.23	3.21	2.89	2.91	39.87	39.93	39.84	39.79	39.80	-84.99	-85.01	-85.00	-85.00	-85.00
S/N ratio – Level 3	3.06	3.27	1.33	3.05	2.99	39.83	39.95	39.77	39.84	39.81	-86.27	-86.95	-85.00	-85.00	-85.00
Delta (max – min)	0.7	1.29	2.78	0.57	0.47	0.25	0.52	0.13	0.15	0.1	2.76	4.5	0.01	0.00	0.00
Rank	3	2	1	4	5	2	1	4	3	5	2	1	3	4	4

4.3.2. TASK C.2: ANOVA METHODS FOR ANALYSIS OUTPUT RESULTS

4.3.2.1. Regression

ANOVA (analysis of variance) is a mathematical tool for analyzing the results to find variation of each effective factor and their contribution (Capozzoli, Gorrino, & Corrado, 2013; Mechri, Capozzoli, & Corrado, 2010). ANOVA results are presented in Table 4.8 using the confidence level and significance level of 95% and 5%, respectively. Note that ANOVA cannot be conducted for capital cost (R_3) since it would be saturated (insufficient degree of freedom for error). The reason is that two factors of upper limit for indoor air temperature (D) and upper limit for floor surface temperature (E) did not affect the capital cost.

F-value of each factor determines its variability between and within groups. The significance of each factor can be realized by checking its F-value as indicated in Table 4.8 where a higher F-value indicates more significance. Therefore, it can be construed that for the peak power consumption (R_1), fan flow rate (C) followed by insulation thickness (B) and concrete slab

thickness (A) has the highest significance. This result is in good agreement with the results showed in Table 4.7.

Table 4.8: ANOVA results based on the data in Table 4.6

Average peak power consumption (R_1)					
Code	Factor name	Degree of freedom (DOF)	Sum of squares (SS)	Mean square (MS)	F-ratio (F)
A	Concrete slab thickness	2	0.019	0.010	37.560
B	Insulation thickness	2	0.070	0.035	137.760
C	Fan flow rate	2	0.263	0.131	514.300
D	Upper limit for air temperature	2	0.011	0.005	21.510
E	Upper limit for floor surface temperature	2	0.008	0.004	15.530
	Error	16	0.004	0.000	–
	Total	26	0.376	–	–
Thermal comfort potential (R_2)					
A	Concrete slab thickness	2	37.913	18.957	34.720
B	Insulation thickness	2	196.591	98.295	180.030
C	Fan flow rate	2	9.665	4.832	8.850
D	Upper limit for air temperature	2	12.930	6.465	11.840
E	Upper limit for floor surface temperature	2	7.724	3.862	7.070
	Error	16	8.736	0.546	–
	Total	26	273.559	–	–

Regression analysis is used to develop functions for the responses (i.e. dependent variables) in terms of independent variables. The functions can be used later for result prediction or conducting optimization. In order to be more comprehensive, interactions among the independent variables were considered and stepwise regression using backward elimination method (with alpha value of 0.1) was used to eliminate insignificant factors.

For average peak power consumption (R_1), the regression results are:

$$R_1 = -11.2 - 1.6 \times 10^{-3} A - 4.73 \times 10^{-4} B - 1.75 \times 10^{-3} C + 5.42 \times 10^{-1} D + 5.01 \times 10^{-1} E - 3.14 \times 10^{-5} A \times B + 8.41 \times 10^{-6} A \times C + 8.36 \times 10^{-6} B \times C - 2.17 \times 10^{-2} D \times E \quad R^2 = 98.18\% \quad (10)$$

where four interactions (i.e. $A \times B$, $A \times C$, $B \times C$, $D \times E$) were found significant.

Regression results for thermal comfort potential (R_2) are:

$$R_2 = 21.34 + 2.13 \times 10^{-1} A + 4.76 \times 10^{-1} B + 1.2 \times 10^{-1} C - 1.51 D + 1.98 E + 7.46 \times 10^{-4} A \times B - 5.04 \times 10^{-4} A \times C - 3.55 \times 10^{-4} B \times C - 1.37 \times 10^{-2} B \times E \quad R^2 = 96.81\% \quad (11)$$

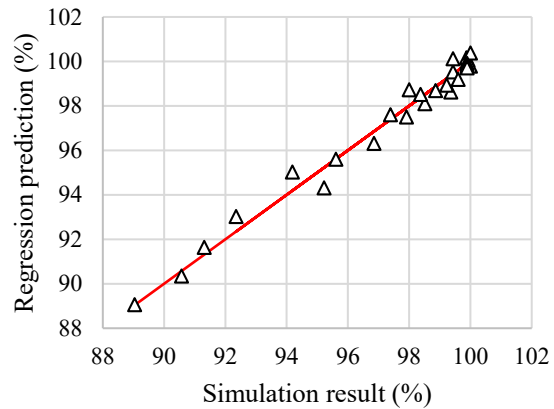
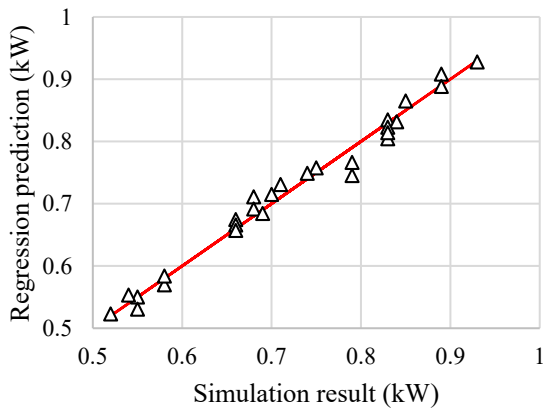
where four interactions (i.e. $A \times B$, $A \times C$, $B \times C$, $B \times E$) were significant.

Finally, for capital cost (R_3):

$$R_3 = 184.66 + 56.17 A + 88.43 B + 3.41 \times 10^{-1} C - 1.75 \times 10^{-3} A \times C \quad R^2 = 100\% \quad (12)$$

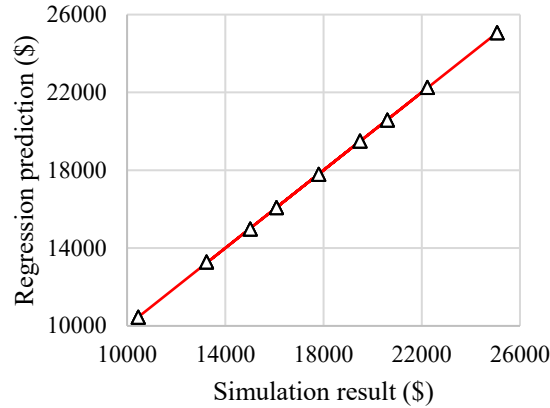
where only one interaction (i.e. $A \times C$) (concrete slab thickness \times fan flow rate) was found significant which was also included for the other responses in Equations (10) and (11), indicating its importance.

The regression model provided the correlation for the data scatter according to comparison of the simulation results and the regression predictions prediction by the Taguchi-ANOVA method in Figure 4.20. According to the figure, an acceptable agreement exists between predictions and simulation results. Quantitatively, the R^2 values of the regression models were above 96%. For instance, as for average peak power consumption (R_1) in Figure 4.20, the range of the peak power is from the 0.5-1 kW, the regression prediction can meet the accuracy in this range, which can indicate the regression model can replace the simulation results in mathematical to do the parametric studies.



Average peak power consumption (R_1)

Thermal comfort potential (R_2)



Capital cost (R_3)

Figure 4.20: Comparison of regression models with simulation results

4.3.2.2. Optimal condition

According to ANOVA results, optimal condition values for each response are identified and are shown in Table 4.9. Moreover, the table shows the overall optimal condition considering equal weight for all the responses. Note that Optimal 3 is not affected by factors D and E as they can be implemented at no cost. Therefore, their levels have been selected according to Optimal 1 and 2. Since none of the optimal conditions have been considered in Table 3.6, verification is required to check whether the optimal conditions (at least) outperform the existing results.

Table 4.9: Optimal condition for each response as well as overall (equal weight)

Factor		Value			
		Optimal 1*	Optimal 2*	Optimal 3*	Overall
A	Concrete slab thickness (mm)	Level 3: 203.2	Level 2: 152.4	Level 1: 101.6	Level 2: 152.4
B	Insulation thickness (mm)	Level 3: 152.4	Level 3: 152.4	Level 1: 50.8	Level 2: 101.6
C	Fan flow rate (CFM)	Level 1: 400	Level 2: 600	Level 1: 400	Level 1: 400
D	Upper limit for air temperature (°C)	Level 3: 24.5	Level 3: 24.5	Level 3: 24.5	Level 3: 24.5
E	Upper limit for floor surface temperature (°C)	Level 3: 28	Level 3: 28	Level 3: 28	Level 3: 28
Already investigated in Taguchi design (see 错误!未找到引用源。)		No	No	No	No

* Optimal 1, 2 and 3 correspond to Response 1, 2 and 3, respectively.

Simulations were conducted for each optimal condition in Table 4.9 to verify their optimized condition. Table 4.10 shows all the results, which confirm the optimal conditions when compared to the output values in Table 4.6.

Table 4.10: Verification of optimal conditions for each output parameter

Response	Optimal 1	Optimal 2	Optimal 3	Overall
Peak power consumption (kW)	0.52	0.65	0.69	0.55
Thermal comfort potential (%)	100.00	100.00	94.14	99.82
Capital cost (\$)	20,597	22,241	10,452	17,769

Compared to the results in Table 4.6, Optimal 1 (in Table 4.10) has the lowest value of average peak power consumption, indicating the highest peak load shifting. The reason can be attributed to the thick concrete (level 3: 203 mm) which can store more energy during off-peak hours. Consequently, lower energy would be needed to meet the demand during the peak hours. Besides, Optimal 2 guarantees the thermal comfort by achieving 100% potential. Note that Optimal 2 possesses the mid value for concrete slab thickness (level 2: 152.4 mm). This indicates that if the thickness is too high (or low) it would store excess (or insufficient) amount of heat, resulting in discomfort. The thicker insulation (level 3: 152 mm) is another effective factor to prevent the heat loss from the concrete slab. In addition, capital cost would be higher for thicker concrete or insulation. Therefore, Optimal 3 provides results with lower capital cost, whereas the peak shifting potential and thermal comfort have undesired values (i.e. 0.69 kW and 94.14%, respectively). Consequently, an overall optimal condition is considered as the trade-off among these three optimal conditions. It has a low peak power consumption (almost the same as the Optimal 1) while guaranteeing thermal comfort (almost 100%) and at the same time having lower capital cost than Optimal 1 or 2.

CONCLUSION

5.1. SUMMARY AND CONCLUSION

The main objective of this study is to develop an advanced controller to enhance the peak shifting potential of EHF system in residential buildings located in cold climate. The inference from the literature review is that various peak shifting control strategies with various TES have been proposed. According to the prediction for storing, control strategies are classified in non-predictive and predictive control strategies. In terms of TES, three main types (thermochemical storage, latent storage and sensible storage) are analyzed integrated with control strategies. The strengths and weaknesses are presented in various peak shifting control strategies with various TES. Consequently, SLC system with sensible heat storage (i.e. basement concrete slab) is selected as the suitable control strategy to operate EHF system in residential buildings located in Quebec.

To investigate the performance of the SLC system for peak shifting and heating cost saving potentials, a TRNSYS-MATLAB model was developed and validated using field measured data. The statistical criteria were in line with the requirements of ASHRAE and FEMP, indicating the validation of the model. Using the validated model, the performance of the SLC system was evaluated for two types of tariff schedules. For the CPP tariff of Quebec, two prediction methods with different temperature categories have been compared in terms of peak shifting potential, thermal comfort and heating cost saving with a reference case and also without SLC. It was found that during the critical days, although the SLC strategy (i.e. **Case Q-SLC-5°C**) required about 5.5% more heating than the other cases, the heating cost could still be reduced. The comparison results show that the peak shifting potential, thermal comfort and heating cost saving potential is better for **Case Q-SLC-5°C**. For this case (**Case Q-SLC-5°C**), heating cost saving of 23.6% was achieved compared to **Case Q-Ref** in the entire winter. For Ontario, the peak energy shaving of 80-100% is achieved, while the heating cost saving potential is 5-30% (i.e. \$0.16 per day on average). Analysis of the results in terms of temperature category indicated that the SLC system is more efficient under CPP tariff settings. These findings can help not only the house owners but

also the utility companies and decision makers in terms of exploiting the existing potential for the heat storage for peak shifting applications in residential sector.

In order to extend the peak shifting, the advanced controller, i.e., SLC system integrated with HES was developed using TRNSYS-MATLAB model to achieve the peak shifting not only in the floor with TES but also in the floor without heat storage facility. Using a fan with different flow rates to ease the overshoot could solve the existing limitation of the SLC (i.e. uncompleted charging) and guarantee the thermal comfort instead of setting the upper limit. Meanwhile, different peak shifting control strategies (RBC and SLC) have been investigated and the respective results were compared. The inference from the result is that both RBC and SLC strategies could guarantee the thermal comfort and at the same time achieve peak shifting and cost saving for the whole building. In RBC, regarded as a simpler control strategy, better performance in thermal comfort was achieved. However, as for peak shifting potential and cost saving, the results of the RBC were worse than the SLC. Advanced controller (SLC with EHF + HES) can provide the solution for completed charging in SLC to extend the peak shifting potential for the whole building (second floor up to 88%) while the RBC can achieve the peak shifting around 45% for the second floor. Meanwhile, advanced controller can avoid to create the new peak in the second off-peak period (shifting 45.92%) and get higher cost saving 35.23%.

In addition, parametric studies for the advanced controller has been investigated using the Taguchi method to provide recommendations on the appropriate design of EHF system and HES. Five parameters were considered (A) concrete slab thickness, (B) insulation thickness, (C) fan flow rate, (D) upper limit for indoor air temperature and (E) upper limit for floor surface temperature. Considering three levels for each parameter an L27 orthogonal array was selected according to Taguchi method. The outputs were (1) average peak power consumption, (2) thermal comfort potential and (3) capital cost. The results indicated that the insulation thickness was the most effective parameter for all individual outputs. Moreover, an overall optimum condition was investigated with equal weight for the outputs, which can provide the reference and guidance for the consumers and supplier. The optimal condition of the advanced controller was found to be a

concrete slab thickness of 152.4 mm, an insulation thickness of 101.6 mm, a fan flow rate of 400 CFM, air indoor upper limit of 24.5 °C and floor surface upper limit of 28 °C.

The overall contributions of this research are summarized here with:

- Peak shifting potential and cost saving for the floor with EHF have been investigated with different electrical tariffs.
- Advanced controller for the SLC together with HES is investigated to extend peak shifting and provide the solution for completed charging in SLC to improve the thermal comfort and peak shifting potential.
- Taguchi-ANOVA method is used in parametric study on peak shifting, thermal comfort and capital cost for the SLC integrated with HES system.

Based on (Canada., 2017), around 1.6 million typical detached houses exist in Quebec with similar characteristics to this investigation. Therefore, this technology is an effective method to decrease the stress of the electrical grid during the peak period once it is implemented.

5.2.FUTURE WORK AND RECOMMENDATIONS

Regarding the limitations of this present study, future work on the proposed SLC with HES to extend the peak shifting potential of EHF is recommended as followings:

- Experimental studies are to be conducted to validate the TRNSYS-MATLAB model with HES in peak shifting performance;
- In terms of the HES, different types of the fans (i.e. flowrate, power and efficiency) should be investigated in influence on peak shifting in simulations/experiments;
- Experiments should be conducted in different residential buildings to test the peak shifting potential and thermal comfort in application.

REFERENCES

- Alexander, B. R. (2010). Dynamic pricing? Not so fast! A residential consumer perspective. *The Electricity Journal*, 23(6), 39-49.
- Alonso, M. J., & Mathisen, H. M. (2017). Analysis of reduction of energy demands for Zero Emission Renovated Office Building by using thermal mass and ventilative cooling. *Energy Procedia*, 132, 592-597.
- Andresen, I., & Brandemuehl, M. (1992). *Heat storage in building thermal mass: a parametric study*. Paper presented at the ASHRAE Winter Meeting, Anaheim, CA, USA, 01/25-29/92.
- ASHRAE. (2013). Standard 55-2013 *Thermal environmental conditions for human occupancy*.
- ASHRAE. (2014). Guideline 14-2014 *Measurement of energy, demand, and water savings*.
- Avcı, M., Erkoç, M., Rahmani, A., & Asfour, S. (2013). Model predictive HVAC load control in buildings using real-time electricity pricing. *Energy and Buildings*, 60, 199-209.
- Bai, J., & Zhang, X. (2007). A new adaptive PI controller and its application in HVAC systems. *Energy Conversion and Management*, 48(4), 1043-1054.
- Balaras, C. (1996). The role of thermal mass on the cooling load of buildings. An overview of computational methods. *Energy and Buildings*, 24(1), 1-10.
- Barzin, R., Chen, J. J., Young, B. R., & Farid, M. M. (2015). Peak load shifting with energy storage and price-based control system. *Energy*, 92, 505-514.
- Bastani, A., & Haghghat, F. (2015). Expanding Heisler chart to characterize heat transfer phenomena in a building envelope integrated with phase change materials. *Energy and Buildings*, 106, 164-174.
- Bastani, A., Haghghat, F., & Kozinski, J. (2014). Designing building envelope with PCM wallboards: design tool development. *Renewable and Sustainable Energy Reviews*, 31, 554-562.
- Bastani, A., Haghghat, F., & Manzano, C. J. (2015). Investigating the effect of control strategy on the shift of energy consumption in a building integrated with PCM wallboard. *Energy Procedia*, 78, 2280-2285.

- Braun, J. E. (2003). Load control using building thermal mass. *Journal of solar energy engineering*, 125(3), 292-301.
- Braun, J. E., Montgomery, K. W., & Chaturvedi, N. (2001). Evaluating the performance of building thermal mass control strategies. *HVAC&R Research*, 7(4), 403-428.
- Canada., S. (2017). “Série ‘Perspective Géographique’, Recensement de 2016.”. Retrieved.
- Capozzoli, A., Gorrino, A., & Corrado, V. (2013). A building thermal bridges sensitivity analysis. *Applied Energy*, 107, 229-243.
- Chen, Y., Norford, L. K., Samuelson, H. W., & Malkawi, A. (2018). Optimal control of HVAC and window systems for natural ventilation through reinforcement learning. *Energy and Buildings*, 169, 195-205.
- Cheng, W., Xie, B., Zhang, R., Xu, Z., & Xia, Y. (2015). Effect of thermal conductivities of shape stabilized PCM on under-floor heating system. *Applied Energy*, 144, 10-18.
- Clauß, J., Finck, C., Vogler-Finck, P., & Beagon, P. (2017). *Control strategies for building energy systems to unlock demand side flexibility—A review*. Paper presented at the IBPSA Building Simulation 2017, San Francisco, 7-9 August 2017.
- Control. (2014). from https://www.coulton.com/What_is_On_Off_Control.html
- De Dear, R. J., & Brager, G. S. (2002). Thermal comfort in naturally ventilated buildings: revisions to ASHRAE Standard 55. *Energy and Buildings*, 34(6), 549-561.
- Electricity pricing and costs. (2018).
- . Energy Efficiency Trends in Canada 1990 to 2013. (2016): Natural Resources Canada.
- Fadejev, J., Simson, R., Kurnitski, J., & Bomberg, M. (2017). Thermal mass and energy recovery utilization for peak load reduction. *Energy Procedia*, 132, 39-44.
- Favre, B., & Peuportier, B. (2014). Application of dynamic programming to study load shifting in buildings. *Energy and Buildings*, 82, 57-64.
- Finck, C., Li, R., & Zeiler, W. (2016). Operational load shaping of office buildings connected to thermal energy storage using dynamic programming. *Proc. 12th REHVA world Congr*, 10.
- Georges, E., Masy, G., Verhelst, C., Andre, P., & Lemort, V. (2014). *Smart grid energy flexible buildings through the use of heat pumps in the Belgian context*. Paper presented at the 3rd International High Performance Buildings Conference at Purdue.

- Greenage. (2019). Time of use tariffs. from <https://www.thegreenage.co.uk/tech/time-of-use-tariffs/>
- Gupta, R., & Irving, R. (2013). Development and application of a domestic heat pump model for estimating CO₂ emissions reductions from domestic space heating, hot water and potential cooling demand in the future. *Energy and Buildings*, 60, 60-74.
- Haines, V., Kyriakopoulou, K., & Lawton, C. (2019). End user engagement with domestic hot water heating systems: Design implications for future thermal storage technologies. *Energy Research & Social Science*, 49, 74-81.
- Hajiah, A., & Krarti, M. (2012). Optimal control of building storage systems using both ice storage and thermal mass—Part I: Simulation environment. *Energy Conversion and Management*, 64, 499-508.
- Halvgaard, R., Poulsen, N. K., Madsen, H., & Jørgensen, J. B. (2012). *Economic model predictive control for building climate control in a smart grid*. Paper presented at the 2012 IEEE PES innovative smart grid technologies (ISGT).
- Heier, J., Bales, C., & Martin, V. (2015). Combining thermal energy storage with buildings—a review. *Renewable and Sustainable Energy Reviews*, 42, 1305-1325.
- Henze, G. P., Dodier, R. H., & Krarti, M. (1997). Development of a predictive optimal controller for thermal energy storage systems. *HVAC&R Research*, 3(3), 233-264.
- Henze, G. P., Felsmann, C., & Knabe, G. (2004). Evaluation of optimal control for active and passive building thermal storage. *International Journal of Thermal Sciences*, 43(2), 173-183.
- Henze, G. P., Kalz, D. E., Felsmann, C., & Knabe, G. (2004). Impact of forecasting accuracy on predictive optimal control of active and passive building thermal storage inventory. *HVAC&R Research*, 10(2), 153-178.
- Henze, G. P., Le, T. H., & Florita, A. R. (2005). *Sensitivity analysis of optimal building thermal mass control*. Paper presented at the ASME 2005 International Solar Energy Conference.
- Henze, G. P., & Schoenmann, J. (2003). Evaluation of reinforcement learning control for thermal energy storage systems. *HVAC&R Research*, 9(3), 259-275.

- Herter, K. (2007). Residential implementation of critical-peak pricing of electricity. *Energy policy*, 35(4), 2121-2130.
- Hu, M., Xiao, F., Jørgensen, J. B., & Li, R. (2019). Price-responsive model predictive control of floor heating systems for demand response using building thermal mass. *Applied Thermal Engineering*.
- Hu, M., Xiao, F., & Wang, L. (2017). Investigation of demand response potentials of residential air conditioners in smart grids using grey-box room thermal model. *Applied Energy*, 207, 324-335.
- Huang, T., & Liu, D. (2011). *Residential energy system control and management using adaptive dynamic programming*. Paper presented at the The 2011 International Joint Conference on Neural Networks.
- Huang, T., & Liu, D. (2013). A self-learning scheme for residential energy system control and management. *Neural Computing and Applications*, 22(2), 259-269.
- Kalnæs, S. E., & Jelle, B. P. (2015). Phase change materials and products for building applications: A state-of-the-art review and future research opportunities. *Energy and Buildings*, 94, 150-176.
- Kattan, P., Ghali, K., & Al-Hindi, M. (2012). Modeling of under-floor heating systems: A compromise between accuracy and complexity. *HVAC&R Research*, 18(3), 468-480.
- Keeney, K., & Braun, J. (1996). A simplified method for determining optimal cooling control strategies for thermal storage in building mass. *HVAC&R Research*, 2(1), 59-78.
- Keeney, K. R., & Braun, J. E. (1997). Application of building precooling to reduce peak cooling requirements. *ASHRAE transactions*, 103(1), 463-469.
- Klein, K., Herkel, S., Henning, H.-M., & Felsmann, C. (2017). Load shifting using the heating and cooling system of an office building: Quantitative potential evaluation for different flexibility and storage options. *Applied Energy*, 203, 917-937.
- Klein, K., Kalz, D., & Herkel, S. (2015). *Grid Impact of a Net-Zero Energy Building With BIPV Using Different Energy Management Strategies*. Paper presented at the Proceedings of International Conference CISBAT 2015 Future Buildings and Districts Sustainability from Nano to Urban Scale.

- Kuboth, S., Heberle, F., König-Haagen, A., & Brüggemann, D. (2019). Economic model predictive control of combined thermal and electric residential building energy systems. *Applied Energy*, *240*, 372-385.
- Lavrova, O., Cheng, F., Abdollahy, S., Barsun, H., Mammoli, A., Dreisigmayer, D., . . . Van Zeyl, C. (2012). *Analysis of battery storage utilization for load shifting and peak smoothing on a distribution feeder in New Mexico*. Paper presented at the 2012 IEEE PES Innovative Smart Grid Technologies (ISGT).
- Le Dréau, J., & Heiselberg, P. (2016). Energy flexibility of residential buildings using short term heat storage in the thermal mass. *Energy*, *111*, 991-1002.
- Li, J., Xue, P., He, H., Ding, W., & Han, J. (2009). Preparation and application effects of a novel form-stable phase change material as the thermal storage layer of an electric floor heating system. *Energy and Buildings*, *41*(8), 871-880.
- Li, X., & Malkawi, A. (2016). Multi-objective optimization for thermal mass model predictive control in small and medium size commercial buildings under summer weather conditions. *Energy*, *112*, 1194-1206.
- Lin, K., Zhang, Y., Xu, X., Di, H., Yang, R., & Qin, P. (2005). Experimental study of under-floor electric heating system with shape-stabilized PCM plates. *Energy and Buildings*, *37*(3), 215-220.
- Liu, L., Fu, L., & Jiang, Y. (2012). A new “wireless on-off control” technique for adjusting and metering household heat in district heating system. *Applied Thermal Engineering*, *36*, 202-209.
- Liu, S., & Henze, G. P. (2006a). Experimental analysis of simulated reinforcement learning control for active and passive building thermal storage inventory Part 1. Theoretical foundation. *Energy and Buildings*, *38*, 142-147.
- Liu, S., & Henze, G. P. (2006b). Experimental analysis of simulated reinforcement learning control for active and passive building thermal storage inventory: Part 2: Results and analysis. *Energy and Buildings*, *38*(2), 148-161.

- Liu, S., & Henze, G. P. (2007). Evaluation of reinforcement learning for optimal control of building active and passive thermal storage inventory. *Journal of solar energy engineering*, 129(2), 215-225.
- Lund, P. D., Lindgren, J., Mikkola, J., & Salpakari, J. (2015). Review of energy system flexibility measures to enable high levels of variable renewable electricity. *Renewable and Sustainable Energy Reviews*, 45, 785-807.
- Luo, N., Hong, T., Li, H., Jia, R., & Weng, W. (2017). Data analytics and optimization of an ice-based energy storage system for commercial buildings. *Applied Energy*, 204, 459-475.
- Ma, J., Qin, J., Salsbury, T., & Xu, P. (2012). Demand reduction in building energy systems based on economic model predictive control. *Chemical Engineering Science*, 67(1), 92-100.
- Ma, Y., Kelman, A., Daly, A., & Borrelli, F. (2012). Predictive control for energy efficient buildings with thermal storage: Modeling, stimulation, and experiments. *IEEE control systems magazine*, 32(1), 44-64.
- Massie, D. D. (2002). Optimization of a building's cooling plant for operating cost and energy use. *International Journal of Thermal Sciences*, 41(12), 1121-1129.
- Masy, G., Georges, E., Verhelst, C., Lemort, V., & André, P. (2015). Smart grid energy flexible buildings through the use of heat pumps and building thermal mass as energy storage in the Belgian context. *Science and Technology for the Built Environment*, 21(6), 800-811.
- Mazo, J., Delgado, M., Marin, J. M., & Zalba, B. (2012). Modeling a radiant floor system with Phase Change Material (PCM) integrated into a building simulation tool: Analysis of a case study of a floor heating system coupled to a heat pump. *Energy and Buildings*, 47, 458-466.
- Mechri, H. E., Capozzoli, A., & Corrado, V. (2010). Use of the ANOVA approach for sensitive building energy design. *Applied Energy*, 87(10), 3073-3083.
- Minitab 18 Statistical Software (2010). (2014.2.14). [Computer software] State College, PA: Minitab, Inc. (www.minitab.com).
- Morgan, S., & Moncef Krarti PhD, P. (2010). Field testing of optimal controls of passive and active thermal storage. *ASHRAE Transactions*, 116, 134.

- Morris, F., Braun, J. E., & Treado, S. (1994). Experimental and simulated performance of optimal control of building thermal storage. *ASHRAE Transactions*, *100*(1), 402-414.
- Mosaffa, A., Farshi, L. G., Ferreira, C. I., & Rosen, M. (2016). Exergoeconomic and environmental analyses of CO₂/NH₃ cascade refrigeration systems equipped with different types of flash tank intercoolers. *Energy Conversion and Management*, *117*, 442-453.
- Nkwetta, D. N., & Haghghat, F. (2014). Thermal energy storage with phase change material—A state-of-the art review. *Sustainable Cities and Society*, *10*, 87-100.
- Nkwetta, D. N., Vouillamoz, P.-E., Haghghat, F., El-Mankibi, M., Moreau, A., & Daoud, A. (2014). Impact of phase change materials types and positioning on hot water tank thermal performance: Using measured water demand profile. *Applied Thermal Engineering*, *67*(1-2), 460-468.
- Olesen, B. W. (2002). Radiant floor heating in theory and practice. *ASHRAE journal*, *44*(7), 19-26.
- Olesen, B. W., & Brager, G. S. (2004). A better way to predict comfort: The new ASHRAE standard 55-2004.
- Olsthoorn, D. (2018). *Determining Key Parameters and Guidelines for the Design of an Electrically Activated Concrete Slab for Peak Shifting in a Light-Weight Residential Building in a Northern Climate*. Concordia University.
- Olsthoorn, D., Haghghat, F., Moreau, A., Joybari, M. M., & Robichaud, M. (2019). Integration of electrically activated concrete slab for peak shifting in a light-weight residential building—Determining key parameters. *Journal of Energy Storage*, *23*, 329-343.
- Omar, F., Bushby, S. T., & Williams, R. D. (2017). A self-learning algorithm for estimating solar heat gain and temperature changes in a single-Family residence. *Energy and Buildings*, *150*, 100-110.
- Patteeuw, D., Henze, G. P., & Helsen, L. (2016). Comparison of load shifting incentives for low-energy buildings with heat pumps to attain grid flexibility benefits. *Applied Energy*, *167*, 80-92.
- Pavlak, G. S., Henze, G. P., & Cushing, V. J. (2015). Evaluating synergistic effect of optimally controlling commercial building thermal mass portfolios. *Energy*, *84*, 161-176.

- Peace, G. Taguchi Methods, A Hands On Approach, 1993: Addison-Wesley Publishing Company, Reading, MA, USA.
- Péan, T. Q., Salom, J., & Costa-Castello, R. (2018). Review of control strategies for improving the energy flexibility provided by heat pump systems in buildings. *Journal of Process Control*.
- Péan, T. Q., Salom, J., & Ortiz, J. (2017). Potential and optimization of a price-based control strategy for improving energy flexibility in Mediterranean buildings. *Energy Procedia*, 122, 463-468.
- Pedersen, T. H., Hedegaard, R. E., & Petersen, S. (2017). Space heating demand response potential of retrofitted residential apartment blocks. *Energy and Buildings*, 141, 158-166.
- Perez, K. X., Baldea, M., & Edgar, T. F. (2016). Integrated HVAC management and optimal scheduling of smart appliances for community peak load reduction. *Energy and Buildings*, 123, 34-40.
- Qian, B., Gregorich, E. G., Gameda, S., Hopkins, D. W., & Wang, X. L. (2011). Observed soil temperature trends associated with climate change in Canada. *Journal of Geophysical Research: Atmospheres*, 116(D2).
- Québec, C. s. l. e. é. d., Lanoue, R., & Mousseau, N. (2014). *Maîtriser notre avenir énergétique: Pour le bénéfice économique, environnemental et social de tous*: Ministère des ressources naturelles.
- Québec, QC - Hourly Forecast. (2018).
- Residential rates. (2018).
- Reynders, G., Diriken, J., & Saelens, D. (2015). *A generic quantification method for the active demand response potential of structural storage in buildings*. Paper presented at the 14th International Conference of the International Building Performance Simulation Association, Hyderabad, India.
- Robillart, M., Schalbart, P., Chaplais, F., & Peuportier, B. (2018). Model reduction and model predictive control of energy-efficient buildings for electrical heating load shifting. *Journal of Process Control*.

- Salpakari, J., Rasku, T., Lindgren, J., & Lund, P. D. (2017). Flexibility of electric vehicles and space heating in net zero energy houses: an optimal control model with thermal dynamics and battery degradation. *Applied energy*, *190*, 800-812.
- Salsbury, T., Mhaskar, P., & Qin, S. J. (2013). Predictive control methods to improve energy efficiency and reduce demand in buildings. *Computers & Chemical Engineering*, *51*, 77-85.
- Schiavon, S., Hoyt, T., & Piccioli, A. (2014). *Web application for thermal comfort visualization and calculation according to ASHRAE Standard 55*. Paper presented at the Building Simulation.
- Schmelas, M., Feldmann, T., & Bollin, E. (2015). Adaptive predictive control of thermo-active building systems (TABS) based on a multiple regression algorithm. *Energy and Buildings*, *103*, 14-28.
- Sharma, A., Saxena, A., Sethi, M., & Shree, V. (2011). Life cycle assessment of buildings: a review. *Renewable and Sustainable Energy Reviews*, *15*(1), 871-875.
- Sharma, I., Dong, J., Malikipoulos, A. A., Street, M., Ostrowski, J., Kuruganti, T., & Jackson, R. (2016). A modeling framework for optimal energy management of a residential building. *Energy and Buildings*, *130*, 55-63.
- Spall, J. C., & Cristion, J. A. (1993). *Model-free control of general discrete-time systems*. Paper presented at the Proceedings of 32nd IEEE Conference on Decision and Control.
- Spall, J. C., & Cristion, J. A. (1998). Model-free control of nonlinear stochastic systems with discrete-time measurements. *IEEE transactions on automatic control*, *43*(9), 1198-1210.
- Standard, A. (2004). Standard 55-2004. *Thermal environmental conditions for human occupancy*, 3.
- Standard, A. (2013). Standard 55-2013. *Thermal environmental conditions for human occupancy*.
- Sun, Y. (2018). *Heat Extraction System for Augmenting the Heating and Peak Shifting Ability of Electrically Heated Floor Residential Buildings*. Concordia University.
- Sun, Y., Panchabikesan, K., Joybari, M. M., Olsthoorn, D., Moreau, A., Robichaud, M., & Haghghat, F. (2018). Enhancement in peak shifting and shaving potential of electrically

- heated floor residential buildings using heat extraction system. *Journal of Energy Storage*, 18, 435-446.
- Sun, Y., Wang, S., & Huang, G. (2010). A demand limiting strategy for maximizing monthly cost savings of commercial buildings. *Energy and Buildings*, 42(11), 2219-2230.
- Thieblemont, H. (2017). *Simplified Predictive Control for Load Management: A Self-Learning Approach Applied to Electrically Heated Floor*. Concordia University.
- Thieblemont, H., Haghghat, F., Moreau, A., & Lacroix, G. (2018). Control of electrically heated floor for building load management: A simplified self-learning predictive control approach. *Energy and Buildings*, 172, 442-458.
- Thieblemont, H., Haghghat, F., Ooka, R., & Moreau, A. (2017). Predictive control strategies based on weather forecast in buildings with energy storage system: A review of the state-of-the art. *Energy and Buildings*, 153, 485-500.
- Thieblemont, H., Moreau, A., Lacroix, G., & Haghghat, F. (2017). *Simplified anticipatory control for load management: application to electrically heated floor*. Paper presented at the Presented at the International Conference & Workshop REMOO 2017.
- Touretzky, C. R., & Baldea, M. (2016). A hierarchical scheduling and control strategy for thermal energy storage systems. *Energy and Buildings*, 110, 94-107.
- Triki, C., & Violi, A. (2009). Dynamic pricing of electricity in retail markets. *4OR*, 7(1), 21-36.
- Turner, W., Walker, I., & Roux, J. (2015). Peak load reductions: Electric load shifting with mechanical pre-cooling of residential buildings with low thermal mass. *Energy*, 82, 1057-1067.
- Varaee, H., & Ahmadi-Nedushan, B. (2011). Minimum cost design of concrete slabs using particle swarm optimization with time varying acceleration coefficients. *World Appl Sci J*, 13(12), 2484-2494.
- Vázquez-Canteli, J. R., & Nagy, Z. (2019). Reinforcement learning for demand response: A review of algorithms and modeling techniques. *Applied Energy*, 235, 1072-1089.
- Wang, X., & Niu, J. (2009). Performance of cooled-ceiling operating with MPCM slurry. *Energy Conversion and Management*, 50(3), 583-591.

- Webster, L., Bradford, J., Sartor, D., Shonder, J., Atkin, E., Dunnivant, S., . . . Schiller, S. (2015). M&V Guidelines: Measurement and Verification for Performance-Based Contracts: Version 4.0, Technical Report.
- Wemhöner, C., Hafner, B., & Schwarzer, K. (2000). Simulation of solar thermal systems with CARNOT blockset in the environment Matlab® Simulink®. *Proceedings Eurosun 2000*.
- Xu, P. (2006). Evaluation of demand shifting strategies with thermal mass in two large commercial buildings. *Proceedings of SimBuild*, 2(1).
- Xu, P., Haves, P., Piette, M. A., & Braun, J. (2004). Peak demand reduction from pre-cooling with zone temperature reset in an office building: Lawrence Berkeley National Lab.(LBNL), Berkeley, CA (United States).
- Yang, L., Nagy, Z., Goffin, P., & Schlueter, A. (2015). Reinforcement learning for optimal control of low exergy buildings. *Applied Energy*, 156, 577-586.
- Yang, Q., Li, G., & Kang, X. (2008). *Application of fuzzy PID control in the heating system*. Paper presented at the 2008 Chinese Control and Decision Conference.
- Yau, Y., & Lee, S. (2010). Feasibility study of an ice slurry-cooling coil for HVAC and R systems in a tropical building. *Applied Energy*, 87(8), 2699-2711.
- Yau, Y., & Rismanchi, B. (2012). A review on cool thermal storage technologies and operating strategies. *Renewable and Sustainable Energy Reviews*, 16(1), 787-797.
- Yin, R., Xu, P., Piette, M. A., & Kiliccote, S. (2010). Study on Auto-DR and pre-cooling of commercial buildings with thermal mass in California. *Energy and Buildings*, 42(7), 967-975.
- Yu, Z. J., Huang, G., Haghghat, F., Li, H., & Zhang, G. (2015). Control strategies for integration of thermal energy storage into buildings: State-of-the-art review. *Energy and Buildings*, 106, 203-215.
- Zhang, X., Pipattanasomporn, M., & Rahman, S. (2017). A self-learning algorithm for coordinated control of rooftop units in small-and medium-sized commercial buildings. *Applied Energy*, 205, 1034-1049.
- Zhu, N., Hu, P., & Xu, L. (2013). A simplified dynamic model of double layers shape-stabilized phase change materials wallboards. *Energy and Buildings*, 67, 508-516.

- Zhu, N., Liu, P., Hu, P., Liu, F., & Jiang, Z. (2015). Modeling and simulation on the performance of a novel double shape-stabilized phase change materials wallboard. *Energy and Buildings*, *107*, 181-190.
- Zhu, N., Wang, S., Ma, Z., & Sun, Y. (2011). Energy performance and optimal control of air-conditioned buildings with envelopes enhanced by phase change materials. *Energy Conversion and Management*, *52*(10), 3197-3205.